This is to certify that the

thesis entitled

SIMULATION AND FEASIBILITY STUDY OF SOLAR WATER HEATING FOR THE FOOD PROCESSING INDUSTRY IN THE MIDWESTERN UNITED STATES

presented by

STEVEN MYRON THOMAS

has been accepted towards fulfillment
of the requirements for

Masters of Science degree in Agricultural Engineering

F.W. Bakker-Arkema
Major professor

Date 10-11-77/my

O-7639

SIMULATION AND FEASIBILITY STUDY
OF SOLAR WATER HEATING
FOR THE FOOD PROCESSING INDUSTRY
IN THE MIDWESTERN UNITED STATES

By

Steven Myron Thomas

A THESIS

Submitted to
Michigan State University
in partial fulfillment of the requirements
for the degree of

MASTER OF SCIENCE

Agricultural Engineering Department

1977

ABSTRACT

SIMULATION AND FEASIBILITY STUDY
OF SOLAR WATER HEATING
FOR THE FOOD PROCESSING INDUSTRY
IN THE MIDWESTERN UNITED STATES

By

Steven Myron Thomas

The feasibility of solar water heating applications in the food processing industry has been studied. Warm water usage surveys were made for three plant sizes; small, medium, and large, for representative plants in the dairy, meat and fruit and vegetable processing industries in the midwestern United States. A computer model, TRNSYS, was used to simulate a solar water heating system. Insolation simulation models were tested for predicting solar insolation data for the average year. The long-term performance for each plant solar water heating system was determined. An economic comparison was made for solar energy with electricity, fuel oil, and natural gas, to determine the current economic feasibility.

Economic feasibility results indicate a significant solar energy contribution can be made by replacing up to 90 percent of the electric and 20 percent of the fossil fuel energy consumption for most plants over a 20-year payback period.

Approved: F. W. Bakker-Arkema
Major Professor 10/10/77

Approved: D. R. Heldman
Department Chairman

ACKNOWLEDGEMENTS

The author wishes to thank the Energy Research and Development Administration (ERDA) and the United States Department of Agriculture (USDA) for their financial support of this study.

Sincere thanks and appreciation is extended to Dr. F. W. Bakker-Arkema (Agricultural Engineering Department) for his professional leadership, encouragement, and personal contribution to the progress and development of the program. The character, confidence and professional spirit of Dr. Bakker-Arkema was of primary importance to the author in the completion of this study.

Appreciation is also extended to Mr. A. L. Rippen (Food Science and Human Nutrition Department) for his helpful guidance and fellowship during the course of the study. Mr. R. Patterson (Agricultural Engineering Department) is also acknowledged for his contribution to the completion of this study.

Special thanks are due to Ms. Shari Cisco for her timely and professional typing of this manuscript.

The Agricultural Engineering faculty and fellow students also contributed significantly to the overall learning experience. Many thanks to these people for their intellectual and personal fellowship.

TABLE OF CONTENTS

Page

Page

LIST OF TABLES

Table | Page

LIST OF FIGURES

Figure | Page

LIST OF SYMBOLS

A	surface area, m^2
A_p	collector perimeter, m
c	specific heat, kJ/kg C
C_h	annual cost of solar energy system, $/year
$C_{h,tot}$	total initial investment for solar energy system, $
CRF	Capital Recovery Factor, $/$/year
COLEF	collector efficiency, %
F′	collector geometric efficiency factor, decimal
h	convection heat transfer coefficient, kJ/hr m^2 C
h_b	back loss coefficient, kJ/hr m^2 C
h_e	edge loss coefficient, kJ/hr m C
H_s	local hour angle measured from solar noon, degrees
i_{ann}	annual interest rate, %
i_{eff}	effective interest rate, %
j	annual rate of fuel price increase, %
k	thermal conductivity, kJ/hr m C
ℓ	thickness of insulation, m
L	latitude, degrees
m	mass flow rate, kg/hr
MCOL	mass flow through collector, kg
P	present value of a sum of money, $
P_o	initial amount of money or savings, $

Q	rate of energy or heat transfer, kJ/hr
Q_b	back loss of collector, kJ/hr
Q_e	edge loss of collector, kJ/hr
Q_t	top loss of collector, kJ/hr
QAUX	auxiliary energy, kJ
QCOL	energy collected by collector, kJ
QENV	energy lost by storage tank, kJ
QHX	energy passing through heat exchanger, kJ
QTANK	energy delivered to load by storage tank, kJ
QTOTAL	sum of QAUX and QTANK, kJ
R	measured daily horizontal insolation, ly/day
R_h	measured hourly horizontal insolation, ly/hr
R*	extraterrestrial daily horizontal radiation, ly/day
R_h^*	extraterrestrial hourly horizontal radiation, ly/hr
RADTOTAL	total radiation striking collector surface, kJ
SOLAR	energy delivered to load by collector, %
SOLAR-total	energy delivered to load by collector, % of QTOTAL
SYSOP	average period of daily collector operation, hrs/day
T'	time period, years
T	temperature, C
T_a	ambient air temperature, C
T_p	mean collector plate temperature, C
U	energy loss coefficient, kJ/m^2 hr C
UA	overall heat transfer coefficient, kJ/hr C
U_L	overall collector loss coefficient, kJ/hr m^2 C
U_t	top loss coefficient of collector, kJ/hr m^2 C
X	future value of a sum of money, $

α	solar altitude angle, degrees
β	collector tilt angle from horizontal, degrees
δ	solar declination, degrees
ε	surface emittance, decimal
σ	Stefan-Boltzman constant, kJ/hr m^2 K
ϕ	solar azimuth, degrees
η	collector efficiency, %
τ	atmospheric transmissivity, and total collector transmittance, decimal

1. INTRODUCTION

Recent years have imposed upon our society a new era of energy awareness. The energy conservationists along with world inflation and changes in international markets have made businessmen, consumers, and legislators realize the urgent need to look to the future and establish a long needed national energy policy dealing with the conservation of current energy sources and further research and development of current and alternate energy sources.

Partially as a result of this increased awareness, more research is being conducted in all areas of fossil energy production and utilization. Because of the magnitude of this effort, the urgency of the need, and economic considerations, researchers are considering all areas of energy consumption including the agriculture industry which represents a small percentage of the total consumption. Energy consumption patterns are very diverse, therefore we must look into every facet and reevaluate the relative costs of resources and products. Small percentages when added up can make a significant contribution to decreasing the overall energy consumption, and therefore concern must be given for every percentage point which can be gained through the use of alternate energy sources or conservation.

The agriculture industry represents 12 to 20 percent (Stout, 1975) of the total energy use in the United States. Currently researchers are looking into using more alternate sources of energy to satisfy certain energy demands in agriculture such as drying of grain crops, fruits, and vegetables, heating livestock housing, and using solar heater water for process cooking, heating of food stuffs, and peripheral functions such as cleaning machinery, product sterilization, and general washing.

This study deals specifically with the possibility of using solar energy as an alternate energy source to replace conventional fossil fuel energy in supplying hot water for processing and cleaning operations in the food industry. For this study the food industry is divided into three general areas, namely the dairy, meat, and fruit and vegetable industries. A small, medium, and large processing plant representative from each of the three areas was selected and surveyed to determine their hot water energy consumption. These plants were taken as representative plants for the midwestern United States and analyzed for solar energy utilization potential at three locations; East Lansing (Michigan), Indianapolis (Indiana), and Columbia (Missouri).

Solar energy as an alternate energy source has certain natural use restrictions which make the system difficult to design and utilize to its fullest capability. A primary concern is its variability and uncertainty of collection, thus making it undependable and necessitating some type of storage or back up energy supply to make it reliable to satisfy the food industry.

Because the utilization of solar energy is inherently dependent upon the weather and system interactions of storage, collection, and usage patterns, the design of such a system requires many calculations to determine its performance. In view of the complexity of this type of analysis a computer simulation lends itself as a viable tool to aid in the design of such a system and to determine its overall use potential.

Such a computer model called TRNSYS was chosen to fulfill the requirements. The TRNSYS program is capable of simulating the desired systems as a function of time, using actual weather data and hot water demand information as inputs. Since it is a transient simulation, calculations are performed at a specified time step over the simulations period. Because of this the accuracy of the simulation is directly related to the accuracy of the measured input weather and insolation data, and concern must be given to the type of data to use.

Hourly weather and insolation data is recommended by the TRNSYS authors. Unfortunately, hourly insolation data suitable for use with TRNSYS is scarce and in most cases only available for a short period of time. Since the performance of any solar installations depends largely on location it would be desirable to be able to use data measured for one location, or use available records of daily or weekly values of insolation and temperature to predict appropriate hourly data. This study will investigate the extent of current weather data availability and test other insolation and weather models to determine the best model to predict the long term performance of the solar water heating systems in supplying the demands of the food processing plants.

When the simulations are completed, basic economic analysis will illustrate the degree to which these solar water heating systems can be economically incorporated into commercial food processing plants.

2. OBJECTIVES

The overall objective of this study is to study the economic and engineering feasibility of heating process water for the food processing industry with solar energy. Specifically, the objectives are:

1. Use the Transient Simulation Program (TRNSYS) to test different types of insolation and temperature data models and determine the applicability, for solar system design, of these models to generate hourly insolation and temperature data, using currently available data, to use in areas where actual measured hourly data is insufficient.
2. Develop solar water heating design parameters and a system configuration applicable to the food processing industry.
3. Use hot water usage surveys and the solar water heating simulation model to predict the long term contribution of solar energy to the total energy demand for each processing plant, system size, and geographic location.
4. Use the simulation results to investigate the real potential for saving fossil fuel and the economic feasiblity of using solar energy at the present state of technology and economics for heating water for food processing plants.

3. REVIEW OF LITERATURE

The solar energy industry is becoming diversified into all areas of energy usage ranging from high temperature steam power generation installations to low temperature drying of agricultural crops (Daniels and Duffie, 1955), not to mention the natural energy conversion performed by plants using photosynthesis. The research and publications resulting from this growing industry is increasing at a fast rate. This study is concerned only with the low temperature application of solar energy for water heating. This review will consider only the simulation models, data inputs and system component designs directly relating to the solar water heating feasibility corresponding to demands from the food processing industry.

3.1 Computer Models

The design and performance analysis of any solar energy system requires many energy balance and transfer calculations. Because solar radiation is a dynamic occurrence, the behavior of the system continues to change over time requiring more calculations to determine its transient performance. A solar energy installation is a system of integrated components such as a collector, heat exchanger, storage tank, pumps, and controls. Mathematical models have been developed for each of these components, consisting of energy balances and sets of algebraic and/or differential equations. Because of the complexity and magnitude of solving these integrated models, the application of modern high speed computers is necessary to determine the long term system performance. With this capability, the analysis of the transient responses of integrated solar energy systems is now possible.

Several attempts have been made at developing reliable programs for this purpose. Ramsey (1975) has developed a flat plate collector computer program for heating liquids and has studied the non-uniform temperature characteristics of the collector and the flow distributions for different collector arrays. Kays and London (1958) presented relationships which describe the performance of different types of heat exchangers.

A few programs have been completed capable of simulating complete systems. Edenburn (1973) developed a specialized "Systems Analysis Computer Program" designed to model the total energy requirements of an entire community. This model is too specific for general use. Graven (1974) discussed several programs and their status such as the Post Office Program, Transient Simulation Program - TRNSYS, and the Jet Propulsion Laboratory program. The Post Office Program deals with building loads and includes no treatment of collector design or storage components. The TRNSYS program contains over 20 routines to model the transient performance of different types of integrated solar energy systems including collectors, storage tanks, and auxiliary heaters. According to Graven (1974) the scope of this model is generally limited to solar energy applications and not applicable to general building loads and other types of energy supplies. The Jet Propulsion program is limited to solar water heating only, thus not generally applicable. Graven (1974) concluded that many programs are still in the process of development and that no single readily available model is generally accepted. Edenburn and Grandjean (1975) and Edenburn (1975) discussed an "Energy System Simulation Computer Program" called SOLSYS developed by Sandia Laboratories. This program is capable of simulating the transient performance of energy systems composed of 21 component subroutines.

The TRNSYS and SOLSYS programs are both capable of simulating solar water heating systems needed for this study. The TRNSYS program was chosen based on its availability, ease of operation, and the results presented by other researchers on its performance and accuracy.

3.2 TRNSYS Program

The development and operation of TRNSYS is completely described by Klein et al. (1974). Instruction is given for connecting the desired components and determining the appropriate parameters. TRNSYS then performs the necessary simultaneous solutions of algebraic and differential equation over a specified time step to determine the system variables. Duffie and Beckman (1974) presented a detailed discussion of the procedures used by TRNSYS, individual component model descriptions, and methods for determining component parameters based on actual component design and application. Modeling considerations and recommendations are also discussed and examples presented to illustrate the behavior of solar systems.

TRNSYS was used by Oonk, Beckman, and Duffie (1975) to model residential heating and cooling performance of the Colorado State University house. Klein et al. (1975) used TRNSYS to simulate a solar water heating system for different system configurations and radiation data inputs. Different runs were made over a one-month period to observe the performance of each system configuration. An 8 percent loss was observed in the amount of solar energy supplied to the load when a heat exchanger component was included in the model. A simulation comparison of input radiation data was made using hourly measured insolation data and hourly mean insolation data based on monthly insolation normals for the same period. The hourly mean insolation data simulation results indicated a 5 to 25 percent increase in performance over the hourly measured insolation data simulation. It was suggested that a probable cause of this result was suggested as being a muting effect by the average data on the effects and irregularity of cloud cover on collector performance. No conclusion was drawn concerning the type of insolation data which should be used.

Gutierrez et al. (1974) used TRNSYS in studying the effects of auxiliary energy supply, load type, and storage capacity variations on total system performance; constant collector design parameters, based on current design practices, were used during this study. It was concluded that a three-layered stratified storage tank gave the best results with respect to accuracy and compute time compared to a higher degree of stratification; also, that the best method of adding auxiliary heat to the warm water is directly to the line coming from the storage tank. The best and worst times of water removal were also examined by the authors, with the most favorable time occurring early afternoon and the least favorable occurring just before sunrise.

3.3 Insolation Data

TRNSYS requires input data values of solar radiation and ambient air temperature at constant time intervals for the duration of the simulation period. The time interval is generally one hour. However, in this study the time interval will be examined for its effect on system performance. Since two data values are needed at each time interval, a distinction will be made wherein: solar radiation data will be referred to as insolation data defined as the total amount of solar radiation received at the surface of the earth (Kreider and Kreith, 1975), while all atmospheric conditions including air temperatures and wind speed will be referred to as weather data.

3.3.1 General availability

Presently, there are 67 collection sites in the United States which measure daily total insolation (Solar Radiation . . ., 1976). Of these, 29 also provide hourly insolation values. The information collected by these stations is gathered and tabulated at the National Climatic Center in Ashville, North Carolina. The period of these collection records range as far back as 1952. Baker and Klink (1975) discussed the quality of this data. Discrepancies of up to 10 percent were accredited to calibration variations, age, and type of absorber surface of the recording instruments. Due to lack of funds and standardization among the different stations the accuracy and reliability of these records is generally questionable. In September 1972 the National Climatic Center ceased publication of radiation data as requested by the

National Weather Service because the errors incorporated were estimated to range from 5 to 30 percent (Solar Radiation . . ., 1976). The National Oceanic and Atmospheric Administration has proposed that a new standardized network of collection stations be established. If and when this occurs, further radiation data will become available for use in solar system design.

3.3.2 Local availability

This study is concerned with solar energy utilization in the midwestern United States. Three locations were chosen, based on the availability of data, geographic location, and the location suitability of food processing plants, in which to study feasibilities. The locations chosen were East Lansing (Michigan), Columbia (Missouri), and Indianapolis (Indiana). All three locations have average daily insolation data available for weekly periods over a period of at least 13 years (Baker and Klink, 1975). Hourly insolation data is also available for 13 years (1946-1958) at the Columbia station and one year (1974-1975) at the East Lansing station. Hourly data is currently not available for the Indianapolis station.

Since proper design requires that system performance is predictable for both good and bad insolation years, more representative and complete data on an hourly basis is desirable.

3.3.3 Insolation models

Extensive work has been done developing models to predict solar insolation necessary for calculating heating and cooling loads of buildings. Although it is impossible to accurately predict future insolation, certain models predict insolation to the degree necessary for certain design problems. Three models have been proposed for simulating hourly horizontal solar insolation at a given location.

The American Society of Heating, Refrigeration, and Air Conditioning Engineers (ASHRAE) has developed tables which can be used to predict clear day hourly insolation based on solar time for different times of the year at different latitudes (ASHRAE, 1974). The purpose of these tables is to yield maximum design values of insolation for collector design. Clear day conditions occur infrequently. Actual insolation will be influenced by cloud cover, dust, water vapor, and other factors which affect the atmospheric transmissivity as described by Fritz (1957) and Threlkeld and Jordan (1957). The use of this insolation model in TRNSYS involves a modification to account for non-clear day operation.

A set of standard curves proposed by Whillier (1956) and further expanded by Liu and Jordan (1960) uses daily insolation totals to determine hourly insolation values based on solar time. This second model was developed and tested in South Africa and gives reasonable accuracy for other locations. Duffie and Beckman (1974) recommended this model to estimate hourly insolation values for input to TRNSYS. Williams, Loomis, and Carter (1974) have developed a Fortran computer program based on the Whillier curves for calculating hourly insolation values given total daily insolation, location, day length, and time of year.

A third model to be tested consists of using daily transmissivities together with a program that calculates extraterrestrial radiation (Furnival, et al., 1969). Equation (3.1) shows the relationship which exists between measured daily horizontal insolation (R), the total horizontal extraterrestrial radiation (R*), and the atmospheric transmissivity (τ) (Baker and Haines, 1969);

$$\tau = R/R^* \tag{3.1}$$

or for hourly insolation values:

$$R_h = \tau x\ R^*_h \tag{3.2}$$

where R_h is hourly horizontal insolation and R^*_h hourly horizontal extraterrestrial radiation. Thomas (1977) discussed the behavior of transmissivity for a one-year (1974-75) period in East Lansing and gives weekly averages of daily transmissivity. All three models can be used to predict insolation for an "average" year based on weekly averages of daily total insolation or daily transmissivity values using 13 year average data contained in Baker and Haines (1969).

Other models for predicting daily insolation have been proposed. Fritz (1957), Moon (1940), Sadler (1974), Threlkeld and Jordan (1957), and Liu and Jordan (1960) discussed the effects of air moisture, dust, air mass thickness, wavelength, location with respect to industrial centers, etc., and other atmospheric properties upon the atmospheric transmissivity and thus the insolation. Much of this work involves solar constant influences on insolation and is fundamental to the basic understanding of solar insolation characteristics. The ASHRAE model includes many of these findings.

Baker and Haines (1969) conducted a study on finding the correlation between the amount of sunshine received per day and the total daily insolation. This study correlated sunshine to insolation to about 0.92. Sunshine duration periods did not give an indication of radiation intensity according to Baker and Haines (1969) thus resulting in some error. Also sunshine records are not widely available for use with such a model. Thomas (1977) developed linear models to predict hourly insolation from hourly inputs of cloud cover, cloud elevation, atmospheric transmissivity, and extraterrestrial radiation. This type of model appears to be quite reliable and applicable to use in a simulation except that hourly cloud information is equally difficult to obtain as the measured insolation itself.

3.4 Weather Data Availability

Necessary inputs to a simulation also include air temperatures and wind speeds. Although wind speed information is not used in this simulation study it should be incorporated for certain collector designs (Klein et al., 1975). Air temperatures are of significant importance. Hourly ambient air temperatures are generally included with records of hourly insolation data. Local Climatological Data contains data on dry and wet bulb temperatures, wind speed, and cloud cover at three hour intervals. These values may be interpolated to produce hourly values with little error if temperature data is needed for combination with existing insolation data (Linvill, 1977). This was done by the author for one year at East Lansing.

Daily average, maximum, and minimum temperatures are also readily available from local weather stations. Annual mean monthly temperatures are available for the three test locations for use in conjunction with long-term average insolation data. East Lansing values are obtainable from the Michigan Department of Agriculture (1974), Indianapolis values from U. S. Department of Commerce (1964), and Columbia values from U. S. Department of Commerce (1968).

3.5 Principles of Heat Transfer

To evaluate the behavior and feasibility of a solar energy system a basic understanding of the modes of heat transfer is necessary. Consideration will be given to three modes of heat transfer, namely conduction, convection, and radiation. A driving force is necessary for heat transfer to occur. The magnitude of the driving force is determined by the temperatures of the bodies involved. From the Second Law of Thermodynamics energy always tends toward a state of greater entropy and for this discussion corresponds to heat transfer from the body with the higher temperature to a body at a lower temperature (Jenkins and Perkins, 1970).

Conductive heat transfer occurs by molecular actions of vibration or rotation (Kreider and Kreith, 1975). The equation describing one dimensional conductive heat transfer is given as:

$$Q = -kA \frac{\partial T}{\partial x} \tag{3.3}$$

where Q is the heat transfer rate, k the thermal conductivity, A the area perpendicular to heat flow, and $\frac{\partial T}{\partial x}$ the temperature gradient in the material.

Convective heat transfer occurs by the motion of a fluid. The describing equation is:

$$Q = hA \, \Delta T \tag{3.4}$$

where h is the heat transfer coefficient, and ΔT the temperature difference between the surface and the fluid.

Radiative heat transfer occurs by means of electro-magnetic radiation and is described by:

$$Q = \varepsilon \; A \; \sigma \; T^4 \tag{3.5}$$

where σ is the Stefan-Boltzmann constant, ε the surface emittance, and T the absolute temperature of the radiating body.

A fourth equation is needed to describe the energy removed by a transport fluid. Equation (3.6) relates the mass flow rate m, specific heat of the fluid c, and the temperature change of the fluid ΔT, to the rate of energy removal Q.

$$Q = mc \; \Delta T \tag{3.6}$$

These relationships may be used to construct energy balances on components to determine their performance as a function of the physical properties of the component and the temperatures at which it is operating.

Basic heat transfer texts such as Holman (1972), Kreith (1973), or Kreider and Kreith (1975) may be referred to for a more detailed discussion of these principles.

3.6 Principles of Solar Radiation

The amount of energy reaching the earth from the sun is called the solar constant, and varies 1.5 percent over the year (Moon, 1940). The degree of variation for most cases is insignificant for design purposes. The accepted value of the solar constant measured normal to the sun rays outside of the earth atmosphere is 1353 J/s/m^2 (ASHRAE, 1974).

The energy which reaches the surface of the earth is dependent upon many factors including: sun-earth orientation, atmospheric properties, and time of day. Figure 3.1 illustrates the spectral distribution characteristics of solar radiation, shows the distribution if the sun were radiating as a black body, the actual solar radiation distribution outside the atmosphere, and the spectral distribution of the radiation which reaches the earth's surface. As solar radiation passes through the atmosphere, a percentage of it is absorbed by water vapor, dust, and gas molecules (Fritz, 1957). As a result, the magnitude of the direct solar (or beam) radiation is decreased and the amount of diffuse or sky radiation is increased. Since the amount of diffuse radiation is largely a function of scattering, sky emissivity, and cloud conditions, it is best described by actual measured data. The performance of a solar collector is dependent upon the relative amounts of direct and diffuse radiation. Duffie and Beckman (1974) described empirical relationships distinguishing diffuse radiation originating near the sun for clear days from that of widely scattered diffuse radiation occurring on very cloudy or hazy days.

When radiation strikes a material it may be transmitted, reflected, absorbed, or a combination of these (Siegel and Howell, 1972). When choosing materials for collector covers and absorbing plates consideration must be given to these properties and how they may influence collector performance. The transmittance of a material is the ratio of energy transmitted to the energy incident. The reflectance of a material is the ratio of reflected energy to the incident energy. Similarly

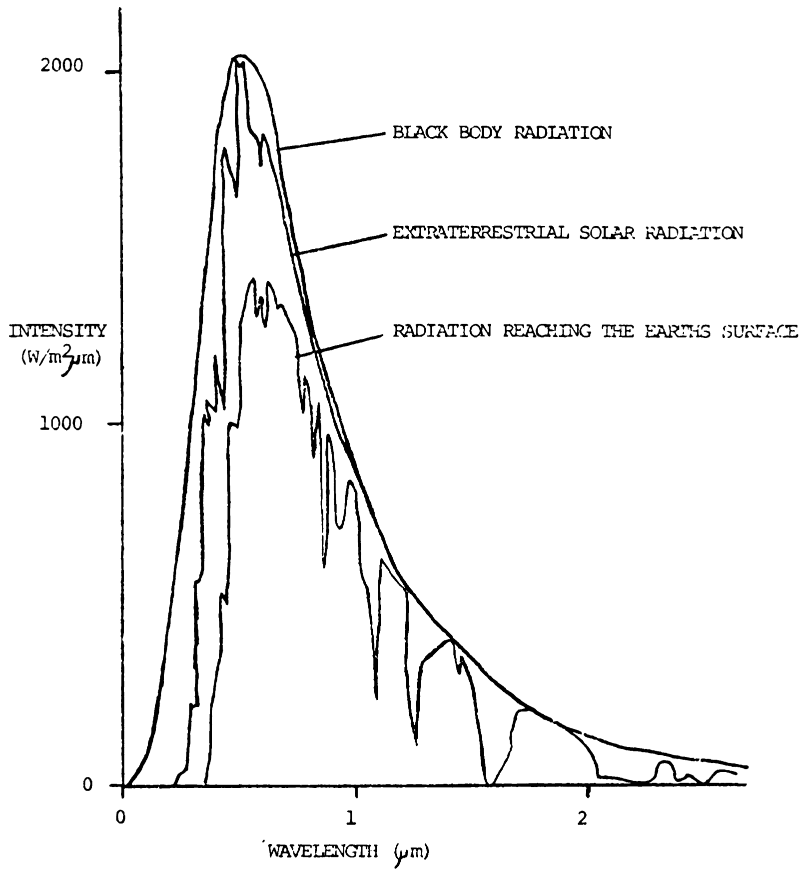

Figure 3.1 Spectral Distribution of Solar Radiation.

absorptance is the ratio of energy absorbed to the amount of energy incident upon the surface. The sum total of these is numerically equal to unity. Emittance is a property describing the radiating characteristics of a body and is defined as the ratio of energy emitted by a material to the amount emitted if it were a black body. Each of these properties is a function of the wavelength and incident angle of the incident energy. When considering collector covers; a low reflectance, emittance, and absorptance material is desirable for all wavelengths and incident angles, while a high transmittance is desirable for wavelengths and incident angles which allow the greatest amount of radiation to pass through. Desirable properties of the collector absorber plate are: low reflectance at all wavelengths and incident angles, zero transmittance, high absorptance for all incident angles and at wavelengths which most incident energy occurs, and low emittance at all angles and at wavelengths corresponding to the greatest intensities of the spectral distribution curve at the plate temperature. A surface in which the absorptance and emittance are not equal is called a selective surface (Kreider and Kreith, 1975), and has a greater potential for use in solar collectors. Materials with these properties are difficult to obtain and generally expensive.

Figure 3.2 identifies the angles which are important in determining the amount of radiation available at a particular location. The altitude angle (α) which the incoming beam radiation makes with the horizontal surface is given by (Kreider and Kreith, 1975):

$$\sin\alpha = \sin L \sin\delta + \cos L \cos\delta \cos H_s \tag{3.7}$$

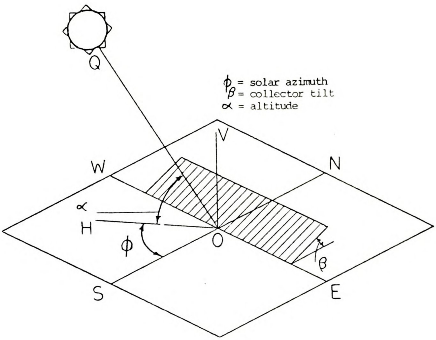

Figure 3.2 Description of Sun-Earth Orientation Angles.

where L is the latitude, δ the solar declination, and H_S the local solar hour angle measured from solar noon. Equation (3.7) can be used to determine the location and elevation of the sun for any time of year, thus allowing for the calculation of collector tilt angles. Most collectors are tilted from the horizontal in order to minimize the angle of incidence of insolation, thus allowing maximum insolation to pass through the glazing to the absorber plate.

3.7 Solar Component Design and Technology

3.7.1 Solar collectors

The basic principles of flat plate solar collector design are illustrated in Figure 3.3. ASHRAE (1974) illustrated fourteen common collector water and air heater designs. The number of covers depends upon the climate and the specific use for the collector. Kreider and Kreith (1975) recommended double glass glazing for most northern climate solar water heater installations. Other glazing materials such as plexiglas, polyvinyl flouride (Tedlar), polyethylene, and others are sometimes used. The choice of such materials depends upon desired performance, costs, life expectancy, maintenance, etc.

Radiation passes through the transparent covers striking the absorber plate. As the radiation strikes the absorber plate, energy is absorbed causing the temperature to increase and heat transfer to occur from the plate to some transport fluid passing through the collector. The absorber plate is covered by some material that has a high absorbtivity and in certain designs, may be a selective surface. Proper collector

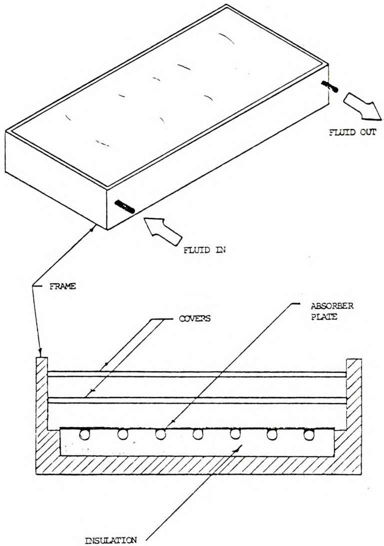

Figure 3.3 Principles of Flat Plate Collector Design.

design must take into consideration heat losses by conduction, convection, and radiation, inefficiencies in transmittance and absorptance of the incident energy, the cost of materials, and the relative trade off of each. There are many commercially available collectors of good quality which have a reasonable long life expectancy. Costs for these collectors range from 100 to 270 dollars per square meter (Solar Research, 1977 and Owens-Illinois, 1977).

Several design parameters are important when determining collector performance. Total transmittance describes the amount of insolation passing through the cover plates which strikes the absorber plate after accounting for reflection and absorption losses. Duffie and Beckman (1974) described the dependance of transmittance on cover thickness, extinction coefficient, number of covers, cover spacing, and incidence angle of the incoming radiation. Based on these relationships Duffie and Beckman (1974) presented figures for the determination of collector transmittance.

Collector plate absorptance is given for several plate coating materials in Table 5.5.1 of Duffie and Beckman (1974). This parameter describes the ability of the collector to collect and retain the incoming radiation. Collector absorptance values range from 0.8 to 0.95 depending upon the coating material.

The overall energy loss coefficient (U_l) is an important parameter influencing the collector performance. Klein (1974) presents a method for calculating this value as a function of top (Q_t), edge (Q_e), and back (Q_b) heat losses:

$$U_l = (Q_t + Q_b + Q_e)/A\ (T_p - T_a) \qquad (3.8)$$

where U_l is the overall energy loss coefficient, A the collector area, T_p the mean collector plate temperature, and T_a the ambient air temperature. Klein (1974) proposes the use of equations (3.9), (3.10), and (3.11) to determine the top, back, and edge heat losses, respectively.

$$Q_t = U_t A \, (T_p - T_a) \tag{3.9}$$

The top loss coefficient U_t in equation (3.9) accounts for radiation and convection losses from the top surface of the absorber plate and is related to the number of cover plates, wind speed, tilt angle, mean plate temperature, and emissivities of the absorber plate and covers. Whillier (1967) presented relationships to calculate the top loss coefficient for several collector designs. Duffie and Beckman (1974) presented curves (Figure 7.4.4 of Duffie and Beckman, 1974) based on an empirical relationship developed by Klein (1974), which can be used to determine the top loss coefficient given the mean collector plate temperature, number of covers, ambient air temperature, plate emissivity and wind speed.

Heat loss from the back side of the collector absorber plate may be obtained from:

$$Q_b = A \, (T_p - T_a)/(\ell/k + 1/h_b) \tag{3.10}$$

where ℓ is the insulation thickness, k the thermal conductivity of the insulation, and h_b the convection coefficient between the bottom of the insulation and the ambient air. Edge losses may be determined by:

$$Q_e = h_e \, (A_p) \, (T_p - T_a) \tag{3.11}$$

where h_e is the convection coefficient between the edge surface and the ambient air, and A_p the collector perimeter.

The actual performance of a collector may be described by the geometric efficiency factor F' (Duffie and Beckman, 1974). This factor is a ratio of the heat transfer resistance between the absorber plate and the ambient air and the heat transfer resistance from the fluid to the ambient air. The collector efficiency factor remains constant for a given collector design and flow rate. Figure 7.5.4 developed by Duffie and Beckman (1974) give values for the geometric efficiency factor given tube spacing, plate conductivity and thickness, overall loss coefficient, and the heat transfer coefficient between the collecting fluid and the inside of the tubes.

The collector efficiency (η) is a term helpful to observe actual collector performance over a simulation period. Kreider and Kreith (1975) describe collector efficiency as the ratio of energy output to the total incident radiant energy. This efficiency is a function of the collector plate temperature and the relative period of operation used to calculate it. Care should be used when comparing efficiencies of different collectors so that equal time periods are used.

3.7.2 Other components

Other components such as heat exchangers, storage tanks, and auxiliary heaters are generally of conventional design. Costs and performance vary according to materials of construction. These components require energy balances to describe their performance over time.

Holman (1972) and Kays and London (1958) described the basic theory for heat exchanger design. Heat exchanger capacity is described by the overall heat transfer coefficient UA. The choice of this design parameter depends upon the heat transfer rate required by the system. Preliminary calculations may be used to estimate the heat exchanger capacity needed for a certain installation. A counterflow type heat exchanger is recommended for applications involving small temperature differentials, as in solar energy systems, because small temperature differences between the warm inlet fluid and the cold exit fluid are characteristically low, thus allowing for maximum heat transfer.

Storage tanks may be divided into segments for modeling with the temperatures at each segment described by a set of differential equations. In order to construct energy balances on these tank segments, the tank losses must be accounted for. An energy loss coefficient (U) for an insulated tank can be determined from Holman (1972).

The capacity of the auxiliary heater may be determined from equation (3.6). The capacity of the heater should be great enough to supply 100 percent of the demand. For simulation testing this criteria should be assumed. In actual design of the physical system the heater capacity may be sized allowing for a minimum energy contribution from the solar collectors and a factor of safety.

3.8 Physical Solar Water Heating Systems

A solar water heating system is a combination of various components designed to collect incident direct and/or diffuse solar insolation and convey this energy, by means of a transport fluid, to a place of utilization and/or storage for future utilization. Clearly such an installation is dependent upon each component in order to give best performance. Löf (1977) emphasized that although individual components are proven to perform under certain conditions, the overall performance and reliability of a system depends upon the proper sizing and combination of related components. Solar water heating is a direct use of solar energy which has been practiced most extensively in the last two decades. Kreider and Kreith (1975) predicted water heating will be the first wide use of solar energy during this period because of the high use factor and low initial cost.

The basic elements of a solar water heater, illustrated in Figure 3.4, are a flat plate collector, storage tank, pump, controller, and an auxiliary heater. For operation in freezing climates an antifreeze solution may be used in the collector with a heat exchanger used to transfer the energy to the water. Duffie and Beckman (1974) stated typical collector dimensions are 1.2 by 1.2 meters with multiple units being connected in a single installation. Common absorber plates are copper or steel with tubes thermally bonded to the plate allowing for the passage of the collector fluid. The absorber plate and glazing covers are installed in a frame with 5 to 10 centimeters of insulation on the back.

Storage tanks should be well insulated. Twenty centimeters of mineral wool insulation is recommended by Duffie and Beckman (1974). Auxiliary energy may be added in three ways as discussed by Gutierrez et al. (1974): directly to the tank, to the water leaving the tank, or directly to the supply water, bypassing the tank. The authors concluded the second method resulted in most efficient operation.

Sizing of system components depends upon the type of load, energy

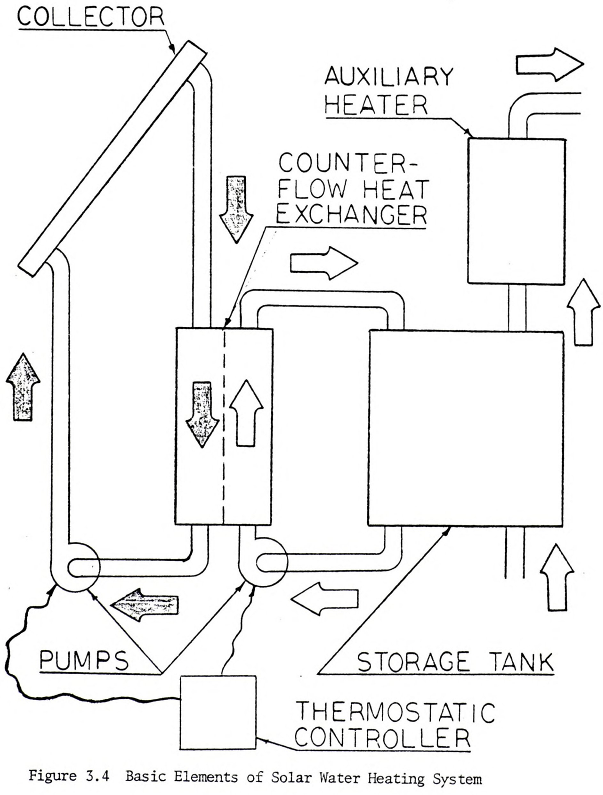

Figure 3.4 Basic Elements of Solar Water Heating System

costs, etc. (Duffie and Beckman, 1974). Kreider and Kreith (1975) presented the following general guidelines for residential installations: 36.8 square meters of collector to supply 100 kilograms of hot water, a storage tank capacity should allow a two-day supply, and a collector fluid flow rate of 40 kilograms per square meter of collector per hour. Guidelines for industrial applications may vary.

3.9 Warm Water Usage

The food processing industry consumes 9.5×10^{17} Joules annually (Reding and Shepard, 1975). The energy consumption for the dairy, meat, and fruit and vegetable industries is given in Table 3.1 (U. S. Department of Commerce, 1974). Recognizing that the warm water use in these processing plants is a significant percentage of this consumption, a potential exists for saving fossil fuel energy by the replacement with solar energy.

Representative processing plants, one each of small, medium, and large from each industry were surveyed by Dansbury (1977) for their warm water consumption. His findings are shown in Tables 3.2, 3.3, and 3.4 and Figures 3.5, 3.6, and 3.7.

3.9.1 Dairy plants

Dairy plants were chosen with an emphasis on fluid milk processing operations. Water usage information obtained from all plants consisted of warm water used for cleaning operations relating to fluid milk processing operations. Table 3.2 shows the volumes and temperatures required.

Table 3.1 - Energy Consumption of the Dairy, Meat, and Fruit and Vegetable Processing Industries (U.S. Department of Commerce, 1974).

INDUSTRY

	Dairy		Meat		Fruit and Vegetable	
	Total	Fluid Milk	Sausage, etc.	Packing	Canning	Freezing
Value of Purchased fuel (1971) (10^6 $)	123.2		130.8 total		124.4 total	
Percent of Product value	0.8		0.5		1.0	
Energy Used (10^{12} KJ)						
1967	230.7		17.0	83.3		
1971	255.2	17.9	24.0	126.8	62.0	21.9
1980	261.7	16.8	27.4	145.5	76.9	30.2
Type of Energy used (% of total)						
Propane		1.8	1.2	2.1	2.9	1.0
Middle distillates		8.1	8.1	3.3	0.9	0.5
Residuals		4.1	3.7	5.2	6.8	2.8
Coal		3.3	0.9	10.1	3.4	3.6
Natural gas		34.9	48.8	48.8	69.6	42.1
Electric		45.8	37.6	30.3	16.4	50.2

Table 3.2 - Dairy Plant Warm Water Usage.

Small:	
Average water temperature	65.53 C
Annual demand schedule	52 weeks
Processing days per week	3 - MWF
Principle use	cleaning
Volume - daily	1940 kg
peak flow	692 kg/hr
weekly	5820 kg
Energy demand - daily	4.28×10^5 kJ
weekly	1.285×10^6 kJ
annual	6.682×10^7 kJ
Medium:	
Average water temperature	66.11 C
Annual demand schedule	52 weeks
Processing days per week	5 - MTWTHF
Principle use	cleaning
Volume - daily	6456 kg
peak flow	717 kg/hr
weekly	32,280 kg
Energy demand - daily	1.44×10^6 kJ
weekly	7.20×10^6 kJ
annual	3.747×10^8 kJ
Large:	
Average water temperature	79.44 C
Annual demand schedule	52 weeks
Processing days per week	6 - MTWTHFS
Principle use	cleaning
Volume - daily	25,000 kg
peak flow	1387 kg/hr
weekly	150,000 kg
Energy demand - daily	6.96×10^6 kJ
weekly	4.182×10^7 kJ
annual	2.17×10^9 kJ

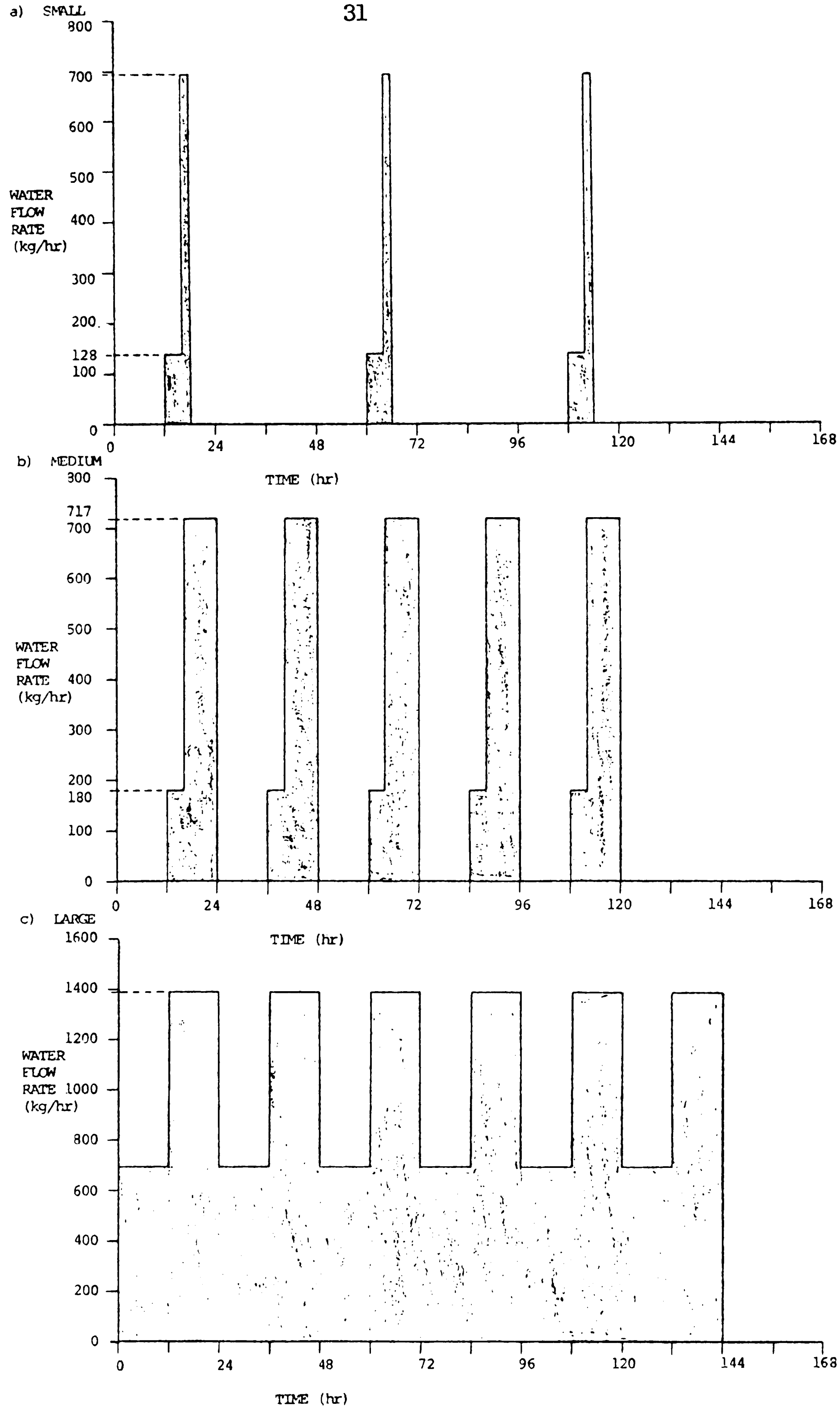

Figure 3.5a,b,c Dairy Processing Plant Water Demand Schedules.

Usage patterns were determined based on plant scheduling, shifts, etc. Dairy plants exhibit a uniform cyclic demand over the entire year. Dansbury (1977) recommended the weekly demand schedules shown in Figure 3.5 for use in computer simulation.

3.9.2 Meat plants

The meat processing plant surveys reflect warm water used for cleaning and washing in slaughter and processing operations. Meat plants operate continuously over the year. Results similar to the dairy plants are given in Table 3.3 and Figure 3.6.

3.9.3 Fruit and vegetable plants

The fruit and vegetable industry is widely diversified. The multitude of agricultural products processed by these plants presented irregular usage patterns throughout the year. The type of processing operations, whether canning or freezing also greatly influenced the warm water energy demand. A cross section of plant operation patterns is represented by the survey results of the three plants.

The small plant is a canning plant which operated during most of the year according to Figure 3.7. Energy demands shown in Table 3.4 include warm water usage for processing and cleaning operations.

The medium plant is a freezing plant that operated 12 months a year. Although this plant produced more product than the small plant it was classified according to the relative energy demands of all three plants.

Table 3.3 - Meat Plant Warm Water Usage.

Small:	
Average water temperature	60.0 C
Annual demand schedule	52 weeks
Processing days per week	5 - MTWTHF
Principle use	cleaning
Volume - daily	3,026 kg
peak flow	504 kg/hr
weekly	15,130 kg
Energy demand - daily	5.98×10^5 kJ
weekly	2.99×10^6 kJ
annual	1.56×10^8 kJ
Medium:	
Average water temperature	71.11 C
Annual demand schedule	52 weeks
Processing days per week	5 - MTWTHF
Principle use	cleaning
Volume - daily	5,410 kg
peak flow	902 kg/hr
weekly	27,050 kg
Energy demand - daily	1.32×10^6 kJ
weekly	6.61×10^6 kJ
annual	3.44×10^8 kJ
Large:	
Average water temperature	71.11 C
Annual demand schedule	52 weeks
Processing days per week	6 - MTWTHFS
Principle use	cleaning
Volume - daily	42,000 kg
peak flow	1800 kg/hr
weekly	2.52×10^5 kg
Energy demand - daily	1.03×10^7 kJ
weekly	6.16×10^7 kJ
annual	3.20×10^9 kJ

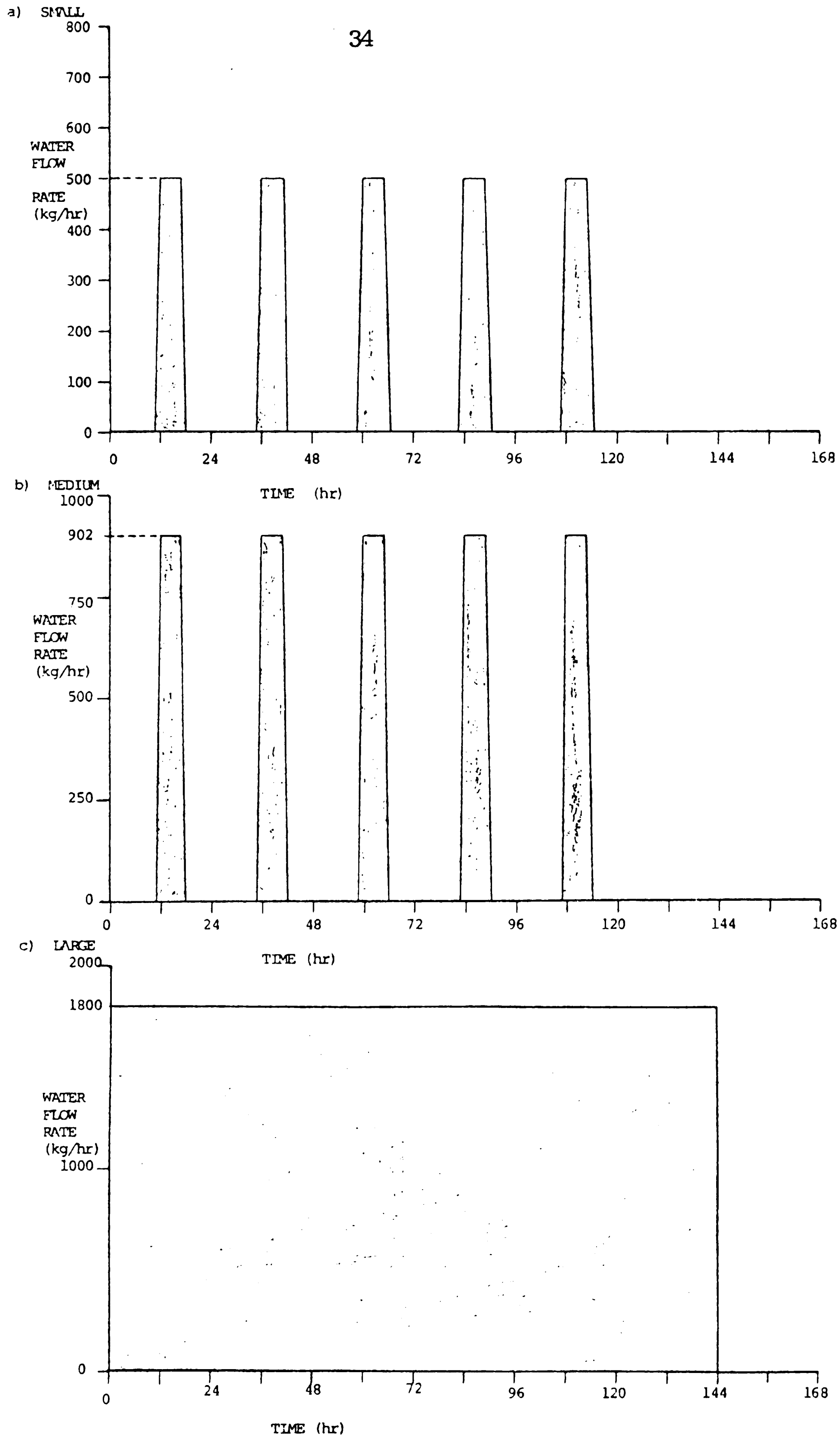

Figure 3.6a,b,c Meat Processing Plant Water Demand Schedules.

Table 3.4 - Fruit and Vegetable Plant Warm Water Usage

Small:	
Type and products	Canning: asparagus, cherries, green beans, apples
Average water temperature	84.8 C
Annual demand schedule	
Period A	36 days starting May 10
Processing days per week	6 - MTWTHFS
Principle use	processing
Volume - daily	25,600 kg
peak flow	2,960 kg/hr
weekly	1.53×10^5 kg
Energy demand - daily	7.72×10^6 kJ
weekly	4.63×10^7 kJ
total for period	2.387×10^8 kJ
Period B	18 days starting June 21
Processing days per week	6 - MTWTHFS
Principle use	processing
Volume - daily	7,670 kg
peak flow	947 kg/hr
weekly	46,000 kg
Energy demand - daily	2.31×10^6 kJ
weekly	1.39×10^7 kJ
total for period	3.006×10^7 kJ
Period C	60 days starting August 1
Processing days per week	5 1/2 - MTWTHFS
Principle use	processing
Volume - daily	76,680 kg
peak flow	4,674 kg/hr
weekly	421,700 kg
Energy demand - daily	2.31×10^7 kJ
weekly	1.271×10^8 kJ
total for period	1.112×10^9 kJ
Period D	60 days starting October 1
Processing days per week	6 - MTWTHFS
Principle use	processing
Volume - daily	7,670 kg
peak flow	947 kg/hr
weekly	44,000 kg
Energy demand - daily	2.31×10^6 kJ
weekly	1.39×10^7 kJ
total for period	1.202×10^8 kJ
Total energy demand	1.501×10^9 kJ

Table 3.4 (continued) Fruit and Vegetable Plant Warm Water Usage .

Medium:	
Type and products	freezing: asparagus, cherries, cabbage, carrots, squash, apples
Average water temperature	84.4 C
Annual demand schedule	
Period A	All year excluding the month of August
Processing days per week	6 - MTWTHFS
Principle use	processing
Volume - daily	48,470 kg
peak flow	2,910 kg/hr
weekly	291,000 kg
Energy demand - daily	1.46×10^7 kJ
weekly	8.76×10^7 kJ
total for period	4.14×10^9 kJ
Period B	30 days of August
Processing days per week	6 - MTWTHFS
Principle use	processing
Volume - daily	60,600 kg
peak flow	3,670 kg/hr
weekly	364,000 kg
Energy demand - daily	1.83×10^7 kJ
weekly	1.10×10^8 kJ
total for period	4.92×10^8 kJ
Total annual energy demand	4.632×10^9 kJ
Large:	
Type and products	canning: green beans
Average water temperature	77.8 C
Annual demand schedule	60 days starting August 1
Processing days per week	6 - MTWTHFS
Volume - daily	507,000 kg
peak flow	31,200 kg/hr
weekly	3.042×10^6 kg
Energy demand - daily	1.382×10^8 kJ
weekly	8.29×10^8 kJ
annual total	8.28×10^9 kJ

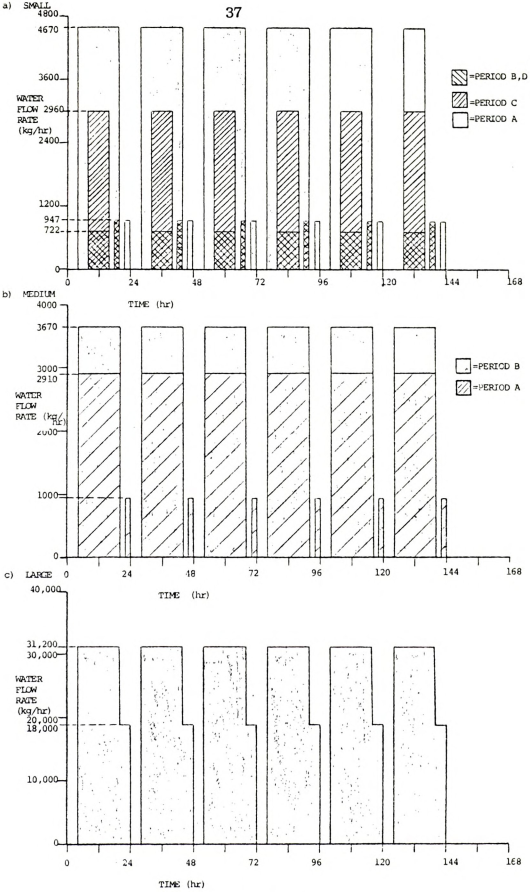

Figure 3.7a,b,c Fruit and Vegetable Processing Plant Water Demand Schedules.

The large plant, a canning plant, represents an extreme peak seasonal use pattern characteristic of many canning plants. This plant is specialized for processing one product for two months during the year as illustrated in Figure 3.7.

3.10 Economic Analysis

Two methods of analyzing solar energy systems described by Kreider and Kreith (1975) may be used to determine the economic feasibility. Solar and conventional energy costs are significant factors in determining overall feasibility.

3.10.1 Life cycle costing method

Life cycle costing is useful for observing the annual operation cost of an installation over its expected lifetime. The annual additional cost of a solar system can be calculated from:

$$C_h = (C_{h,\ tot})\ (CRF) \tag{3.12}$$

where C_h is the annual additional cost of solar system, $C_{h,tot}$ the total additional initial investment in the solar system, and CRF the capital recovery factor obtained from tables (Table C.6, Kreider and Kreith, 1975). The CRF factor is a function of annual interest rate and expected life of the system.

3.10.2 Cost effectiveness method

The method of cost effectiveness for solar systems illustrates the economic benefits of future increase in the cost of conventional energy sources. Equation (3.13) relates the future value of a present sum of money (Kreider and Kreith, 1975):

$$X = P\ (1 + i_{ann})^{t'} \qquad (3.13)$$

where X is the value of a future sum, P the present value of the sum, i_{ann} the annual interest rate, and t the period of years. Equation (3.14) gives the present worth (P) of an initial amount of money (P_o) paid annually for a period of t' years where the annual payment is increasing at an annual rate j.

$$P = P_o\ (1 + i_{eff})^{t'-1}/i_{eff}(1 + i_{eff})^{t'} \qquad (3.14)$$

The effective interest rate (i_{eff}) is given by:

$$i_{eff} = (1 + i_{ann})/(1 + j) - 1 \qquad (3.15)$$

Using these models the costs of solar energy utilization and conventional fuel sources may be compared.

3.10.3 Solar system costs

Collector component cost estimates were presented in 1975 dollars by Kreider and Kreith (1975). A double glass cover, selective surface collector costs 145 dollars per square meter including materials and a 35 percent overhead. Approximate costs of other system components were also shown as: 0.12 dollars per kilogram of water stored and 5.5 dollars per square meter of collector for pumps, piping, etc. A constant cost for controls and miscellaneous items should also be included.

3.10.4 Conventional energy costs

The present cost of energy to the consumer is dependent upon the geographic location, type of fuel, and method of conversion. Common conversion efficiencies presented by Fryling (1966) are necessary for estimating the energy costs. Current price ranges for three energy sources were chosen after discussion with commercial suppliers of oil, gas, and electricity: 3.5 to 4.5 cents per kilowatt hour for electricity, 0.10-0.13 dollars per kilogram for #2 fuel oil, and 3.20-4.25 dollars per 1000 cubic meters for natural gas.

4. METHODOLOGY

4.1 Insolation Test Models

The lack of insolation data necessary for solar energy simulation design at the chosen test locations has necessitated the construction of an insolation model for determining hourly insolation and air temperature data for computer simulation.

Five models for predicting hourly insolation and air temperature data were chosen for comparison with a control model which uses actual measured values of hourly insolation and air temperature. All five models use a constant air temperature obtained by averaging the hourly air temperatures over the 336-hour simulation period. For non-daylight periods for all test models, insolation was assumed zero with the ambient air temperature remaining constant. The five models are: the control model with constant temperature, the ASHRAE model using daily total insolation, the ASHRAE model using weekly averages of daily total insolation, the Whillier model, and the Transmissivity model. The model which best compares with the control model will be used for simulating long-term performance of the solar water heating system.

It was also desired to observe the effect of averaging insolation and air temperature data over periods greater than one hour. Hourly measured data was averaged for three and six hour periods and simulated together with the original hourly data for a period of 1000 hours. Although three, six and other average insolation data, excluding 24 hour averages (daily totals), are not readily available, the objective was twofold. First to examine the behavior of average data on the simulation results, and second, to observe the potential for interpolating daily total insolation data into three or six hour averages.

It should be stated that measured hourly insolation values are hourly averages of instantaneous insolation. The best possible method would be to use instantaneous data for input to a simulation. Since TRNSYS calculates transient responses over a designated time step, the input data need not be averaged over a period less than this time step in order to maintain the desired accuracy. TRNSYS uses a linear interpolation routine to calculate insolation at each time step. The error incurred by using hourly data compared to average data interpolated over the time step is thus minimized.

4.1.1 Control model

The control model was used for comparing the simulation results of the other insolation models. This model uses actual measured values of hourly insolation and air temperature for 1974 at the East Lansing test location, based on Eastern Standard Time. This data is also used to construct daily total insolation and the average air temperature for the period used in the other test models.

4.1.2 Control model with constant temperature

The purpose of this model was to determine the influence of air temperatures on system performance. Since the other insolation models use constant average air temperatures for the simulation period, the effect of constant average air temperature must be distinguished from that of actual air temperatures. The same temperature used with this model was used for all test models. The insolation data used for this model was the same hourly measured values used with the control model.

4.1.3 ASHRAE model using daily totals

Chapter 59 of ASHRAE (1974) contains tables of clear day insolation values based on solar time, for a given day and latitude. These tables were constructed to give maximum design values for designing a solar energy system. Hourly insolation values in this table are the same for morning and afternoon. The procedure consists of using the total and hourly insolation values taken on a horizontal surface at 40 degrees north latitude, interpolated according to the time of year of the control simulation to calculate a ratio of hourly insolation to daily total insolation for each daylight hour (Appendix A). Daily total insolation values were obtained by summing the hourly insolation values for each day of the simulation period. These totals were then multiplied by the ratios of hourly insolation and total insolation to obtain the simulated hourly values. The resulting data corresponds to solar time with the maximum value occurring between 11:30-12:30 during solar noon. Since the morning and afternoon ratios are the same, a symmetric insolation curve results, which is not realistic in the strictest sense since atmospheric conditions influence radiation intensities. The use of actual daily totals with this model tends to compensate for the clear day conditions on which these ratios are based. This method assumes the ratios remain constant for all atmospheric conditions. The validity of this assumption for use with modeling is questionable and can best be determined by simulation and comparison with actual insolation data results.

4.1.4 ASHRAE model using weekly averages

Weekly averages of daily total insolation data for 13 years in East Lansing are available from Baker and Klink (1975). To use this data, a model to construct hourly values from these weekly averages is needed. This ASHRAE model is similar to the one previously described except it uses weekly averages of daily insolation instead of daily totals to calculate hourly insolation. The daily total insolation values used in the first ASHRAE model are averaged over weekly periods and used as inputs to test this model. This model using the same ratios given in Appendix A, may be used to predict the hourly insolation values for an "average" year for all three test locations.

4.1.5 Whillier model

Whillier (1956) developed a set of curves relating the ratio of hourly insolation to daily total insolation and daylength for all types of atmospheric conditions. These curves are based on solar time. The maximum ratio occurs during the hours before and after solar noon (11:00-12:00 or 12:00-1:00). Since daylengths are necessary for determining these ratios, a computer program named SOLAR (Furnival et al., 1969) was used to obtain daylengths for the test periods. Appendix B contains a table of daylengths generated by this program for East Lansing

(1974). Using this table ratios were interpolated from the Whillier curves (Whillier, 1956) and given in Appendix C.

Using this information and daily insolation for the test periods, a data set similar to the ASHRAE data, was constructed and used in the test simulations.

The Whillier model also reflects the symmetry described for the ASHRAE models. Whillier (1956) showed that a difference exists between morning and afternoon insolation for areas exhibiting effects of industrial smoke or haze from mountain ranges. East Lansing exhibited none of these characteristics, and therefore any weighting of morning or afternoon insolation values was neglected.

4.1.6 Transmissivity model

The Transmissivity model uses values of weekly atmospheric transmissivity and hourly extraterrestrial radiation to predict hourly insolation. Thomas (1977) analyzed the 1974-75 radiation data at East Lansing and calculated weekly atmospheric transmissivity values based on hourly measured insolation and hourly extraterrestrial radiation data obtained from program SOLAR. These transmissivities are given in Appendix D. The SOLAR program was modified to calculate hourly extraterrestrial radiation corresponding to Eastern Standard Time. A listing of the modified program is given in Appendix E. A data file was then constructed for testing this model. The model may be extended to predict hourly insolation for the "average" year using data from Baker and Haines (1969).

4.2 Energy Demand Loads

Dairy, meat, and fruit and vegetable plant surveys of warm water usage were conducted by Dansbury (1977). Tables 3.2, 3.3, and 3.4 illustrate the results of these surveys. To incorporate this information into the simulation, TRNSYS requires a demand function indicating the water flow rates at different times of the day. Since all plants operated less than seven processing days per week and were different in their peak flows, a seven day cycle was used to establish the demand functions. Special consideration is given to the fruit and vegetable plants which operate in seasonal patterns.

Information was obtained concerning the number of shifts per day, working days per week, and time spent for processing cleaning operations. From this information, functions were developed describing the periods of warm water use. Figures 3.5, 3.6, and 3.7 show the scheduling used in the simulations for the dairy, meat, and fruit and vegetable processing plants, respectively. These figures along with Tables 3.2, 3.3, and 3.4 adequately describe the amount, temperature, and distribution of water usage. Each simulation period begins according to these functions and cycles every seven days. These schedules primarily constitute a daily cycle corrected by accounting for the slack weekend period.

Dairy and meat plants both exhibit a constant demand cycle during the year. Fruit and vegetable plants, as shown in Figure 3.7, present a vastly different situation compared to the dairy and meat plants. Unless the plant is widely diversified, as the medium plant was in this survey, the fruit and vegetable plants generally reflect a strong seasonal dependence for their processing and energy consumption patterns together with much higher water flow rates and temperature requirements.

Since periods of highest production occur during periods of higher insolation, solar energy appears to be well suited to these plants. The economics of plants with only summer period energy demand depend upon finding a full-time use for or a storage system to collect the off season energy.

Simulation runs were conducted on these plants in a slightly different manner. During the off production periods for the small and large plants the solar energy system was assumed to produce heat for space heating of warehouses and offices. Actual simulation runs for space heating were not performed. Estimates based on simulation runs made during processing were used to evaluate the total energy contribution made by the solar system for economic considerations.

4.3 Physical Solar Water Heating System Design

A simple solar water heating concept is employed in this study to determine the contributions that solar energy can make to decrease the fossil fuel energy consumption of the food industry. It should be recognized that new solar energy technology is constantly being developed in areas of collection, storage, and construction materials. The solar water heating system presented attempts to represent the state of the art for the design of flat plate collectors and other system components.

The physical system considered is represented by Figure 3.4. Due to overall climatic conditions in the midwest region the system was designed for cold weather operation. South facing selective surface flat plate collectors with a variable tilt angle were assumed. The collector fluid was chosen to be an anti-freeze solution in order to prevent freezing damage to the collectors during periods of off operation. Double glazed, insulated collectors compatible with cold weather operation were chosen.

The collector fluid is pumped through a closed loop consisting of a collector and counterflow heat exchanger. A second loop uses water to remove the energy from the heat exchanger for storage in a tank to be delivered to the load. The proposed storage tank is insulated and located inside of a building maintained at constant temperature. Water is pumped between the heat exchanger and storage tank by a separate pump. The tank capacity and pump capacities were chosen based on system parametric tests. The storage tank will hold approximately twice the daily demand volume for the plant. System operation is controlled by an on/off thermostatic controller which senses the difference between the collector plate temperature and storage tank temperature. The controller turns the pumps on when the collector temperature becomes greater than the storage tank temperature. Warm water delivered by the system leaves the storage tank and passes through an auxiliary heater which, if needed, raises the water to the desired temperature. Replacement water is supplied directly to the storage tank from the main water supply at a constant temperature.

This system can be readily modeled by TRNSYS. Other system configurations can also be devised depending upon specific plant requirement for warm water recycling, removal of heat exchanger, or inclusion of other components such as a heat pump. These other considerations will not be analyzed in the basic study of the processing plants.

4.4 System Modeling

With the basic solar water heater concept established, a matching computer simulation model was developed with TRNSYS. An illustration of the subroutines used and the pattern of information flow is given in Figure 4.1. A sample control card deck and output results are given in Appendix F. Changes, made to the control card deck, when simulating different plants were accomplished by changing values on the parameter cards of selected routines.

There are thirteen subroutines together with the main executive program used in these simulations. Seven of these units correspond to physical system components, while the other six involve the manipulation of input and output data necessary for modeling. Each routine, as shown in Figure 4.1, is identified by a unit number. This number is used internally by TRNSYS to identify the variables and allow for communication and information flow between the executive program and each subroutine.

Each input, output, and parameter is organized specifically for each subroutine and is identified in the TRNSYS manual. The function and purpose of the pertinent units will be discussed in detail. All of the routines are interconnected. Therefore, units will be described according to their approximate order of appearance. For complete discussion of the facilities and necessary considerations for using TRNSYS, the operation manual should be consulted (Klein, 1974).

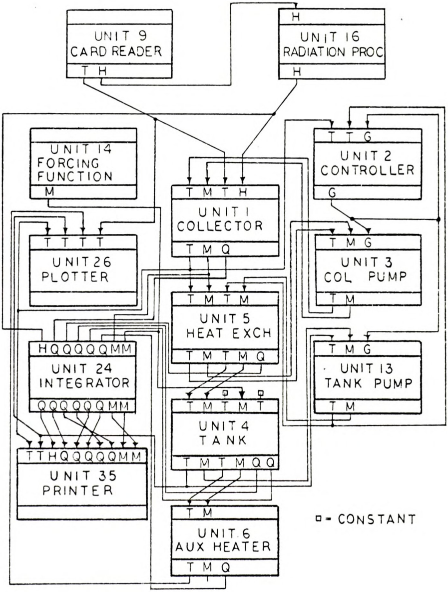

Figure 4.1 Subroutine and Information Flow Diagram of the TRNSYS Solar Water Heating Model.

4.4.1 Simulation considerations

The execution procedure used by TRNSYS consists of calculating the variables of all the units during a given time step and then proceeding to the next time step, repeating the process using the values calculated during the previous time step. Some variables are common to more than one unit. The overall behavior of the system is represented by a set of algebraic and/or differential equations. During a given time step, TRNSYS iterates among the units until the variables converge to within a specified tolerance from their value of the previous interation. The magnitude of the tolerance is set in the control card deck by the TOLERANCES card. The smaller the tolerance the more iterations necessary to achieve convergence, the more compute time required, and the more accurate the results. After a set number of iterations, if the tolerances are not satisfied, TRNSYS will execute the next time step with the values of the variables at the last iteration regardless of their convergence status. If this happens repeatedly, the simulation will terminate in error. The number of iterations allowed is set by the LIMITS card. The size of the time step has a significant effect upon the calculation effort, accuracy, and allowable tolerances. The choice of the time step and tolerances is dependent upon the type of system being simulated. Units containing sets of differential equations generally require a smaller time step and a larger tolerance than a system modeled by algebraic equations.

The values used in this study were selected as a compromise between compute time and accuracy requirements. A time step of 0.2 hours and a tolerance of 0.1 were used for all plant simulations. Preliminary work used for selecting these values indicated that the stratified storage tank unit would not operate satisfactorily under these restraints. In light of the multitude of simulation runs to be made and the resulting computer time required, it was decided to exclude the use of a stratified storage tank. The result of this decision is that the output data represent a conservative behavior of the solar system with respect to the amount of energy delivered by the storage tank.

To simulate the solar water heating system for 336 hours approximately 30 seconds of CP time were required, at a cost of $2.50. For simulating an entire year of 8712 hours approximately 760 seconds of CP time were required at a cost of about $62.00. Stability requirements were generally satisfied. Exceptions occurred when an input data point was in error or during rapid changes in the input insolation data. For these cases the iteration limit would be exceeded for that time step and TRNSYS would execute to the next time step, and display a warning message. The occurrences were infrequent and introduced no significant error into the final results.

4.4.2 Card reader

Unit 9 is a card reader routine used to read input temperature and insolation data at a designated time interval from the input file. Since the input variable units of existing data files are degrees Fahrenheit and Langleys per hour, a unit conversion technique is used to convert these values to degrees Celcius and kilo-Joules per hour per square meter, respectively. This unit also performs a linear interpolation on the given input data to provide appropriate values corresponding to the specified simulation time step.

This unit supplies input data of hourly ambient air temperature to the collector, unit 1, and measured horizontal insolation to the solar radiation processor, unit 16.

4.4.3 Radiation processor

Unit 16 is a solar radiation processing routine which converts the input total horizontal measured insolation to total radiation incident on a tilted collector surface. This routine may operate in one of several modes depending upon the type of input radiation data and the method of calculating amounts of direct and diffuse radiation. The techniques used are described in detail by Liu and Jordan (1960). For this study it is assumed that the diffuse radiation originated near the sun which is most accurate for clear day conditions. This unit supplies input insolation data to the collector, unit 1.

4.4.4 Flat plate collector

The collector routine, unit 1, also has multiple modes of operation. In this study the collector loss coefficient (U_l) and total transmittance (τ) are assumed to remain constant. Other modes consider these parameters as functions of collector temperature and radiation incidence angle. All simulations use the same collector design parameters with exception of collector area.

The collector unit requires four inputs. The first two, fluid inlet temperature and flow rate, come from the collector pump, unit 3.

The third input, ambient air temperature comes from the card reader, unit 9. The fourth input is total incident radiation striking the collector, and comes from the radiation processor, unit 16.

From the information of temperatures, collector flow rate, insolation, and the collector loss coefficient an energy balance is made on the collector. This analysis yields a value for the net energy collected. This value is then used to calculate the collector fluid exit temperature.

There are three outputs from unit 1. The first and second are fluid exit temperature and flow rate. These variables are used as inputs to the heat exchanger and thermostatic controller. The third output is the total energy collected during the time step; this variable is integrated and printed out periodically so collector performance can be evaluated.

4.4.5 Controller

The thermostatic controller, unit 2, determines when the collector system operates by sensing the temperature difference between the collector outlet fluid and the storage tank. In order to maintain system stability this unit contains a feedback hysteresis characteristic to eliminate the possibility of repeatedly switching the system on and off. The parameters needed are upper and lower dead band temperature differentials to control the degree of hysteresis. The output of this unit is a control variable, either on (1) or off (0), which is sent to the collector and heat exchanger pumps. The control output function is also used as an input to unit 2, thus acting as a feedback variable to indicate the status during the previous time step.

4.4.6 Heat exchanger

Unit 5 is a zero capacitance heat exchanger model capable of modeling crossflow, parallel flow, counterflow or constant effectiveness heat exchangers. The counterflow mode was used in this system to allow for maximum heat transfer characteristic of this design. The overall heat transfer coefficient (UA) is used to calculate heat exchanger effectiveness for each time step. From this value, the fluid exit temperatures are determined from the flow rates and inlet temperatures. Inputs to this unit are the fluid temperature and mass flow rates from the collector, unit 1, and the tank pump, unit 13, respectively. Five outputs are utilized from this routine. The warm side fluid temperature and flow rate is input to the collector pump, unit 3. Cold side fluid temperature and flow rate pass directly to the storage tank, unit 4. The fifth output is the total heat transferred during the time step and is integrated and printed out in the results.

4.4.7 Pumps

The system contains two pumps, one for the collector fluid, and another for the heat exchanger-storage tank loop. These routines are simple on/off components controlled by the controller, unit 2. Maximum mass flow rates are specified parameters, and whenever the pump is operating, this flow rate is used. There is no temperature change of the fluid in either pump when the fluid passes through. Temperature inputs and outputs are used only to maintain uniformity in the information flow process. Inputs to the collector pump come from the warm side of the heat exchanger, unit 5, and the controller, unit 2. Inputs to the tank pump, unit 13, are from the storage tank, unit 4, and the controller, unit 2.

4.4.8 Storage tank

The storage tank component is identified as unit 4. This study assumes an unstratified storage tank. The routine has the capacity to model a stratified storage tank for determining water temperature at different heights in the tank. The modeling of such a storage tank involves the solving of a set of simultaneous differential equations. Because of stability problems caused by the choice of time step and the extra computer time required, it was decided to use an unstratified storage tank. Since the volumes of water used in processing plants are large, the accuracy of using a stratified model is suspected.

Inputs to the tank are fluid temperature and flow rate from the heat exchanger, unit 5, and a constant temperature and variable flow rate of the replacement fluid as determined by a forcing function routine, unit 14.

The tank is insulated and assumed to be full at all times. An energy loss coefficient (U) must be specified for determining tank losses. Tank volume and height are specified parameters. Given the loss coefficient, the model calculates the area of the tank, assuming a cylindrical shape, to determine the total environmental heat loss for the time period. An energy balance is made on the tank and accounts for energy delivered from the heat exchanger, delivered to the load, and lost by conduction from the tank to its surroundings. The energy lost and the total energy delivered by the tank to the load are outputs of the unit and are integrated and included in the simulation results. Other outputs of this unit are the fluid inlet temperature and flow rate to the heat exchanger, unit 5, and fluid temperature and flow rate to the auxiliary heater, unit 6.

4.4.9 Auxiliary heater

An auxiliary heating component, unit 6, is included for determining the amount of energy needed to supply the total demand when the solar collector system cannot meet the load. This is an on/off component routine controlled by an internal thermostat set at the desired constant demand temperature. Inputs to the unit are water temperature and mass flow rate from the storage tank, unit 4. The auxiliary heater adds energy to the water to bring it up to the minimum supply temperature. If the inlet temperature is greater than the heater temperature setting, the outlet temperature is set equal to the inlet temperature. For these cases the water supplied to the load is warmer than necessary. This condition is not allowed for in the model, since the flow rates, controlled by the forcing function, determine the system energy demands. Allowances for this condition are made in the analysis and discussion. The outputs of unit 6 are fluid temperature, fluid flow rate and energy added to the water. The energy is integrated for the entire simulation period and given in the results.

4.5 Design Parameters

Each unit has one or more parameters which need to be established prior to simulation. These parameters are discussed for each component in the system. In two cases, parametric test runs were conducted to determine the best parameter for the processing plant simulations. Table 4.1 gives a summary of the necessary parameters and their SI units.

4.5.1 Radiation processor

The solar radiation processor, unit 16, requires seven parameters. Mode is the first and is equal to 1. The second parameter is the day of the year at the start of the simulation. Table 4.2 illustrates the day of the year for which each simulation begins together with the approximate duration of the simulation. Latitude is the third parameter. Values for latitude taken from Baker and Klink (1975) are 42° 42' for East Lansing, 38° 58' for Columbia, and 39° 44' for Indianapolis. Collector tilt angle, measured from the horizontal is the fourth parameter. Kreider and Kreith (1975), generally recommend an annual optimum tilt angle for residential water heating, equal to the latitude. Latitude plus 15 degrees is accepted as best for annual residential space heating. The design of this solar water heater was assumed to have the capability of varying the collector tilt. Since no accepted rule exists for best tilt angles to use at different periods, an assumption was made. The collector tilt angle was assumed to be optimum when calculated as the complement angle of the solar altitude calculated at 15 degrees from local solar noon averaged over the period of the simulation.

Table 4.1 - Summary of Simulation Parameters and Their SI Units.

Radiation Processor - Unit 16			
Parameter:	1	Mode	integer
	2	Day of the year at beginning of simulation	integer
	3	Latitude	degrees
	4	Collector tilt angle from horizontal	degrees
	5	Collector southern orientation	degrees
	6	Solar constant	kJ/m^2 hr
	7	Ground reflectance	decimal
Collector - Unit 1			
Parameter:	1	Mode	integer
	2	Collector surface area, A	m^2
	3	Collector geometric efficiency factor, F'	decimal
	4	Specific heat of collector fluid	kJ/kg C
	5	Collector plate absorptance	decimal
	6	Collector overall loss coefficient	kJ/m^2 hr C
	7	Total cover transmittance	decimal
Controller - Unit 2			
Parameter:	1	Stick control	integer
	2	Upper dead band temperature	C
	3	Lower dead band temperature	C
Pump - Units 3 and 13			
Parameter:	1	Maximum fluid mass flow rate	kg/hr
Heat Exchanger - Unit 5			
Parameter:	1	Mode	integer
	2	Overall heat transfer coefficient, UA	kJ/hr C
	3	Specific heat of warm fluid	kJ/kg C
	4	Specific heat of cold fluid	kJ/kg C
Storage Tank - Unit 4			
Parameter:	1	Volume	m^3
	2	Tank height	m
	3	Specific heat of storage fluid	kJ/kg C
	4	Mass density of fluid	kg/m^3
	5	Overall loss coefficient, U	kJ/m^2 hr C
Auxiliary Heater - Unit 6			
Parameter:	1	Maximum heating rate	kJ/hr
	2	Minimum supply temperature	C
	3	Dead band temperature	C
	4	Specific heat of fluid	kJ/kg C

Table 4.2 - Starting Day of Simulations.

Data Source	Season	Duration	Day of Year	Comments
East Lansing, 1974	spring	2160	60	medium dairy
		500	131	small F & V
	summer	2160	152	medium dairy
		2160	172	small F & V
			213	all F & V plants
1965	fall	2160	244	medium dairy
		336	244	all plants
		2160	273	small F & V
	winter	2160	334	medium dairy
Columbia, 1949, 52	spring	2160	57	medium dairy
		500	131	small F & V
	summer	2160	146	medium dairy
		2160	172	small F & V
			213	all F & V plants
	fall	2160	238	medium dairy
		336	244	all plants
		2160	273	small F & V
	winter	2160	330	medium dairy
Average Year	spring	2160	60	medium dairy
	summer	2160	152	medium dairy
	fall	2160	244	medium dairy
	winter	2160	334	medium dairy

Equation (3.7) was used to calculate the altitude angle with H_s equal to 15 and declination values interpolated from ASHRAE (1974). Ground reflectance was assumed to be zero.

4.5.2 Collector

The collector, unit 1, requires seven parameters. The first parameter, collector mode is equal to 1. The second parameter, collector area, measured in square meters, is of primary importance in the design of the appropriate system size for each food processing plant. This parameter is used to scale storage tank volume, pump flow rates, and heat exchanger capacity. The initial collector areas to be simulated were chosen based on preliminary simulations according to the total daily energy requirement of the processing plant. A method was needed for selecting proper collector areas to simulate for each processing plant. It was desired to make runs which would result in a solar contribution to the total demand, in the range of 30 to 80 percent. Several preliminary runs were used to determine an approximate ratio of collector area to energy supplied to use as guideline for selecting collector areas to simulate. The resulting ratios were: 245 square meters of collector per million kiloJoules would supply approximately 70 percent of the demand, and 62 square meters of collector per million kiloJoules would supply approximately 30 percent of the demand. Using these criteria, the following rule was used to establish the collector areas to be simulated: the largest initial area was determined by taking the total daily energy demand in millions of kJ and multiplying it by 245, the smaller area was determined by using a factor of 62. For some cases of the fruit and vegetable plants, a smaller collector area was chosen because of the limited use characteristics of the plant. Table 4.3 summarizes the collector areas used in the food processing plant simulations.

The fourth parameter is the specific heat of the collector fluid. A value of 2.386 kJ/kg C for ethylene glycol at 20 degrees C was obtained from Holman (1972). The fifth parameter is the collector plate absorptance. A selective absorber surface approximating lampblack in epoxy was chosen based on Table 5.5.1 of Duffie and Beckman (1974). An absorptance of 0.9 was estimated for long term collector performance. The seventh parameter, cover transmittance, was taken from Figure 6.2.1 in Duffie and Beckman (1974) for a collector with two glass covers exhibiting a thickness-extinction coefficient product of 0.0125 per sheet, at an average incidence angle of 20 degrees. The figure shows a transmittance of 0.833 allowing for reflection and absorption. This value was held constant during all simulation runs.

The sixth parameter, collector loss coefficient (U_1), was determined according to the method described by Klein (1974). This method, discussed in Chapter 3, uses equations (3.8), (3.9), (3.10), and (3.11). The top (Q_t), edge (Q_e), and back (Q_b) heat losses are calculated for a given collector design. For this analysis a collector with the following properties was assumed: collector dimension of 2x2 meters, surface area (A) of 4 square meters, edge perimeter (A_p) of 8 meters, two glass covers, absorber plate emissivity (ε_p) of 0.95, average plate temperature (T_p) of 85 degrees C, ten centimeters of back insulation with a resistance of 0.697 kJ/m^2hr C. The following ambient conditions were assumed: wind speed of 10 m/s and an ambient air temperature of 10 degrees C. Values for the edge and back heat transfer coefficients were taken as

Table 4.3 - Summary of Collector Areas Choosen for Testing (collector area in square meters).

Scale:	a	b	c	d	e
Small Dairy	25	40	65	100	
Medium Dairy	80	140	200	330	
Large Dairy	400	700	1000	1600	
Small Meat	35	65	100	150	
Medium Meat	80	140	200	320	
Large Meat	600	1050	1600	2400	
Small F & V	670	1340	2340	3340	5365*
Medium F & V	525	1050	1850	2650	4200*
Large F & V	4015	8030	14050	20070	32100*

*for East Lansing location only

1.8 kJ/m hr C and 45.0 kJ/m^2hr C, respectively, as recommended by Klein (1974). This results in a collector top loss coefficient of 15.8 kJ/m^2hr C using Figure 7.4.c from Duffie and Beckman (1974). Equation (3.9) was used to calculate the top heat loss. The edge loss (Q_e) was calculated as 1080 kJ/hr from equation (3.11) and a back loss (Q_b) of 21 kJ/hr from equation (3.10). A resulting overall loss coefficient of 20 kJ/m^2hr C was calculated using equation (3.8). This value was assumed constant for all simulations.

The collector efficiency factor, F', the third parameter, is important for describing collector performance. The determination of this value is dependent upon detailed collector design such as: bond conductance, tube spacing, etc. Figures 7.5.4b,c from Duffie and Beckman (1974), were used to choose a typical value. Using a collector loss coefficient of 20, a plate conductivity thickness product (k) of 0.4 and a tube spacing of 12 centimeters, an efficiency factor of 0.95 was estimated for use in all simulations.

4.5.3 Heat exchanger

The heat exchanger unit requires four parameters: mode, specific heats of the cold and warm fluids, and the overall heat transfer coefficient, UA. Mode 2, the counterflow type, was used. The specific heat of the cold side water was taken as 4.186 kJ/kg C, and 2.386 kJ/kg C for the warm collector fluid.

The overall heat transfer coefficient for the exchanger was chosen based upon a design assumed for a given system capacity in a preliminary run. Preliminary analysis showed an approximate daily usage of 500,000 kJ/day for a small dairy plant. Assuming the collector operated 5 hours per day, a heat transfer rate in the heat exchanger has to be 100,000 kJ/hr. An average temperature difference across the heat exchanger of 5.6 degrees C, based on recommendations for the design of heat transfer equipment from Jennings (1970), was used to obtain an overall design heat transfer coefficient from the following relation:

$$Q = UA \, \Delta T \tag{4.1}$$

UA was found to be 19,000 kJ/hr C. This value was standardized with a collector area of 100 m^2. The resulting ratio of 190 kJ/hr C per square meter of collector was used to determine the heat exchanger capacities for other processing plants.

4.5.4 Tank pump

The tank-heat exchanger pump, unit 13, requires a maximum flow rate specification. The choice of this value relates to the determination of the heat exchanger capacity. In order to remove 100,000 kJ/hr at 5.6 degrees C from the heat exchanger, the fluid flow rate is restricted by equation (3.6). The maximum flow rate calculated was 4540 kg/hr. This parameter was also standardized for a collector area of 100 m^2. A ratio of 45.4 kg/hr per square meter of collector area was used to determine the proper pump size relative to the other units when simulating different size systems.

4.5.5 Collector pump

The collector pump, unit 3, also requires a flow rate specification. Initially in preliminary runs this value was set equal to the tank pump flow rate. This parameter was desired to be partially optimized for a system size of 100 m^2 of collector with a load for the small dairy, in order to allow for actual operational characteristics of the system during simulation. Five collector pump flow rates were tested for collector performance, ranging from 1135 to 5675 kg/hr. From these results a collector pump flow rate to collector area ratio of 34.11 kg/hr per square meter of collector was obtained and used to scale collector flow rates for the processing plant simulations.

4.5.6 Storage tank

Five parameters: tank volume, tank height, specific heat of the storage fluid, mass density of fluid, and heat loss coefficient, are required for unstratified storage tank operation. For simulating different size systems a ratio of tank volume to collector area was needed for proper scaling.

The tank volume ratio was chosen from parametric test simulations based on the tank size which supplied the greatest percentage of energy to the load. Sizes, ranging from 1.89 to 11.36 m^3, were tested. A final ratio of 0.03785 m^3/m^2 of collector was used for scaling processing plant simulations.

The tank height specification was based on approximate dimensions of commercially available steel tanks. Where large tanks were needed the tank height was assumed to be 4 meters. A height of 2 meters was chosen for the smaller tanks. These specifications were chosen somewhat arbitrarily since actual tank design depends upon available space, etc., at each plant.

The specific heat and mass density for water was specified as 4.186 kJ/kg C and 1000 kg/m^3, respectively. The loss coefficient for the tank was taken constant for all simulations. Eight centimeters of fiber insulation was assumed with a resulting loss coefficient, including film resistance, of 6.96 kJ/m^2C. This loss could be decreased by the addition of more insulation.

4.5.7 Auxiliary heater

The auxiliary heater requires the specification of fluid specific heat, minimum temperature, and maximum heating rate. The temperature settings, corresponding to the type of processing plant being simulated, were obtained from Tables 3.2, 3.3, and 3.4. Using these temperatures and the maximum flow rate for each plant, the maximum heating rate was calculated using equation (3.6), assuming the auxiliary heater supplied 100 percent of the demand. This condition allows for total system reliability if the solar energy system fails.

4.6 Simulation Periods

This study deals with simulating a solar water heating system for 2 parametric tests, 9 insolation model tests, 9 energy demand loads, 3 geographic locations, 4 seasons, 5 years, varying durations, and at least 4 different collector areas for each demand load. Because of the number of simulations and complexity in identifying each simulation the following method was developed to accurately describe each simulation run.

Each simulation is identified by a code containing information relating to the type of plant, time of simulation, etc. Table 4.4 gives the legend which describes the meaning of each category. Each code contains 8 symbols which identify the: group, type, location, year, season, model, period, and scale for each simulation.

Runs are classified in one of eight groups labeled A through H. Group A includes all hourly insolation test model simulations. Group B contains the simulations performed on the hourly average test models. Group C contains parametric test simulations for storage tank size determination. Group D contains parametric tests simulations of collector flow rate determination. Groups E, F, and G contain simulations for the three food processing plants: dairy, meat, and fruit and vegetable, respectively. Group H contains simulations for the "average" year.

Each group is identified according to plant type. Three plant types are outlined: S for small, M for medium, and L for large. Not every type is specified for each group. This is also true for other classifications. For example, Group A simulations were only performed on a small dairy plant. There were no Group A simulations for a medium or large plant.

The location identifier describes the geographic location corresponding to the data used in the simulation. For each type there are three possible location specifications: 1 represents East Lansing

Table 4.4 Legend for Simulation Identification.

Group:	A - Insolution Test Models
	B - Hourly Average Tests
	C - Storage Tank Parametric Tests
	D - Collector Fluid Flow Rate Parametric Tests
	E - Dairy Processing Plants
	F - Meat Processing Plants
	G - Fruit and Vegetable Plants
	H - "Average" Year Tests
Type:	S - Small size plant
	M - Medium
	L - Large
Location:	1 - East Lansing (Michigan)
	2 - Indianapolis (Indiana)
	3 - Columbia (Missouri)
Year:	49 - 1949
	52 - 1952
	65 - 1965
	74 - 1974
	A - "Average" year according to Baker and Klink (1975)
Season:	SP - Spring beginning March 1
	SU - Summer beginning June 1
	FA - Fall beginning September 1
	WI - Winter beginning November 30
Model:	K - Control model using measured hourly insolution data
	L - Control model using constant air temperature
	M - ASHRAE model using daily total insolution inputs
	N - ASHRAE model using weekly average daily insolution
	O - Whillier model
	P - Transmissity model
	Q - 1 hour average model
	R - 3 hour average model
	S - 6 hour average model

Table 4.4 (Continued) Legend for Simulation Identification.

Period:	336 hours
	1000 hours
	2160 hours
	etc.
Scale:	a - Smallest system size or parameter specification for the period
	b - next smallest
	c - etc.
	d -
	e - Largest system size or parameter specification

(Michigan), 2 for Indianapolis (Indiana), and 3 for Columbia (Missouri).

The year classification indicates the year the input data was recorded. Corresponding to each location classification there may be five year specifications: 65 representing the year 1965, 74 for 1974, 49 for 1949, 52 for 1952, and A for the "average" year.

The season classification indicates the time of year the simulation takes place. There may be four season classifications for each year: SP representing spring, SU for summer, FA for fall, and WI for winter.

The model specification indicates the origin of the input insolation data. There are 9 models, K through S, which may be used for each season: Model K is the basic control model which uses measured hourly values of insolation and air temperature, L is the control model which uses constant air temperatures, M is the ASHRAE model which uses daily total insolation, N is the ASHRAE model which uses weekly averages of daily total insolation, O is the Whillier model, P is the Transmissivity model, Q is the 1-hour average model, R is the 3-hour average model, and S is the 6-hour average model.

The duration of each simulation is identified by the period specification. The number of hours for each simulation is equal to the numerical value of the period specification. Most simulations were 336, 1000, or 2160 hours long. Thus following each model specification the period is specified: 336,1000,2160, etc.

Finally, a description of system size is identified by the scale specification. This specification describes the parameter variations of collector area, collector flow rate, etc., occurring for each period. Up to five scale specifications may be given for each period as follows: a,b,c,d,e. Scale "a" indicates the smallest and scale "e" the largest collector area, etc., for each period.

Each category is always specified for each simulation run to eliminate confusion. Some repetition exists in the description of models, types, etc. For the purpose of completeness, this repetition is tolerated. All simulations use the same solar water heater configuration as discussed under the System Modeling section. Two examples are given to illustrate the use of this method.

Example One: A:S:1:74:SP,SU:K,N:336:d

This code describes 4 simulation runs: an insolation model test (A) for the small plant (S) at the East Lansing location (1) in 1974 (74) for two seasons, spring (SP) and summer (SU), for models using hourly measured insolation (K), and ASHRAE weekly model (N) for a simulation time period of 336 hours with a collector area of 100 m^2 (scale d).

Example Two: G:M:3:49:FA:K:336:a,b,c,d

This code describes 4 simulation runs: a fruit and vegetable plant (G) of medium size (M), at the Columbia location (3), occurring in 1949 (49), during the fall (FA) using actual measured insolation data (K), for a period of 336 hours for four different collector sizes (a,b,c,d).

4.6.1 Insolation modeling - Group A

Four time periods, to observe seasonal influences, of 336 hours each were used to test the validity of the 5 hourly insolation models with the control during 1974 at East Lansing, Michigan. The four periods started on March 1, June 1, September 1 and November 30. These test runs were performed for a small dairy demand with a higher heater temperature than shown in Table 3.2. A collector area of 100 m^2 was used. Table 4.5 describes the parameters and total energy demand for each run in this group.

4.6.2 Hourly averages - Group B

Group B simulations compare the effect of averaging insolation data on the simulation results. Three runs were made of 1000 hours each beginning March 1, 1974 at East Lansing, Michigan. A demand function for a small dairy plant was used with a collector area of 80 m^2. Table 4.6 illustrates the parameters used in these runs.

4.6.3 Storage tank tests - Group C

Two time periods of 336 hours beginning June 1 and November 30 for 1974 at East Lansing, Michigan were used to evaluate storage tank parameter selection. Five storage tank sizes ranging from 1.892 to 11.36 m^3 were tested. Table 4.7 illustrates the conditions used for these simulations.

4.6.4 Collector fluid flow rate tests- Group D

Simulations for optimizing collector flow rate were performed for the same conditions as the storage tank tests. The collector flow rates

Table 4.5 Group A Simulations: Insolation Test Models.

- Type: S
  - Location: 1
    - Year: 74
      - Season: SP
      - Model: K
      - Period: 336
      - Scale:

	d
Collector area[1]	100.0
Tilt angle[2]	49.9
Ambient air temperature[3]	variable
Collector fluid flow rate[1]	4540
Heat exchanger coefficient[1]	190.000
Exchanger pump flow rate[1]	4540
Storage volume[1]	7.57
Tank height[1]	6.0
Supply water temperature[1]	10.0
Heater capacity[1]	105,000
Heater temperature[1]	68.33
Demand flow-weekly[1]	5820
Energy demand - total[1]	2.842×10^6

- Models: L, M, N, O, P
- Period: 336
- Scale:

	d
Ambient air temperature[3]	3.5

- Season: SU
- Model: K
- Period: 366
- Scale:

	d
Tilt angle[2]	24.3
Ambient air temperature[3]	variable

- Season: SU
- Models: L, M, N, O, P
- Period: 336
- Scale:

	d
Ambient air temperature[3]	19.17

Table 4.5 Group A Simulations: Insolation Test Models (Continued).

Season: FA
Model: K
Period: 336
Scale:

	d
Tilt angle[2]	39.0
Ambient air temperature[3]	variable

Season: FA
Models: L, M, N, O, P
Period: 336
Scale:

	d
Ambient air temperature[3]	16.11

Season: WI
Model: K
Period: 336
Scale:

	d
Tilt angle[2]	65.9
Ambient air temperature[3]	variable

Season: WI
Models: L, M, N, O, P
Period: 336
Scale:

	d
Ambient air temperature[3]	-1.56

---

[1]Constant for group

[2]Constant for season

[3]Constant for model(s)

Table 4.6 - Group B Simulations: Hourly Average Tests.

Type: S - Small Dairy

Location: 1 - East Lansing

Year: 74

Season: SP

Models: Q, R, S

Period: 1000

Scale:

	<u>a</u>
Collector area	80
Tilt angle	50
Ambient air temperature	variable
Collector fluid flow rate	4540
Heat exchanger coefficient	19,000
Exchanger pump flow rate	4540
Storage volume	9.46
Tank height	3.6
Supply water temperature	10.0
Heater capacity	105,000
Heater temperature	74.0
Demand flow - bi-daily	3240
Energy demand - bi-daily	8.68×10^5
Energy demand - Total	1.823×10^7

Table 4.7 - Group C Simulations: Storage Tank Tests.

Type: S

Location: L

Year: 74

Season: SU

Model: K

Period: 336

Scale:	a	b	c	d	e
Collector area[1]	100				
Tilt angle[2]	30				
Ambient air temperature[1]	variable				
Collector fluid flow rate[1]	4540				
Heat exchanger coefficient[1]	19,000				
Exchanger pump flow rate[1]	4540				
Storage volume[1]	1.892	3.785	5.680	7.57	11.36
Tank height[1]	6.0				
Supply water temperature[1]	10.0				
Heater capcity[1]	105,000				
Heater temperature[1]	68.33				
Demand flow-weekly[1]	5820				
Energy demand-total[1]	2.842×10^6				

Season: WI

Model: K

Period: 336

Scale:	a
Tilt angle[2]	60.0

---

[1]Constant for group

[2]Constant for season

tested ranged from 1135 to 5675 kg/hr in the summer and 1135 to 4540 kg/hr in the winter. Table 4.8 presents the specific conditions and periods for these runs.

4.6.5 Dairy plants - Group E

A two-week period starting September 1 was chosen to simulate all dairy plants for two years (65,74) at East Lansing, Michigan and two years (49,52) at Columibia, Missouri. Indianapolis insolation data was not available for simulation. These simulations serve as a base for comparing the performance of different sizes and types of plants for a given year. Each plant was simulated for 4 collector sizes. The medium dairy plant at one collector size (140 m^2) was chosen to simulate for an entire year (1974) at East Lansing, Michigan, and for 2 years (1949, 1952) at Columbia, Missouri. This is the only plant which was simulated for an entire year. Annual performance of all other plants was projected from the results of these annual runs. The annual runs were broken into 4 periods of 2160 or 2184 hours each. The purpose for this was to facilitate the changing of the collector tilt angle.

Table 4.9 describes in detail the parameters and energy demands for each dairy plant simulation.

4.6.6 Meat plants - Group F

All meat plants were simulated for 4 collector sizes at the two-week September period for 2 years (65,74) at East Lansing, Michigan and 2 years (49,52) at Columbia, Missouri. The annual operation of these

Table 4.8 - Group D Simulations: Collector Flow Rate Tests.

Type: S

Location: 1

Year: 74

Season: SU

Model: K

Period: 336

Scale:

Collector area[1]	100
Tilt angle[2]	30
Ambient air temperature[1]	variable
Collector fluid flow rate[1]	1135
Heat exchanger coefficient[1]	19,000
Exchanger pump flow rate[1]	4540
Storage volume[1]	7.57
Tank height[1]	6.0
Supply water temperature[1]	10.0
Heater capacity[1]	105,000
Heater temperature[1]	68.33
Demand flow-weekly[1]	5820
Energy demand-total[1]	2.842×10^6

Season: WI

Model: K

Period: 336

Scale:

	a
Tilt angle[2]	60.0

---

[1]Constant for group

[2]Constant for season

Table 4.9 -Group E Simulations: Dairy Plants.

Type: S

Location: 1

Years: 65, 74

Season: FA

Model: K

Period: 336

Scale:

	a	b	c	d
Collector area[2]	25	40	65	100
Tilt angle[3]	39.0			
Ambient air temperature[1]	variable			
Collector fluid flow rate[2]	853	1364	2217	3411
Heat Exchanger Coefficient[2]	4750	7600	12,350	19,000
Exchanger pump flow rate[2]	1135	1816	2951	4540
Storage volume[2]	0.946	1.514	2.460	3.785
Tank height[2]	2.0			
Supply water temperature[1]	12.78			
Heater capacity[2]	170,000			
Heater temperature[2]	65.53			
Demand flow-weekly[2]	5820			
Energy demand-total[2]	2.57×10^6			

Location: 3

Years: 49, 52

Season: FA

Model: K

Period: 336

Scale:

	b
Tilt angle[3]	37.5

Type: M

Location: 1

Years: 65, 74

Season: Fa

Model: K

Period: 336

Table 4.9 - Group E Simulations: Dairy Plants (Continued).

Scale:	a	b	c	d
Collector area[2]	80	140	200	330
Tilt angle[3]	39.0			
Collector fluid flow rate[2]	2730	4775	6822	11,260
Heat exchanger coefficient[2]	15,200	26,600	38,000	62,700
Exchanger pump flow rate[2]	3632	6356	9080	14,980
Storage volume[2]	3.03	5.30	7.57	12.50
Tank height[2]	2.0			
Heater capacity[2]	170,000			
Heater temperature[2]	66.11			
Demand flow-weekly[2]	32,280			
Energy demand-total[4]	1.411×10^7			

Year: 74

Season: SP

Model: K

Period: 2184

Scale:	b
Tilt angle[5]	49.9
Energy demand-total[4]	9.367×10^7

Season: SU

Model: K

Period: 2184

Scale:	b
Tilt angle[5]	24.3

Season: FA

Model: K

Period: 2160

Scale:	b
Tilt angle[5]	39.0

Season: WI

Model: K

Period: 2184

Scale:	b
Tilt angle[5]	65.9

Table 4.9- - Group E Simulations: Dairy Plants (Continued).

Location: 3
Years: 49, 52

Season: SP	
Model: K	
Period: 2184	
Scale:	b
Tilt angle[5]	33.8
Energy demand-total[5]	9.367×10^7
Season: SU	
Model: K	
Period: 2184	
Scale:	b
Tilt angle[5]	23.6
Energy demand-total[5]	9.367×10^7
Season: FA	
Model: K	
Period: 336	
Scale:	d
Tilt angle[6]	37.5
Energy demand-total[6]	1.441×10^7
Period: 2184[7]	
Scale:	b
Tilt angle[6]	48.3
Energy demand-total	9.367×10^7
Season: WI	
Model: K	
Period: 2160	
Scale:	b
Tilt angle[5]	61.3
Energy demand-total[5]	9.367×10^7

Table 4.9 - - Group E Simulations: Dairy Plants (Continued).

Type: L

Location: 1

Years: 65, 74

Season: FA

Model: K

Period: 336

Scale:	a	b	c	d
Collector area[2]	400	700	1000	1600
Tilt angle[3]	39.0			
Collector flow rate[2]	13,640	23,880	34,110	54,580
Heat exchanger coefficient[2]	76,000	133,000	190,000	304,000
Exchanger pump flow rate[2]	18,160	21,780	45,400	72,640
Storage volume[2]	15.10	26.50	37.85	60.60
Tank height[2]	2.0	4.0	4.0	4.0
Heater capacity[2]	405,000			
Heater temperature[2]	79.44			
Demand flow-weekly[2]	149,850			
Energy demand-total[2]	8.363×10^7			

Location: 3

Years: 49, 52

Season: FA

Model: K

Period: 336

Scale:	a
Tilt angle[3]	37.5

---

[1]Constant for group

[2]Constant for type

[3]Constant for location

[4]Constant for year(s)

[5]Constant for season

[6]Constant for period

[7]late portion of 49 run had bad weather data and was truncated at 1320 hours

plants is similar to the dairy plants. The operation of the plant during the September simulation period is the same as for the rest of the year, similar to the dairy plants. The September simulations serve as a means of comparing the meat plants with the annual performance of the medium dairy plant. Table 4.10 shows the parameters used for these simulations.

4.6.7 Fruit and vegetable plants - Group G

Simulation periods for these plants required individual attention since each one varied in its periods of production. All plants were modeled according to their September demand for the same two-week periods as the meat and dairy plants for comparison. Also, each plant was modeled for most of one year's processing demand for 1974 at East Lansing, Michigan and 1952 at Columbia, Missouri.

All vegetable plants required separate runs during the year because of their seasonal periods of operation as shown in Table 3.4. The small vegetable plant was simulated for the loads according to Figure 3.7 for 864 hours starting the 131th day for period A, 360 hours starting the 173rd day for period B, 432 hours starting the 214th day for period C, and 1440 hours starting the 274th day for period D. The medium plant exhibits only two different demands, with the largest occurring in August. This high demand load was used for a 432 hour simulation. The performance for the remainder of the year was drawn from previous yearly dairy runs.

The large vegetable plant exhibited a very high short duration demand. This period was simulated for 432 hours. Table 4.11 presents the specific

Table 4.10 - Group F Simulations: Meat Plants.

Type: S

Location: 1

Years: 65, 74

Season: FA

Model: K

Period: 336

Scale:

	a	b	c	d
Collector area[2]	35	65	100	150
Tilt angle[3]	39.0			
Ambient air temperature[1]	variable			
Collector fluid flow rate[2]	1194	2217	3411	4687
Heat exchanger coefficient[2]	6650	12,350	19,000	28,500
Exchanger pump flow rate[2]	1589	2951	4540	6810
Storage volume[2]	1.32	2.46	3.785	5.68
Tank height[2]	2.0	2.0	2.0	2.0
Supply water temperature[1]	12.78			
Heater capacity[2]	100,000			
Heater temperature[2]	60.0			
Demand flow-weekly[2]	15,130			
Energy demand-total[2]	5.98×10^6			

Location: 3

Years: 49, 52

Season: FA

Model: K

Period: 336

Scale:

	a
Tilt angle[3]	37.5

Type: M

Location: 1

Years: 65, 74

Season: FA

Model: K

Period: 336

Table 4.10 - Group F Simulations: Meat Plants (Continued).

Scale:

	a	b	c	d
Collector area^2	80	140	200	320
Tilt angle^3	39.0			
Collector fluid flow rate^2	2730	4775	6833	10,920
Heat exchanger coefficient^2	15,200	26,600	38,000	60,800
Exchanger pump flow rate^2	3632	6356	9080	1453
Storage volume^2	3.03	5.30	7.57	12.11
Tank height^2	2.0	2.0	2.0	2.0
Heater capacity^2	221,000			
Heater temperature^2	71.11			
Demand flow-weekly^2	27.050			
Energy demand-total^2	1.321×10^7			

Location: 3

Years: 49, 52

Season: FA

Model: K

Period: 336

Scale:

	a
Tilt angle^3	37.5

Type: L

Location: 1

Years: 65, 74

Season: FA

Model: K

Period: 336

Scale:

	a	b	c	d
Collector area^2	600	1050	1600	2400
Tilt angle^3	39.0			
Collector fluid flow rate^2	20,500	35,800	54,580	81,860
Heat exchanger coefficient^2	114,000	199,500	304,000	456,000
Exchanger pump flow rate^2	27,240	47,670	72,640	109,000
Storage volume^2	22.7	40.0	60.6	90.1

Table 4.10 - Group F Simulations: Meat Plants (Continued).

Tank height[2]	4.0	4.0	4.0	4.0
Heater capacity[2]	450,000			
Heater temperature[2]	71.11			
Demand flow-weekly[2]	252,000			
Energy demand - total[2]	1.231×10^8			

Location: 3

Years: 49,52

Season: FA

Model: K

Period: 336

Scale:

	a
Tilt angle[3]	37.5

---

[1]Constant for group

[2]Constant for type

[3]Constant for location

parameters and energy demand information for each simulation.

4.6.8 ASHRAE averages - Group H

The medium dairy plant, using the same collector size as previous annual simulations, was simulated for complete years at East Lansing, (Michigan) Indianapolis (Indiana) and Columbia (Missouri) for the "average" year using the ASHRAE model for weekly averages of daily insolation, Model N. Weekly average values of daily insolation were obtained from Baker and Klink (1975) for use with this model. Monthly mean temperatures were obtained for the tests locations from the sources indicated in Chapter 3. The average simulation data files were constructed as described for the ASHRAE weekly average test model.

Four simulation periods of 2160 hours each were made at each location. The results of these simulations were used to determine the long-term performance of solar water heaters for all processing plants. The complete description of these runs is given in Table 4.12. Appendices E and F contain temperature and insolation data, respectively, used to calculate data for the "average" year simulations.

4.7 Description of Simulation Results

4.7.1 Simulation outputs

To observe the behavior and performance of the solar water heating simulation model, values such as the energy collected and delivered by the system need to be determined. The TRNSYS model prints out 8

Table 4.11 - Group G Simulations - Fruit and Vegetable Plants.

Type: S

Location: 1

Year: 65, 74

Season: FA

Model: K

Period: 336

Scale:	a	b	c	d	e
Collector area[2]	670	1340	2340	3340	5365
Tilt angle[3]	39.0				
Ambient air temperature[1]	variable				
Collector fluid flow rate[2] ($\times 10^4$)	2.285	4.571	7.982	11.39	18.30
Heat exchanger coefficient[2] ($\times 10^5$)	1.273	2.546	4.446	6.346	10.19
Exchanger pump flow rate[2] ($\times 10^4$)	3.042	6.084	10.62	15.16	24.36
Storage volume[2]	25.4	50.7	88.6	126.0	203.0
Tank height[2]	2.0	2.0	2.0	2.0	2.0
Supply water temperature[1]	12.78				
Heater capacity[2]	2,536,000				
Heater temperature[2]	84.8				
Demand flow-weekly[2]	423,700				
Energy demand - total[3]	2.555×10^8				

Table 4.11 - (Continued).

Year: 74	
Season: SP	
Model: K	
Period: 864	
Scale:	b
Tilt angle[3]	27.6
Energy demand total[3]	2.387×10^8
Season: SU	
Model: K	
Period: 384	
Scale:	b
Tilt angle[4]	23.6
Energy demand-total[4]	3.238×10^7
Season: SU	
Period: 432	
Scale:	b
Tilt angle[4]	31.3
Energy demand-total[4]	3.482×10^8
Season: FA	
Model: K	
Period: 1440	
Scale:	b
Tilt angle[4]	52.4
Energy demand - total[4]	1.202×10^8

Table 4.11 -(Continued).

Location: 3

Year: 49,52

Season: FA

Model: K

Period: 336

Scale:	a
Tilt angle[3]	37.5

Year: 52

Season: SP

Model: K

Period: 864

Scale:	b
Tilt angle[3]	24.5
Energy demand - total[3]	2.387×10^8

Season: SU

Model: K

Period: 360

Scale:	b
Tilt angle[4]	20.7
Energy demand-total[4]	3.006×10^7

Period: 432

Scale:	b
Tilt angle[4]	28.1
Energy demand - total[4]	3.482×10^8

Table 4.11 - (Continued).

Season: FA

Model: K

Period: 1440

Scale:

	b
Tilt angle[4]	49.0
Energy demand - total	1.202×10^8

Type: M

Location: 1

Year: 65, 74

Season: FA

Model: K

Period: 336

Scale:

	a	b	c	d	e
Collector area[2]	525	1050	1850	2650	4200
Tilt angle	39.0				
Collector flow rate[2] ($\times 10^4$)	1.79	3.58	6.31	9.04	14.33
Heat exchanger coefficient[2] ($\times 10^4$)	9.975	19.95	35.15	50.35	79.8
Exchanger pump flow rate[2] ($\times 10^4$)	2.385	4.77	8.40	12.03	19.07
Storage volume[2]	20.0	40.0	70.0	100.0	159.0
Tank height[2]	2.0	2.0	2.0	2.0	2.0
Heater capacity[2]	17,600,000				
Heater temperature[2]	84.4				
Demand flow-weekly[2]	291,800				
Energy demand - total[3]	1.750×10^8				

Table 4.11 - (Continued).

Year: 74	
Season: SU	
Model: K	
Period: 432	
Scale:	<u>b</u>
Tilt angle[3]	31.3
Energy demand-total[3]	2.917×10^8
Location: 3	
Year: 49,52	
Season: FA	
Model: K	
Period: 336	
Scale:	<u>b</u>
Tilt angle[3]	37.5
Year: 52	
Season: SU	
Model: K	
Period:	
Scale: 432	<u>b</u>
Tilt angle[3]	28.1
Energy demand-total[3]	2.917×10^8

Table 4.11 -(Continued).

Type: L

Location: 1

Year: 65, 74

Season: FA

Model: K

Period: 336

Scale:	a	b	c	d	e
Collector area[2]	4015	3030	14050	20070	32100
Tilt angle[3]	39.0				
Collector flow rate[2] ($\times 10^5$)	1.370	2.74	4.79	6.85	10.96
Heat exchanger coefficient[2] ($\times 10^5$)	7.63	15.26	26.70	38.10	61.00
Exchanger pump flow rate[2] ($\times 10^5$)	1.825	3.65	6.38	9.11	14.60
Storage volume[2]	152.0	304.0	530.0	760.0	1215.0
Tank height[2]	2.0	2.0	2.0	2.0	2.0
Heater capacity[2]	8.49×10^7				
Heater temperature[2]	77.78				
Demand flow-weekly[2]	3.041×10^6				
Energy demand-total[3]	8.274×10^8				

Year: 74

Season: SU

Model: K

Period: 432

Scale:	b
Tilt angle[3]	31.3
Energy demand-total[3]	2.206×10^9

Table 4.11 - (Continued).

Location: 3		
Year: 49, 52		
Season: FA		
Model: K		
Period: 336		
Scale:	a	
Tilt angle[3]	37.5	
Year: 52		
Season: SU		
Model: K		
Period		
Scale:		b
Tilt angle[3]		28.1
Energy demand-total[3]		2.206×10^9

---

[1]Constant for group

[2]Constant for type

[3]Constant for season

[4]Constant for period

Table 4.12 - Group H Simulations - ASHRAE Averages.

Type: M

Location: 1

Year: A

Season: SP

Model: N

Period: 2160

Scale:

	b
Collector area[1]	140
Tilt angle[2]	49.9
Ambient air temperature[1]	constant monthly averages
Collector fluid flow rate[1]	4775
Heat exchanger coefficient[1]	26,600
Exchanger pump flow rate[1]	6356
Storage volume[1]	5.3
Tank height[1]	2.0
Supply water temperature[1]	12.78
Heater capacity[1]	170,000
Heater temperature[1]	61.11
Demand flow - weekly[1]	32,380
Energy demand - total[1]	9.367×10^7

Season: SU

Model: N

Period: 2160

Scale:

	b
Tilt angle[2]	24.3

Season: FA

Model: N

Period: 2160

Scale:

	b
Tilt angle[2]	39.0

Table 4.12 - Group H Simulations - ASHRAE Averages (Continued).

Season: WI
Model: N
Period: 2160
Scale: b
Tilt angle[2] 65.9

Location: 2
Year: A
Season: SP
Model: N
Period: 2160
Scale: b
Tilt angle[2] 34.5
Season: SU
Model: N
Period: 2160
Scale: b
Tilt angle[2] 24.2
Season: FA
Model: N
Period: 2160
Scale: b
Tilt angle[2] 49.0
Season: WI
Model: N
Period: 2160
Scale: b
Tilt angle[2] 60.3

Location: 3
Year: A
Season: SP
Model: N
Period: 2160
Scale: b
Tilt angle[2] 33.8

Table 4.12 - Group H Simulations - ASHRAE Averages (Continued).

Season: SU	
Model: N	
Period: 2160	
Scale:	b
Tilt angle[2]	23.6
Season: FA	
Model: N	
Period: 2160	
Scale:	b
Tilt angle[2]	37.5
Season: WI	
Model: N	
Period: 2160	
Scale:	b
Tilt angle[2]	61.3

---

[1]Constant for group

[2]Constant for season

integrated system variables in the final results. Six of these are total energy flows and two are total mass flows during the simulation. Each of the variables, unique to each run, are included in the tables of simulation results in Appendices I, J, and K. A sample table is presented in Chapter 5, Table 5.9.

The total radiation striking the collector surface is identified as RADTOTAL. This variable is the output of the radiation processor. QCOL is the total energy collected by the collector after accounting for losses encountered in the collector. QTANK represents the net energy removed from the tank which is delivered to the load. QAUX is the total energy required by the auxiliary heater to heat the water coming from the storage tank to the required temperature. The sum of QTANK and QAUX is given as QTOTAL. This value is the total energy delivered by the entire system. In most cases this value is equal to the design load specified for each plant. However, QTOTAL may be larger than this value due to collection periods which cause the tank temperature to exceed the demand temperature. For these cases the system delivers more energy than required.

QENV is the total energy loss to the environment by the storage tank. This value is only used to observe the increase in system losses at higher operating temperatures. The total energy passing through the heat exchanger is identified by QHX. This value is not used directly in the results analysis, however the overall effect of the heat exchanger may be observed by calculating the system efficiency.

The total water demand during the simulation is also printed out by the model. This value is not included in the results and was used only as a check to make sure the energy demand simulated was the same as the desired demand. For all cases this value was the same as the design demand and can be observed in the tables describing the simulation parameters and energy demands.

The total mass flow through the collector is identified as MCOL. This value was obtained for determining the average daily operation of the collectors. Since the mass flow rate of the collector pump is constant when the pump is on, this total mass flow directly relates the length of time which the system collected energy.

4.7.2 Description of performance results

The integrated values from the simulation results are used to calculate 6 values useful for observing the system performance all of which are shown in the tables of simulation results in Appendices I, J, and K.

The overall collector efficiency, COLEF, describes the collector performance during all periods of poor insolation and changing air temperatures. This value is determined by dividing QCOL, the total energy collected, by RADTOTAL, the total incident energy.

The energy delivered to the demand by the solar collector is represented as SOLAR. This value is the percent calculated by dividing QTANK, the energy delivered by the collector to the load, by the total design load for the plant. This value assumes any oversupply, due to temporary high tank temperatures, is used as part of the design load. This is reasonable for most cases since the duration of the higher tank temperature lasts only until sufficient cool supply water lowers the temperature below the demand temperature. If a thermostatically controlled mixing value were used to control the maximum temperature of the water supplied to the load this oversupply could easily be utilized, thus causing the auxiliary energy demand to decrease. For periods during the summer and where large collectors are used, this assumption is less accurate. For these cases, the effects of long cloudy periods, which require a significant auxiliary energy supply, will be overshadowed by the oversupply during peak insolation periods. This results in a larger error as the percent SOLAR approaches 100 percent.

When the degree of oversupply is significant, the "SOLAR-total" value is calculated. This quantity indicates the percent of solar energy supplied with respect to QTOTAL. SOLAR-total is presented in the simulation results for cases where a significant deviation occurs from the value of SOLAR.

The average period of daily system operation is given by SYSOP in hours per day. This value is calculated by dividing the total collector flow, MCOL, by the number of days and the maximum flow rate of the collector pump. This value is an average for the simulation period and does not indicate a maximum or minimum daily operation period.

The percentage of collected energy (QCOL) lost by the storage tank to the environment is calculated as TANK LOSS.

The average temperature of water supplied by the storage tank is represented in the simulation results as "Avg. Temp". This value is calculated by dividing the energy delivered by the tank, QTANK, by the mass flow and specific heat of the water. This results in an average temperature increase of the water as it passes through the tank. The exit temperature is then determined by summing this temperature increase and the constant cold water supply temperature.

4.8 Projection of Results

4.8.1 Method

The amount of energy delivered by the solar energy system to the demand load, SOLAR, is of interest for economic considerations. Performance projections for each plant are made only for this performance criteria.

The method for determining the annual system performance was chosen based on preliminary simulation results. One reference plant is simulated for a short period and an annual period. The ratio of SOLAR for the short period to SOLAR for the annual period is considered a function of the year and is assumed constant for that year. Other plants are simulated for the same short period as the reference plant. The SOLAR for the short period of each plant is then multiplied by the ratio for the reference plant to determine annual performance. The annual demand characteristics for each plant are necessary for determining the base periods for comparison of performance. The dairy and meat plants are similar in their demands and thus allowed the annual performances of each plant to be determined from one reference plant simulation, while the fruit and vegetable plants required a slightly different method as described in the following sections.

4.8.2 Dairy and meat plants

The dairy and meat plants exhibit similar annual demand schedules which enable a direct comparison between the plants during different times of the year. All dairy and meat plants were simulated for 336 hours in September. The medium dairy plant was simulated for the entire year at one collector area. A ratio of the September to the annual performance was used to project the annual performance for each plant and collector area for that year using the September simulation results. "Average" year simulation results for the medium dairy plant at East Lansing and Columbia, using the ASHRAE weekly insolation model were used to construct a ratio using the September results, to predict the average long-term performance of the dairy and meat plants. The average long-term results for Indianapolis were then interpolated from the average year simulation results for all three locations and the projections for each plant from East Lansing and Columbia.

For East Lansing and Columbia, two years of September data were available for simulation. For determining the average long-term performance, the results of the September simulations for each loaction were averaged.

4.8.3 Fruit and vegetable plants

Fruit and vegetable plants do not exhibit a constant annual demand schedule. September simulations similar to the dairy and meat plants were performed on the fruit and vegetable plants for means of comparison with the dairy and meat plant results. The medium fruit and vegetable plant results for September were used to partially predict the annual performance.

Each fruit and vegetable plant was simulated for their seasonal demand periods for one year using one collector area at East Lansing and Columbia.

These results were used to determine the annual performance of each plant by summing up the seasonal energy demands and the contributions made by the solar collector to each demand period. The average long-term performance projections at East Lansing and Columbia were then calculated using the fruit and vegetable plant annual results and the medium dairy plant ratio of annual results for the same year and the average simulation results using the ASHRAE weekly model.

4.9 Economic Analysis

4.9.1 Conventional energy costs

The cost of solar energy was compared with conventional energy sources of electricity, fuel oil, and natural gas. All energy costs were described as the cost in dollars to supply one million kilo-Joules.

Typical energy conversion efficiencies for industrial boilers were taken from Fryling (1966). Electricity was assumed to have a conversion efficiency of 85 percent. The current price to residential consumers was chosen for this analysis as 3.32 cents per kilowatt-hour. The result is an energy cost for electricity of 10.85 $/MKJ.

The current price of No. 2 fuel oil was found to be 45.9 cents per gallon. Using a conversion efficiency of 80 percent and a heat content of 132,000 BTU per gallon a final cost of 4.12 $/MKJ was calculated.

Natural gas was taken at a price of 3.2 dollars per 1000 cubic feet, a heat content of 1000 BTU per cubic foot, and a conversion efficiency of 76 percent to yield a cost of 3.98 $/MKJ.

4.9.2 Solar system capital investments

The following equation based on estimates from Kreider and Kreith (1975) was used to calculate the capital investment (CI in dollars) for constructing solar water heating systems:

$$CI = 2000 + 150(A) + 120(V) \quad (4.1)$$

where A is the collector area in square meters and V the storage volume in cubic meters. The cost of collector and piping were estimated from Kreider and Kreith (1975). A constant value of 2000 dollars was estimated for fixed costs such as controls and thermostats.

4.9.3 Solar energy costs

A life cycle cost technique was used to determine the annual operating cost of the solar energy system. A 20-year solar energy system life expectancy and an annual interest rate of 10 percent were used to determine a Capital Recovery Factor (CRF) of 0.1175. The annual operating cost was then calculated from equation (3.12) for each collector size. The annual operating cost for each solar water heating system was divided by the annual amount of energy supplied by the system to determine the cost of each million kilo-Joules for comparison with the cost of conventional energy sources.

4.9.4 Cost effectiveness using capital investment analysis

The cost effectiveness of the solar water heating system is determined by comparing the capital investment of a solar energy system and the allowable investment determined from the value of the conventional energy replaced by solar energy over a 20-year period, at an annual interest rate of 10 percent and a fuel increase of 5 percent per year. Equations (3.14) and (3.15) were used to determine the relationship between the allowable investment and the present value of the conventional energy saved, P_o. A simplified relationship of equation (3.14) for the above criteria is shown in equation (4.2):

$$P = (P_o)(16.6) \tag{4.2}$$

The value of P_o was determined by multiplying the annual energy supplied by the solar energy system, by the energy cost in dollars per million kilo-Joules, for each conventional fuel; electricity, oil, or gas. The allowable investment, P, was then determined for each energy source for comparison with the investments required by the solar water heating system.

5. SIMULATION RESULTS AND DISCUSSION

5.1 Insolation Models - Group A

The simulation results for the 6 insolation models for each season are given in Tables 5.1, 5.2, 5.3 and 5.4. Each table shows the total insolation striking the collector (RADTOTAL), the total energy collected (QCOL), the total energy delivered to the load by the tank (QTANK), and the total fluid flow through the collector (MCOL). From this information, the overall collector efficiency (COLEF), percentage of the demand supplied by collectors (SOLAR), and the average temperature of the water supplied by the tank were determined for each model.

The seasonal behavior of each model generally resulted in a decrease in the solar energy supplied to the load. Table 5.5 summarizes the percent SOLAR for each run and compares the annual percentage for each model. The annual percentages were calculated by summing the energy delivered by the tank for each season and dividing it by the total design load. The percent deviation of each test model from the control model and the control model with constant temperature is illustrated.

The seasonal performance variations of each model is further illustrated in Figure 5.1. This figure shows the total insolation (RADTOTAL) striking the collector for each test model. The daily ASHRAE model (M) shows a higher insolation in the summer period and a lower insolation

Table 5.1 -Group A Simulation Results for Spring.

A:S:1:74:SP:K, L, M, N, O, P:336:d

Radiation Model:	K Control (hourly T)	L Control (constant T)	M ASHRAE (daily)	N ASHRAE (weekly)	O Whillier	P Trans
RADTOTAL ($X10^7$KJ)	2.076	2.076	2.084	2.095	2.058	2.032
QCOL ($X10^6$KJ)	5.870	5.704	5.819	4.938	5.588	4.896
QTANK ($X10^6$KJ)	1.533	1.439	1.467	1.561	1.415	1.522
MCOL ($X10^5$kg)	3.941	3.777	3.805	4.958	3.768	4.640
COLEF (%)	28.3	27.5	27.9	23.6	27.2	24.1
SOLAR (%)	53.9	50.6	51.6	54.9	49.8	53.6
AVG.TEMP.(C)	41.5	39.5	40.1	42.0	39.0	41.2

Table: 5.2 -Group A Simulation Results for Summer.

A:S:1:74:SU:K, L, M, N, O, P:336:d

Radiation Model:	K Control (hourly T)	L Control (constant T)	M ASHRAE (daily)	N ASHRAE (weekly)	O Whillier	P Trans
RADTOTAL ($X10^7$KJ)	2.572	2.572	2.723	2.504	2.602	2.556
QCOL ($X10^6$KJ)	7.767	7.567	7.511	7.040	7.366	6.952
QTANK ($X10^6$KJ)	2.308	2.230	2.269	2.231	2.188	2.157
MCOL ($X10^5$kg)	4.685	5.008	5.916	5.339	5.661	6.043
COLEF (%)	30.2	29.4	27.6	28.1	28.3	27.2
SOLAR (%)	81.2	78.5	79.8	78.5	77.0	75.9
Ave. Temp. (°C)	57.4	55.8	56.6	55.8	54.9	54.3

Table 5.3 -Group A Simulation Results for Fall.

A:S:1:74:FA:K, L, M, N, O, P:336:d

Radiation Model:	K Control (hourly T)	L Control (constant T)	M ASHRAE (daily)	N ASHRAE (weekly)	O Whillier	P Trans
RADTOTAL ($X10^7$KJ)	2.274	2.274	2.266	2.508	2.269	2.222
QCOL ($X10^6$KJ)	6.876	6.537	6.438	7.301	6.504	6.129
QTANK ($X10^6$KJ)	2.176	2.061	2.050	2.253	2.065	1.905
MCOL ($X10^5$kg)	4.449	4.363	4.581	4.831	4.545	5.316
COLEF (%)	30.2	28.7	28.4	29.1	28.7	27.6
SOLAR (%)	76.6	72.5	72.1	79.3	72.7	67.0
Avg. Temp. (°C)	54.7	52.3	52.1	56.2	52.4	49.1

Table 5.4 -Group A Simulation Results for Winter.

A:S:1:74:WI:K, L, M, N, O, P:336:d

Radiation Model:	K Control (hourly T)	L Control (constant T)	M ASHRAE (daily)	N ASHRAE (weekly)	O Whillier	P Trans
RADTOTAL ($X10^7$KJ)	1.507	1.507	1.322	1.649	1.135	0.715
QCOL ($X10^6$KJ)	3.993	3.969	3.634	4.368	2.722	2.381
QTANK ($X10^6$KJ)	1.431	1.433	1.362	1.412	1.085	0.899
MCOL ($X10^5$kg)	2.624	2.551	2.125	3.387	2.143	1.371
COLEF (%)	26.5	26.3	27.5	26.5	24.0	33.0
SOLAR (%)	50.4	50.4	47.9	49.7	38.2	31.6
Avg. Temp. (°C)	39.4	39.4	38.0	39.0	32.3	28.4

Table 5.5 -Group A Simulation Results Summary.

A:S:1:74:SP, SU, FA, WI: K, L, M, N, O, P:336:d

Radiation Model:	K Control (hourly T)	L Control (constant T)	M ASHRAE (daily)	N ASHRAE (weekly)	O Whillier	P Trans
SOLAR						
SPRING (%)	53.9	50.6	51.6	54.9	49.8	53.6
SUMMER(%)	81.2	78.5	79.8	78.5	77.0	75.9
FALL(%)	76.6	72.5	72.1	79.3	72.7	67.0
WINTER (%)	50.4	50.4	47.9	49.7	38.2	31.6
Annual Average (%)	65.5	63.0	62.8	65.6	59.4	57.0
Deviation from K (%)	0	3.8	-4.0	0.2	-9.3	-13.0
Deviation from L (%)	4.0	0	-0.2	0.2	-5.7	-9.5

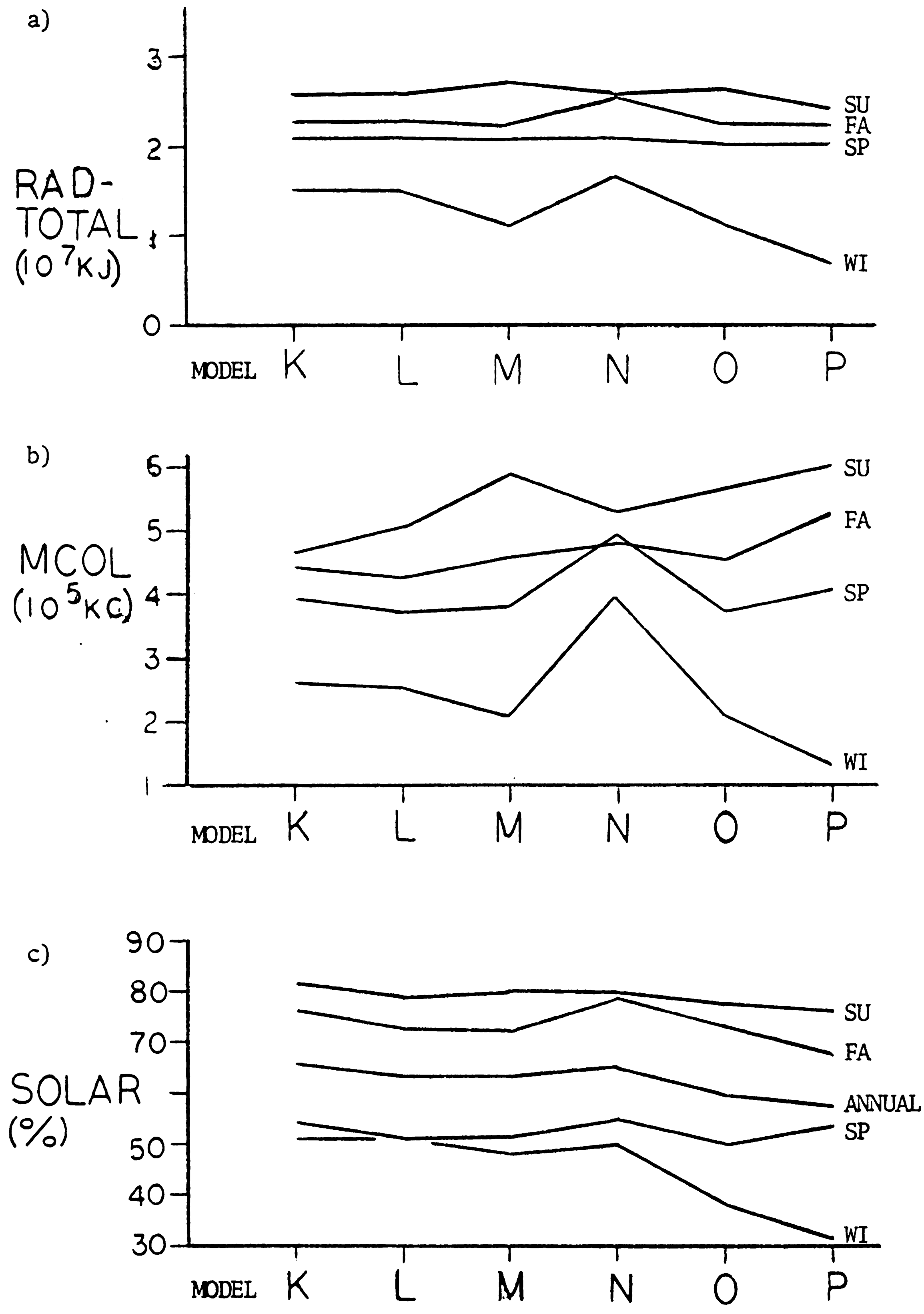

Figure 5.1 Insolation Model Test Results.

during the winter. Just the opposite is true for the weekly ASHRAE model (N). During the spring and fall, only slight variations are apparent among all models. For the winter, only the weekly ASHRAE model (N) showed an increase in insolation.

Figure 5.1b shows the total mass flow through the collector. This value reflects the time which solar energy was collected. For the spring, summer, and fall, most models showed an increase in operation time. Actual measured insolation data reflects periods of high and low insolation intensity which results in a variable rate of energy collection during the periods of operation. The symmetry characteristic of the other insolation models tends to remove any rapid changes in intensity, caused by temporary cloudy periods, etc. The result is a uniform distribution of insolation allowing the system to operate every day during the peak insolation periods regardless of cloud cover, thus accounting for these increases in operation time.

The winter simulation shows a drastic decrease in the collector mass flow. Cloud cover during this period is greater than for other periods. The peak insolation periods produced by the test models are apparently not sufficient to raise the collector to a temperature greater than the storage temperature. The control however still accounts for short periods of high insolation, thus accounting for the higher collector flow rate. The effect of weekly average insolation data used by the ASHRAE model (N) apparently compensates for the day to day variability of the other models, resulting in a greater collector flow rate.

Figure 5.1c illustrates the system efficiencies for each season and the total year. All models except the ASHRAE weekly model (N), show a decrease in system efficiency for all seasons compared to the control (K). The ASHRAE model (N) shows an increase in system efficiency during the spring and fall periods, with an annual efficiency within 0.2 percent to that of the control (K).

Based on these results the ASHRAE weekly model (N) is recommended for generating insolation data for simulation on the long-term basis. For short-term periods either the ASHRAE daily model (M) or the Whillier model (O) appear acceptable. The Transmissivity model (P) is inadequate for predicting insolation within the accuracy needed for design. If accuracy with 5-10 percent is acceptable, the Whillier (O) and ASHRAE daily model (M) may be used for simulating annual system performance.

The effect of using constant temperature in Model L results in a 3.8 percent decrease in annual predicted system performance. The ASHRAE weekly model (N) compensates for this loss, and allows for the continued use of constant temperatures for predicting simulation data.

The performance of the ASHRAE weekly model (N) in these tests has made it the reasonable choice for predicting the long-term performance of solar energy systems for food processing plants. Because of the close correlation with this model and the control model, the performance of the ASHRAE weekly model (N) was assumed to predict accurately the performance of a solar system for any year.

5.2 Hourly Average Models - Group B

The effect of averaging insolation data over periods greater than 1 hour results in a significant decrease in system performance as shown in Table 5.6. A decrease of over 6 percent resulted from averaging 1-hour data over a 3-hour period. A 14 percent decrease occurs using 6-hour averages. The advantages of using a transient computer simulation are destroyed when using such averages. It appears that hourly insolation data is necessary for accurately simulating a solar system. When hourly data is not available, it is recommended that a method of predicting hourly insolation, as described in the previous section, be used. Hourly averages for insolation over a period greater than one hour are unacceptable.

5.3 Storage Tank Simulation Results - Group C

Parametric test results for storage tank volume determination are shown for the summer and winter periods in Table 5.7. Five tank volumes were tested with a collector of 100 m^2.

The function of a large storage tank serves to increase the reliability of the system during cloudy periods and for demands which require a reliable hot water supply. A large storage tank also increases the amount of energy lost to the tank environment.

As the size of the tank increases the capacity of the system to collect energy during periods of high insolation increases, resulting in a more constant average storage temperature. Figure 5.2 illustrates the effects of storage tank variations on system performance.

As the tank volume increases, the energy collected (QCOL) increases in a linear fashion. However, due to system losses, the energy supplied to the load indicates a maximum, clearly indicating a point of optimum performance. For economic considerations of storage tank cost, etc.,

Table 5.6 -Group B Simulation Results for Hourly Averages.

B:S:1:74:SP:Q, R, S:1000:a

Model:	Q (1 hour)	R (3 hour)	S (6 hour)
RAD TOTAL ($X10^7$KJ)	4.769	4.542	3.582
QCOL ($X10^7$KJ)	1.484	1.426	1.040
QTANK ($X10^6$KJ)	7.965	6.755	5.344
COLEF (%)	31.1	31.4	29.0
SOLAR (%)	43.7	37.1	29.3

Table 5.7 - Storage Tank Design Simulation Results.

Run - C:S:1:74:SU, WI:K:336:a, b, c, d, e

Season: SU

Scale:	a	b	c	d	e
STORAGE VOLUME (m^3)	1.892	3.785	5.680	7.570	11.36
QCOL (10^6KJ)	6.983	7.080	7.326	7.607	8.177
QTANK (10^6KJ)	2.221	2.376	2.338	2.265	2.109
QAUX (10^6KJ)	0.715	0.519	0.526	0.586	0.733
MCOL (10^5Kg)	4.358	4.404	4.522	4.613	4.949
SOLAR (%)	78.1	83.6	82.3	79.7	74.2

Season: WI

Scale:	a	b	c	d	e
STORAGE VOLUME (m^3)	1.892	3.785	5.680	7.570	11.36
QCOL (10^6KJ)	3.621	3.735	3.840	3.953	4.203
QTANK (10^6KJ)	1.446	1.511	1.475	1.416	1.293
QAUX (10^6KJ)	1.315	1.268	1.302	1.357	1.473
MCOL (10^5Kg)	2.579	2.515	2.579	2.615	2.742
SOLAR (%)	50.9	53.2	51.9	49.8	45.5

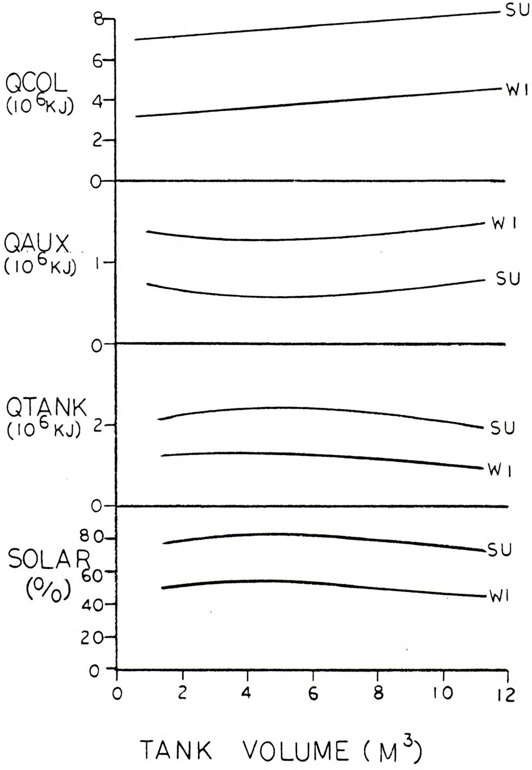

Figure 5.2 Tank Volume Parametric Test Results.

the tank size which supplies the greatest percentage of energy to the load is optimum. For this study a tank size of 3.785 m^3 was chosen (see Table 5.7). For the purpose of system scaling, a storage volume to collector area ratio was determined as 0.03875 m^3 of storage volume per m^2 of collector area.

5.4 Collector Fluid Flow Rate Test Results - Group D

The collector fluid flow rate, in effect, controls the mean collector plate temperature and the temperature rise across the collector. At a higher flow rate the mean plate temperature is decreased which decreases the instantaneous environmental energy loss of the collector. Thus, the flow rate has a direct influence on collector efficiency.

Results of the parametric tests on collector fluid flow rates are given in Table 5.8. Tests were run for the summer and winter period. The table shows the energy collected (QCOL), energy delivered to load (QTANK), auxiliary energy (QAUX), mass flow through the collector (MCOL), and system efficiency (SOLAR). Figure 5.3 illustrates the behavior of these variables. The flow rate which yields the maximum system performance is 3411 kg/hr. This value was assumed optimum for these conditions and scaled for the processing plant simulations.

5.5 Processing Plant Results and Projections

5.5.1 Sample simulation results

A sample computer printout for a small dairy plant is given in

Table 5.8-Collector Flow Rate Simulation Results.

Run - D:S:1:74:SU, WI:K:336:a, b, c, d, e

Season: SU

Scale:	a	b	c	d	e
Collector Flow Rate (Kg/hr)	1135	2270	3411	4540	5675
QCOL (10^6KJ)	6.650	7.249	7.471	7.607	7.725
QTANK (10^6KJ)	2.134	2.261	2.274	2.265	2.250
QAUX (10^6KJ)	0.711	0.590	0.477	0.586	0.599
MCOL (10^5Kg)	1.217	2.311	3.459	4.613	5.823
SOLAR (%)	75.1	79.6	80.0	79.7	79.2

Season: WI

Scale:	a	b	c	d
Collector Flow Rate (Kg/hr)	1135	2270	3411	4540
QCOL (10^6KJ)	3.445	3.810	3.887	3.953
QTANK (10^6KJ)	1.313	1.403	1.423	1.416
QAUX (10^6KJ)	1.457	1.371	1.350	1.357
MCOL (10^5Kg)	0.683	1.317	1.958	2.615
SOLAR (%)	46.2	49.4	50.1	49.8

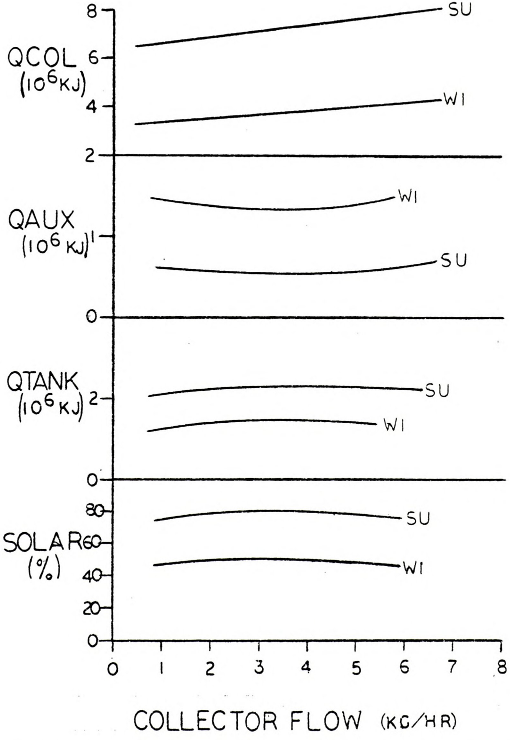

Figure 5.3 Collector Fluid Flow Rate Parametric Test Results.

Tables H.1, H.2, and H.3 in the Appendix. Table H.1 is a listing of the control cards which determine the type of system to be simulated. At the end of the control card deck an output reference map describes the configuration and information flow for the simulation. Table H.2 is the output results for this sample simulation. The first column indicates the time of the simulation. The remaining columns contain energy flows, etc., as described in the control card deck and in Chapter 4. Table H.3 is a plot of the temperature profiles for the storage fluid, collector and ambient air. This aids in visualizing the transient behavior of the system.

Selected variables from the printouts are tabulated for each plant simulation in Appendices I, J, and K. A sample table for small dairy simulations results for September, 1974, at East Lansing, Michigan, is given in Table 5.9. This table contains eight values taken directly from the computer output. Six other values, as described in Chapter 4, are also presented.

The system behavior represented in this table is characteristic of all plant simulations. Each column from left to right, corresponding to increasing system scale, describes the performance of a different system size. Observe that RADTOTAL, QCOL, QTANK, QENV, and QHX all increase with an increase in system scale and collector area, while QAUX decreases. QTOTAL remains relatively constant. The mass flow rate through the collector also increases with collector size and corresponds to the average daily operation of the system, SYSOP. Collector efficiency, COLEF, consistently decreases with increasing scale. This is because the higher operating temperatures in the collector SOLAR percentages increase with increasing scale. SOLAR-total

Table 5.9 - Small Dairy Plant Simulation Results For September 1974 - East Lansing.

Run: E:S:1:74:FA:K:336:a,b,c,d

Scale:	a	b	c	d
Collector area (m^2)	25	40	65	100
RADTOTAL (10^6KJ)	5.685	9.096	14.78	22.74
QCOL (10^6KJ)	2.099	3.036	4.310	5.802
QTANK (10^6KJ)	1.190	1.567	1.966	2.297
QAUX (10^6KJ)	1.390	1.025	0.654	0.385
QTOTAL (10^6KJ)	2.580	2.592	2.620	2.682
QENV (10^6KJ)	0.324	0.521	0.860	1.321
QHX (10^6KJ)	1.886	2.697	3.805	5.094
MCOL (10^5Kg)	0.947	1.419	2.124	3.084
COLEF (%)	36.9	33.4	29.2	25.5
SOLAR (%)	46.3	61.0	76.5	89.4
SOLAR - total (%)	46.1	60.5	75.0	85.6
SYSOP (hrs/day)	7.9	7.4	6.8	6.5
TANK LOSS (%)	15.5	17.2	19.9	22.8
Avg. Temp. (^oC)	37.2	44.9	53.1	59.9

is not included in all tables. This value indicates the amount of energy supplied by the system relative to QTOTAL. For some collector sizes QTOTAL is greater than the design load Q, representing a degree of oversupply during periods of large insolation. For cases when QTOTAL is equal to the design load, the SOLAR-total values are identical to the SOLAR values and not included in the tables. TANK LOSS percentages increase with increasing scale because of the higher storage tank temperatures. The average tank temperature is given at the bottom of each table and is seen to increase with an increase in the collector size.

5.5.2 Dairy plants - Group E

A summary of the percent solar energy supplied to the demand loads of the daily plants is given in Table 5.10. This table shows the results of the two-week September simulations which were made on all processing plants for two years at East Lansing, Michigan, and Columbia, Missouri. Percentages range from 32 for the small scale medium dairy at East Lansing, 1974, to 135 for the large scale small dairy at Columbia, 1952. A significant increase in the amount of energy delivered by the collector is evident in the Columbia test results compared to the East Lansing results. Several runs indicate over 100 percent solar energy supply for Columbia. This is expected since Columbia is at a lower latitude with a higher average daily insolation. For the two years at East Lansing, 1974, gives a slightly better system performance than the 1965 year for the larger collector areas. For the lower collector areas, the results for 1965 tend to be slightly higher. The exact

Table 5.10- Summary of September Simulation Results for Dairy Plants (Percentage of demand supplied by solar energy).

Scale:		a	b	c	d
Small Plant					
Collector area		25	40	65	100
East Lansing,	1965	46.7	60.4	74.7	86.6
	1974	46.3	61.0	76.5	89.4
Columbia,	1949	67.0	87.5	107.3	124.0
	1952	77.4	98.0	117.7	135.2
Medium Plant					
Collector area		80	140	200	330
East Lansing,	1965	33.5	48.2	58.8	73.8
	1974	32.4	48.0	59.2	75.5
Columbia,	1949	46.7	67.4	82.5	104.6
	1952	51.9	74.0	90.1	113.1
Large Plant					
Collector area		400	700	1000	1600
East Lansing,	1965	33.9	46.0	54.1	65.0
	1974	33.2	46.0	54.9	66.8
Columbia,	1949	41.5	58.4	70.5	87.2
	1952	51.7	70.7	83.6	100.7

cause of this is not obvious. It is suspected that a combination of insolation values and air temperatures caused greater energy losses for the larger systems during 1965. The simulations for Columbia show a distinct decrease in system performance for 1949 compared to 1952.

The annual simulation runs for the medium dairy plant are presented in Table 5.11. This table contains one full year run for 1974 at East Lansing, Michigan, and two full year runs for 1949 and 1952 at Columbia, Missouri, using actual measured insolation data, and an average year for Indianapolis, Indiana. Also presented are the ASHRAE "average" year results for all three test locations. The seasonal results for each year are presented together with the annual percentage. The average year results are assumed to be indicative of the results obtained if an "average" year of measured data were used. This assumption is made based on the results presented earlier for this ASHRAE test model.

From Table 5.11 the 1974 year at East Lansing appears to be a relatively poor year for insolation compared to the average year. This agrees with the conclusion of Thomas (1977), when he compared the weekly average daily insolation values for 1974 with 16-year average values.

For Columbia, both test years, 1949 and 1952, are found to give better results than the average year. The differences between these results may reflect several possible factors: (1) an inaccuracy of the ASHRAE weekly model for Columbia, (2) differences in the Columbia data compared to the averages due to age or type of instruments used, and (3) the possibility that 1949 and 1952 were above average insolation

Table 5.11- Summary of Annual Simulation Results for Medium Dairy Plant (Percentage of demand supplied by solar energy).

Season:	SP	SU	FA	WI	Annual Total
East Lansing, 1974	38.5	59.5	40.7	27.9	41.7
Average Year	41.5	61.9	46.4	32.7	45.6
Indianapolis					
Average Year	45.9	64.4	54.9	36.7	50.5
Columbia, 1949	53.9	74.8	69.7	32.7	56.5
1952	57.0	75.4	77.2	47.8	64.3
Average Year	49.9	67.7	57.8	42.2	54.6

years. The latter condition will be assumed since there is no evidence to indicate otherwise.

The results from the Indianapolis average simulation cannot be compared to actual measured data. However, the annual percentage of 50.5 follows the trend expected for the performance at the three test locations.

Dairy plant projections for the annual percent solar energy supplied to the load for 1974, East Lansing and for 1949 and 1952, Columbia are given in Table 5.12. These projections are based on the annual and September period results for these three years. The values underlined for the medium dairy plant are the actual simulation results.

The results presented in Table 5.12 are not used for projecting the average year plant performance. They are presented to compare the annual performance of the dairy plants with the meat and fruit and vegetable plants.

The long-term dairy plant results are given in Table 5.13. These values were obtained from the average year and the September period simulation as described in Chapter 4. A small dairy system with a collector size of 40 m^2 is shown to supply 14 percent more energy for a plant located in Columbia than for one located in East Lansing. This trend is consistent for all size plants and collector areas and will have a definite effect upon the economic feasibilities of solar water heating systems for each location. The percentages presented in Table 5.13 are used to construct performance curves for determining the economic feasibility of solar water heating for dairy plants.

Table 5.12 -Annual Projected Performance Of Solar Water Heating System For Dairy Plants (Percentage of demand supplied by solar energy).

Scale:	a	b	c	d
Small Plant				
Collector area	25	40	65	100
East Lansing, 1974	40.2	53.0	66.5	77.7
Columbia, 1949	56.2	73.3	89.9	103.9
Columbia, 1952	67.3	85.2	102.3	117.5
Medium Plant				
Collector area	80	140	200	330
East Lansing, 1974	28.1	41.7[1]	51.4	65.5
Columbia, 1949	39.1	56.5[1]	69.1	87.7
Columbia, 1952	45.1	64.3[1]	78.3	98.3
Large Plant				
Collector area	400	700	1000	1600
East Lansing, 1974	28.9	40.0	47.7	58.0
Columbia, 1949	37.8	49.0	59.1	73.9
Columbia, 1952	44.9	61.4	72.6	87.5

[1] Actual simulation results

Table 5.13 Long Term Annual Performance of Solar Water Heating System For Dairy Plants At All Test Locations (Percentage of Demand Supplies By Solar Energy).

Scale:		a	b	c	d
Small Plant					
	Collector area	25	40	65	100
	East Lansing	44.1	57.5	71.7	83.4
	Indianapolis	50.4	65.2	80.0	92.5
	Columbia	55.7	71.6	86.9	100.1
Medium Plant					
	Collector area	80	140	200	330
	East Lansing	30.7	45.6	56.2	71.6
	Indianapolis	34.7	50.5	61.9	78.4
	Columbia	38.0	54.6	66.7	84.1
Large Plant					
	Collector area	400	700	1000	1600
	East Lansing	31.8	43.6	51.7	62.5
	Indianapolis	34.0	47.0	55.9	67.9
	Columbia	35.9	49.8	59.4	72.5

5.5.3 Meat plants - Group F

The method used for determining the average year performance of the meat processing plant systems is similar to that used by the dairy plants. Because of the similarity of the demand loads for the two plant types (see Figure 3.6), yearly simulation runs were not made for the meat plants. Annual projections are made using the yearly simulation results for the medium dairy plant.

September simulation results, showing the percent solar energy supplied to each meat plant demand are summarized in Table 5.14. The collector areas for the small, medium, and large meat plants are approximately the same as the dairy plants. The demand for the meat plants generally require a lower supply temperature. The percent supplied by the solar system for the meat plants is generally higher than the dairy plants. The relative performance of each year with respect to the year and location is the same as described for the dairy results for September since the same data files were used for both plants.

Using these results and the annual results for the medium dairy plant, projections were made for annual performance of the meat plants for 3 years: 1974 at East Lansing, 1949 and 1952 at Columbia. These results are presented in Table 5.15. This table is similar to Table 5.12 and shows the same characteristics of a decrease in performance at East Lansing compared to Columbia.

Table 5.16 shows the long-term average performance of the meat plants at each test location. This table was constructed using the ASHRAE average results for the medium dairy from Table 5.11 and the

Table 5.14 - Summary of September Simulation Results for Meat Plants (Percentage of demand supplied by solar energy).

Scale:		a	b	c	d
Small Plant					
Collector area		35	65	100	150
East Lansing	1965	44.6	62.7	75.8	87.9
	1974	44.8	63.3	77.1	90.4
Columbia	1949	59.0	85.4	105.9	134.7
	1952	68.4	95.8	115.9	134.7
Medium Plant					
Collector area		80	140	200	320
East Lansing	1965	42.2	56.0	65.0	76.2
	1974	42.4	56.6	66.1	78.7
Columbia	1949	56.7	77.1	90.5	107.6
	1952	64.3	84.2	99.5	117.0
Large Plant					
Collector area		600	1050	1600	2400
East Lansing	1965	35.6	49.2	60.3	71.1
	1974	35.0	49.4	62.3	73.1
Columbia	1949	43.1	62.1	78.3	94.9
	1952	53.8	75.0	92.4	109.6

Table 5.15 - Annual Projected Performance of Solar Water Heating System for Meat Plants (Percentage of demand supplied by solar energy).

Scale:		a	b	c	d
Small Plant					
Collector area		35	65	100	150
East Lansing,	1974	38.9	55.0	67.0	78.6
Columbia,	1949	49.4	71.7	88.0	103.2
Columbia,	1952	59.4	83.3	100.7	117.1
Medium Plant					
Collector area		80	140	200	320
East Lansing,	1974	36.8	49.2	57.4	68.4
Columbia,	1949	47.5	64.6	75.8	90.2
Columbia,	1952	55.9	65.4	86.5	101.7
Large Plant					
Collector area		600	1050	1600	2400
East Lansing,	1974	30.4	42.9	53.3	63.5
Columbia,	1949	36.1	52.0	65.6	79.5
Columbia,	1952	46.8	65.2	80.3	95.2

Table 5.16-Long Term Annual Performance of Solar Water Heating System For Meat Plant At All Test Locations (Percentage of Demand Supplied By Solar Energy).

Scale:		a	b	c	d
Small Plant					
	Collector area	35	65	100	150
	East Lansing	42.4	59.7	72.4	84.6
	Indianapolis	46.1	65.3	79.4	92.8
	Columbia	49.2	69.9	85.3	99.6
Medium Plant					
	Collector area	80	140	200	320
	East Lansing	40.1	53.4	62.1	73.4
	Indianapolis	43.7	56.4	68.2	80.6
	Columbia	46.7	59.0	73.3	86.7
Large Plant					
	Collector area	600	1050	1600	2400
	East Lansing	33.4	46.7	57.6	68.3
	Indianapolis	35.5	50.0	62.1	74.1
	Columbia	37.3	52.8	65.8	78.9

September meat plant simulations results from Table 5.14. The performance results in Table 5.16 are used for construction performance curves for economic feasibility analysis in Chapter 6.

5.5.4 Fruit and vegetable plants - Group G

The September simulation results for the fruit and vegetable plants are shown in Table 5.17. These results correspond to the September results obtained for the dairy and meat plants.

Fruit and vegetable plant simulation results for the seasonal demand loads are given in Table 5.18. The demand periods illustrated in this table correspond to the demand schedules for each plant shown in Table 3.4. The small plant has four different seasonal demands, the medium plant two, and one for the large plant. The results for the large plant and the small plant for scale C show two values. The first one is the result of the August simulation, the second is for September. Both use the same demand load. For the small plant, results indicate that for periods B and D the solar energy supplied over 100 percent of the demand. The demand loads for these periods are less than period C. This illustrates a problem unique to the fruit and vegetable plants, namely that for periods of low demand, the solar system produces more energy than needed. The energy delivered by the collectors above the 100 percent demand load cannot be justified as usable energy in the economic analysis. In order to get the full usefulness from the solar system, a use should be found for this energy. This problem is further illustrated when considering the off season energy production potential of the system. In the following chapter, consideration is given to

Table 5.17 - Summary of September Simulation Results for Fruit and Vegetable Plants (Percentage of demand supplied by solar energy).

Scale:	a	b	c	d	e
Small Plant					
Collector area	670	1340	2340	3340	5365
East Lansing, 1965	23.1	35.0	45.8	53.1	62.3
East Lansing, 1974	22.8	35.2	47.1	55.1	65.4
Columbia, 1949	27.7	44.2	60.6	71.6	
Columbia, 1952	34.3	52.6	70.0	81.4	
Medium Plant					
Collector area	525	1050	1850	2650	4200
East Lansing, 1965	25.7	38.4	49.8	57.3	66.2
East Lansing, 1974	25.3	38.6	51.1	59.2	69.2
Columbia, 1949	30.3	47.5	64.5	76.0	
Columbia, 1952	38.4	58.1	84.9	75.9	
Large Plant					
Collector area	4015	8030	14050	20070	32100
East Lansing, 1965	23.4	36.1	48.4	56.4	67.1
East Lansing, 1974	22.7	35.9	49.0	58.0	69.8
Columbia, 1949	27.1	43.7	61.2	72.9	
Columbia, 1952	34.7	54.4	73.3	83.5	

Table 5.18 - Summary of Yearly Simulation Results for Fruit and Vegetable Plants (Percentage of demand supplied by solar energy).

Demand Period:	A	B	C	D
Small Plant				
Collector area 1340				
East Lansing, 1974	57.8	75.9	32.1 (35.2)*	134.2
Columbia, 1952	86.8	118.8	50.7 (52.6)*	184.1
Medium Plant				
Collector area 1050				
East Lansing, 1974	38.6	31.0		
Columbia, 1952	58.1	49.1		
Large Plant				
Collector area 8030				
East Lansing, 1974	32.7 (35.9)*			
Columbia, 1952	51.9 (54.4)*			

*September results

off season demand and its contribution to the overall economic feasibility.

Table 5.19 gives the annual performance projections for the small fruit and vegetable plant for two years: 1974 at East Lansing and 1952 at Columbia. For each location the performance for each demand period is given. For demand period C, scale b at both locations the value is the average for two simulations, indicated by the bar over the number, occurring at different times during the plant demand. Several periods indicate over 100 percent supply to the load. A low and high annual percentage is given for both locations. The difference between these two percentages represents the amount of oversupply of the solar system for certain periods of the year. For the large scale, the amount of oversupply for each location is over 14 percent. Since only the low annual percentage can be justified for the normal plant demand, it is used to determine the average annual percentage for each location.

The annual performance results for the medium fruit and vegetable plant are presented in Table 5.20. The medium plant exhibits a demand 12 months per year. For a period in August the demand is greater corresponding to demand period B. To determine the annual performance for this plant the annual percentage of solar supply taken for the September demand was calculated and is shown as demand period A (annual) in the table. An allowance for high demand period B was made to determine the actual annual system performance. The annual performance for the East Lansing location ranges from 21.6 to 58.9 percent for scales a through e and 32.9 to 75.5 for scales a through d at the Columbia location. These values are used to predict the average annual performance for fruit and vegetable plants at all three test locations.

Table 5.19 - Annual Projected Performance of Solar Water Heating System for Small Fruit and Vegetable Plants (Percentage of demand supplied by solar energy).

Scale:	a	b	c	d	e
Collector area	670	1340	2340	3340	5365
East Lansing, 1974					
Demand Period					
A	37.7	57.8	77.3	90.5	107.4
B	49.2	75.9*	101.6	118.8	141.0
C	21.8	33.7	45.1	52.8	62.6
D	86.9	134.2	179.2	210.0	249.3
Annual					
High	30.0	38.2	62.1	73.0	86.3
Low	30.0	35.3	55.7	63.5	72.3
Columbia, 1952					
Demand Period					
A	56.6	86.8	115.5	134.3	
B	77.5	118.8*	158.1	184.0	
C	33.6	51.6	68.7	79.9	
D	120.0	184.1	245.0	285.0	
Annual					
High	45.0	69.2	92.0	107.0	
Low	43.5	62.0	76.8	85.1	

*actual simulation results

Table 5.20 - Annual Projected Performance of Solar Water Heating System for Medium Fruit and Vegetable Plant (Percentage of demand supplied by solar energy).

Scale:	a	b	c	d	e
Collector area	525	1050	1850	2650	4200
East Lansing, 1974					
Demand Period					
A	25.3	38.6	51.1	59.2	69.2
A (annual)	22.0	33.5	44.4	51.4	60.1
B	20.3	31.0	41.0	47.5	55.6
Annual	21.6	32.9	43.5	50.4	58.9
Columbia, 1952					
Demand Period					
A	38.4	58.1	76.4	88.1	
A (annual)	33.4	50.5	66.4	76.6	
B	32.5	49.1	64.6	74.5	
Annual	32.9	49.8	65.5	75.5	

Table 5.21 gives the annual projections for the large plant. Since this plant has only one demand period, determining the annual solar contribution can be simplified. Runs for August and September periods were made for this plant at the two locations shown. These runs were assumed to give reasonable indication of the performance of the system for the total 8-week demand period. The September and August percentages were averaged to give the annual performance. These annual results for each system scale are used to predict the average long-term performance for the large plant at all three test locations.

The final results of all three fruit and vegetable plants are shown in Table 5.22. The results were obtained using the ASHRAE weekly average model similar to the dairy and meat plants except that the simulated annual performance for each plant was used instead of the September simulation results in the other plants. The Indianapolis results were interpolated from the projections at East Lansing and Columbia based on the average year simulations for the medium dairy plant. These results are combined with similar results for the dairy and meat plants in the next chapter for a discussion of the economic feasibility.

The overall simulation results for the processing plants are presented as the percentage of the annual demand which can be supplied by the solar collectors. This long-term annual percentage, used for economic considerations, does not indicate the actual seasonal or year to year performance of these systems. It must be understood that day to day performance may fluctuate from 0 to 100 percent. Actual design of a solar system needs to be based on other factors besides the long-term performance.

Table 5.21 - Annual Projected Performance of Solar Water Heating System for Large Fruit and Vegetable Plant (Percentage of demand supplied by solar energy).

Scale:	a	b	c	d	e
Collector area	4015	8030	14050	20070	32100
East Lansing, 1974					
Demand Period					
August		32.7*			
September	22.7	35.9*	49.0	58.0	69.8
Average	21.7	34.3	46.8	55.4	66.7
Columbia, 1952					
Demand Period					
August		51.9*			
September	34.7	54.5*	73.7	86.6	
Average	33.9	53.2	71.9	84.5	

*actual simulation results

Table 5.22 Long Term Annual Performance of Solar Water Heating System for Fruit and Vegetable Plants at all Test Location (Percentage of demand supplied by Solar energy).

Scale:	a	b	c	d	e
Small plant					
Collector area	670	1340	2340	3340	5365
East Lansing	32.8	38.6	60.9	69.5	79.1
Indianapolis	35.0	46.2	63.2	71.0	
Columbia	36.9	52.6	65.2	72.3	
Medium Plant					
Collector area	525	1050	1850	2650	4200
East Lansing	23.6	36.0	47.6	55.1	64.4
Indianapolis	25.9	39.4	52.0	60.0	
Columbia	32.9	49.8	65.5	75.5	
Large Plant					
Collector area	4015	8030	14050	20070	32100
East Lansing	23.7	37.5	51.2	60.6	73.0
Indianapolis	26.5	41.7	56.6	66.6	
Columbia	28.8	45.2	61.1	71.7	

6. FEASIBILITY RESULTS AND DISCUSSION

This chapter discusses the economics of solar water heating for each size dairy, meat, and fruit and vegetable plant. Each plant type; dairy, meat, and fruit and vegetable is discussed separately.

The economic analysis presented shows only the general feasibility trends. The costs of conventional energy, life time of the system, and interest rates assumed for this discussion represent present day economic conditions. It should be realized that changes in or deviations from these assumptions can significantly affect the economic results. In future years changes in these assumptions will have a positive effect upon the feasibility of solar water heating for food processing plants.

6.1 Dairy Plant Feasibility

Dairy plant solar water heating annual performance curves, shown in Figures 6.1a, b, c, were constructed from simulation results given in Table 5.13. The abscissa shows the collector areas (system size), the left ordinate shows the predicted annual percentage of total energy demand supplied by the solar water heater, and the right ordinate gives the corresponding value of this energy. Each geographic test location is shown by a single curve. Identification is made using the method described in Table 4.4. For example: E:S:2 represents the small dairy plant at the Indianapolis test location. Table 3.2, showing the warm

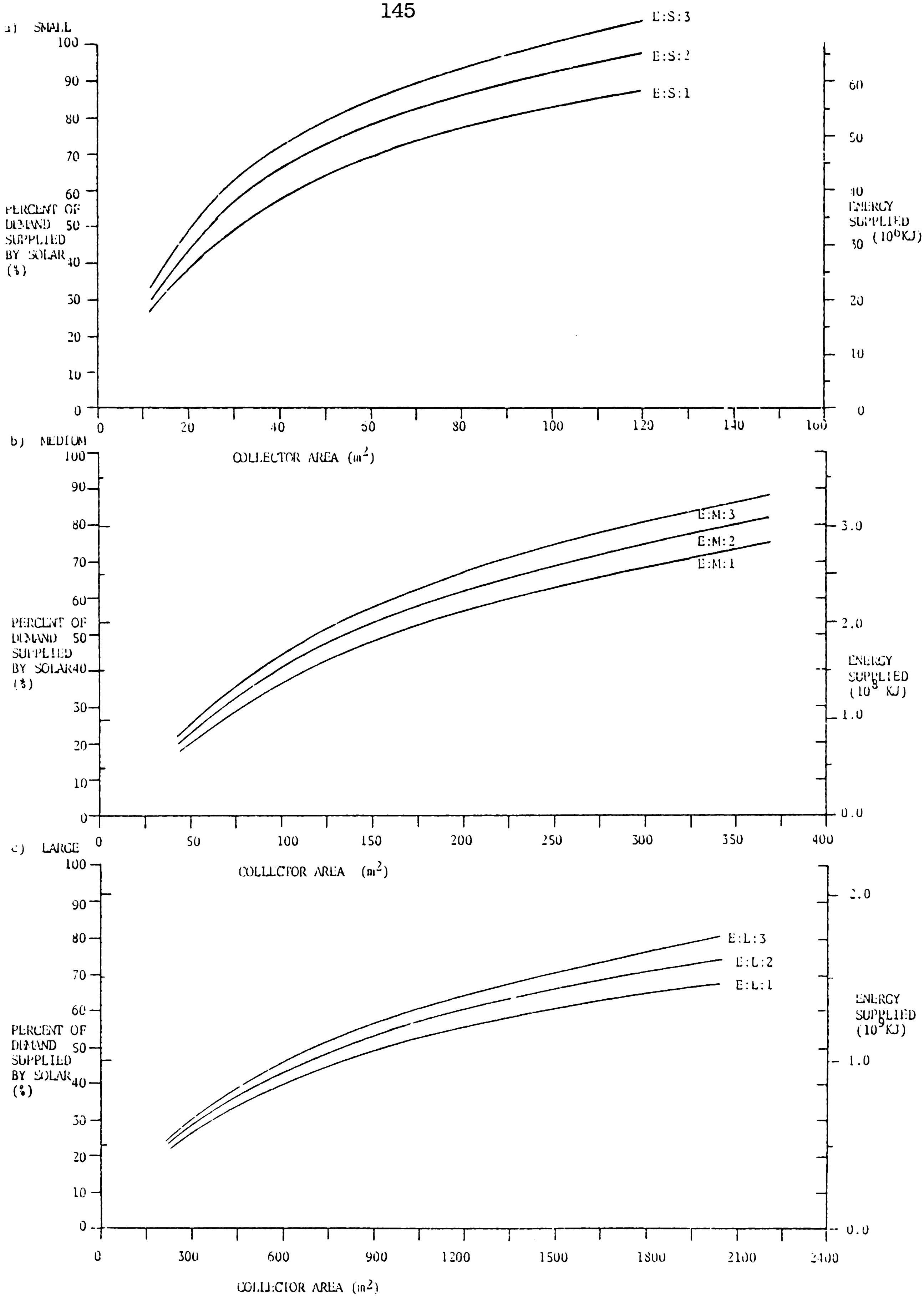

Figure 6.1a,b,c Dairy Plant Solar Water Heater Performance Curves.

water usage, and Figure 3.5, showing the demand schedules for each plant size are useful for interpreting these results.

All performance curves in Figure 6.1 exhibit a decreasing rate of increase of the percent of energy supplied by the solar energy system as the collector area increases. This is expected since at the higher system operating temperatures, corresponding to large collector areas, energy losses increase and collector efficiencies decrease because higher collector operating temperatures cause a decrease in the daily period of energy collection. Each size plant; small, medium, and large, exhibits a similar performance trend. Differences in performance due to the energy demand loads for each plant are not evident in these curves.

The effect of geographic location is clear. The East Lansing test location shows the worst performance while the Columbia location the best. The Indianapolis location appears approximately midway between the Columbia and East Lansing locations.

The values for percent of demand supplied by solar (is shown in Figure 6.1) are used in the following analysis as an indication of system size. These curves serve to relate a given percentage to the appropriate collector size for determining the cost of the solar energy system.

The present day[1] energy costs, for each size plant, of solar energy, electricity, fuel oil, and natural gas are shown in Figure 6.2. The abscissa indicates the percentage of demand supplied by the solar energy system. The ordinate indicates the energy costs for each source for one million kilo-Joules, on an annual basis.

---

[1]These costs include boiler inefficiencies, operating costs, etc., as recommended by Fryling (1966).

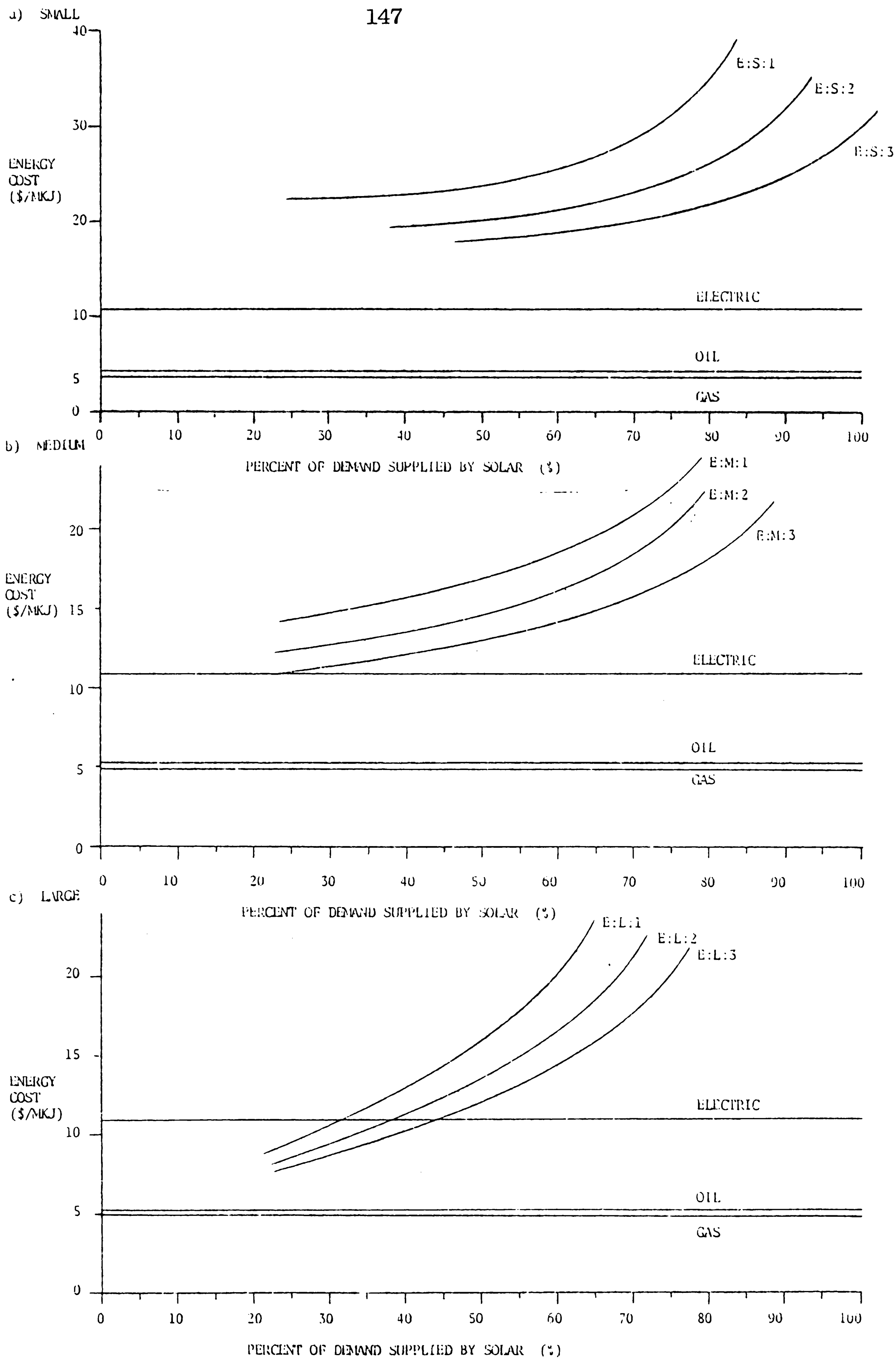

Figure 6.2a,b,c Dairy Plant Solar Water Heater Energy Cost Comparison.

The costs of conventional sources (electricity, fuel oil, and natural gas) are constant. Since each of these is a high grade (meaning capable of producing high temperatures) energy source, the cost is the same for producing one million kilo-Joules at any temperature. In actual practice, energy losses, due to low efficiencies, also increase for these energy sources at high temperatures. Also, large volume consumers of petroleum fuels and electricity often receive rate cuts for using more energy. However, these factors of conversion efficiency and unit costs are assumed constant for this analysis.

Each plot of solar energy costs in Figure 6.2 shows a gradual and then rapid increase in the cost of energy as the percent of demand supplied by the collectors increases. The East Lansing curves for each plant size exhibit the largest cost and the Columbia curves the lowest.

The small dairy plant shows a much higher energy cost than either the medium or large plant. Costs for the small plant nearly level off below the 40 percent supply level at the East Lansing location at a cost of 23 $/MKJ and below the 50 percent supply level for the Columbia location at a cost of 18 $/MKJ. At higher percentages the costs increase rapidly. The medium and large plants show costs below 15 and 13 $/MKJ, respectively, at the same percentages. One reason for the high costs of the small plant is evident from Figure 3.5. The small plant uses energy only 3 days per week at a temperature lower than the other plants (Table 3.2). Although the lower temperature tends to increase the percentage of solar delivered to the load, the off days and weekends appear to decrease the economic usability of the system.

The medium size dairy plant curve for Columbia from Figure 6.2, shows a comparable present day cost to that of electricity at the 20 to 25 percent supply level. The cost of solar energy at Indianapolis and East Lansing approaches the cost of electricity at a much lower percentage. Costs for oil and gas remain far below the costs of solar energy at the lowest percentages.

The large dairy plant shows the most favorable result. At 33 to 45 percent of the energy demand, solar energy compares favorably with electricity for all locations. As the percentage supplied approaches zero, the cost of solar energy nears the cost of oil and gas. The lower costs of the large plant compared to the medium plant appear to be related to the demand schedule. Figure 3.5 shows a longer and more constant demand for the large plant compared to the intermittent 5-day demand of the medium plant. From Table 3.2 the large plant also requires a higher temperature than either of the smaller plants. Thus, the overall use capacity appears to be higher for the large plant.

Based on this cost comparison, the benefit of using a solar water heater appears negative for the small dairy and limited to less than 30 percent for the large and medium plants when the current energy source is electricity. For oil and gas, there is still a large cost differential. Since most dairy plants use petroleum fuel to generate warm water, the benefit of using solar energy for this purpose appears unacceptable at this time. As oil and gas prices increase the cost differential will decrease. However, the present day energy cost comparison presented in this section does not consider future energy price increases.

The long-term feasibility of solar water heating can be evaluated by comparing the total cost of supplying hot water using different types of energy over a 20-year time period. A break even point is reached when the capital investment cost of a solar energy system becomes equal to the allowable investment. The allowable capital investment, for oil and electricity, is equal to the present value of the future cost of energy which can be supplied by the solar system over a period of 20 years at an interest rate of 10 percent and a fuel price increase of 5 percent per year. From this comparison the size of solar water heater which is justified can be determined. This comparison was made for the solar energy system, electricity, oil, and gas in order to observe the possible benefits of using solar energy in the long term.

Figure 6.3 shows the result of the capital investment analysis for each size dairy plant. For each plant a plot of capital investment is drawn as a function of percent of demand supplied by solar. The capital investment[1] (from equation 4.1) required to construct solar water heaters at each test location and the allowable capital investments for electricity and oil are shown. Curves for natural gas are not included because of the present day small price difference between oil and natural gas.

From Figure 6.3a the small dairy results indicate a capital investment break even point with electricity for all test locations below the 50 percent range. This result appears marginal and offers no real incentive to invest in a solar energy system. The medium and large plants shown in Figure 3.6b, c, show a significant advantage compared to electricity below the 70 percent supply range.

The break even point of the solar energy system compared to oil is nearly reached by the large and medium plant at the 20 percent supply level. Compared to the present energy costs in Figure 6.2, these results

---

[1]The capital investment for the solar energy system does not include annual operating costs for maintenance and electricity. These factors must be considered along with similar considerations for conventional energy installations.

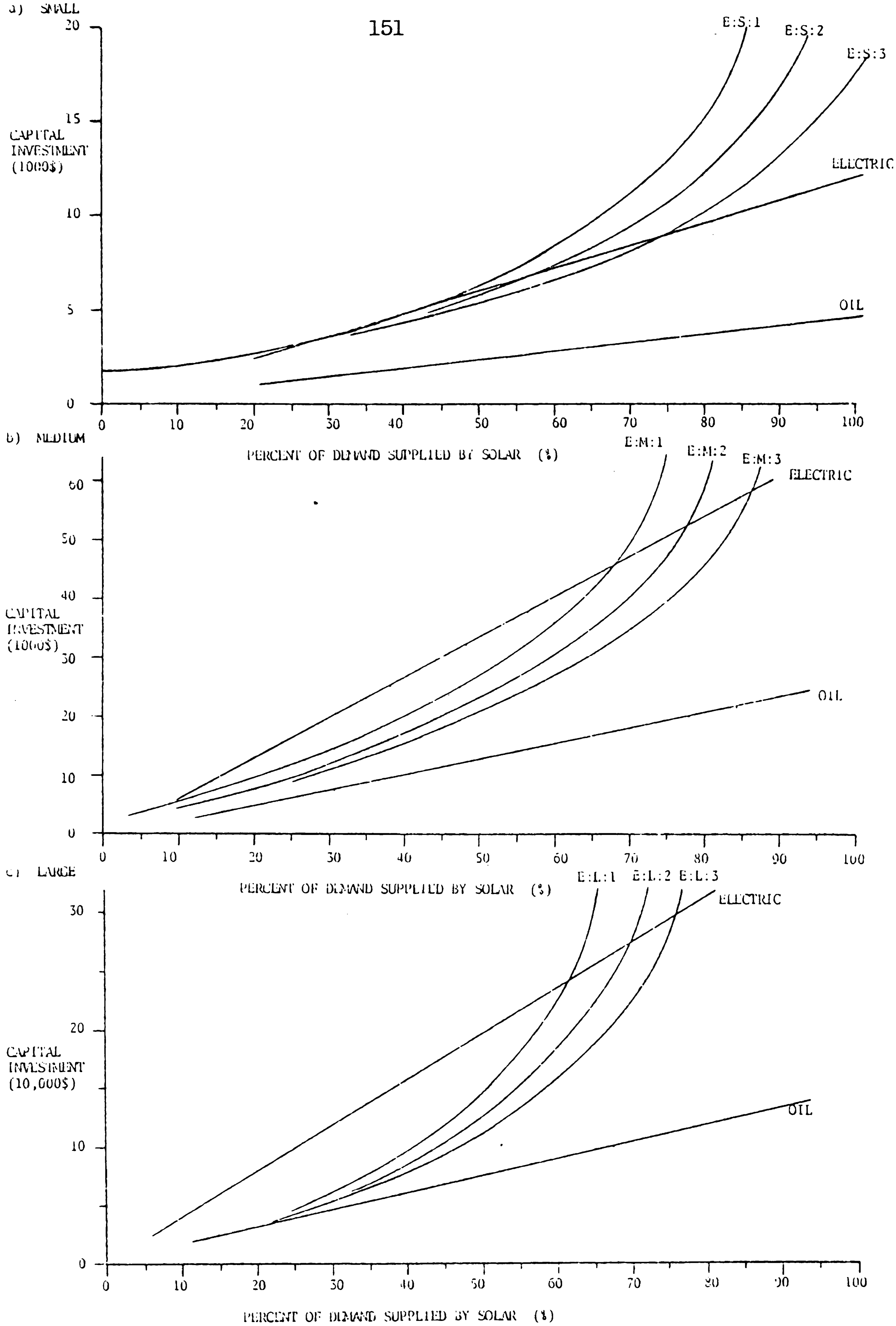

Figure 6.3a,b,c Dairy Plant Solar Water Heater Capital Investment Comparison.

indicate a significant advantage in the long run for using solar energy to replace 30 to 60 percent of the electric energy demand for the large and medium plants. A small contribution can be made to replace the petroleum demand.

The overall feasibility in the dairy industry appears to be limited to a solar energy contribution of less than 20 percent of the total demand in view of the present day primary industry dependence on oil and gas. The use factor has an important effect upon the overall feasibility. The small dairy may be able to justify solar energy use by expanding its processing periods or finding other uses for the solar heated warm water.

6.2 Meat Plant Feasibility

Meat plant solar water heater performance curves are shown in Figure 6.4a, b, c. These curves are similar to those described for the dairy plants. The decreasing rate of supply with increasing collector area and the increase in system performance for Columbia over East Lansing is easily observed.

Figure 6.5 gives the energy cost comparisons for the meat processing plants. All three plants show a favorable comparison of solar energy with electricity at the 30 to 50 percent supply range, with the medium and large plants showing an advantage over the small plant. Both of these larger plants also show a slightly greater decreasing rate of energy cost compared to the small plant. This trend indicates a favorable comparison of these plants with oil and gas at the less than 10 percent supply range.

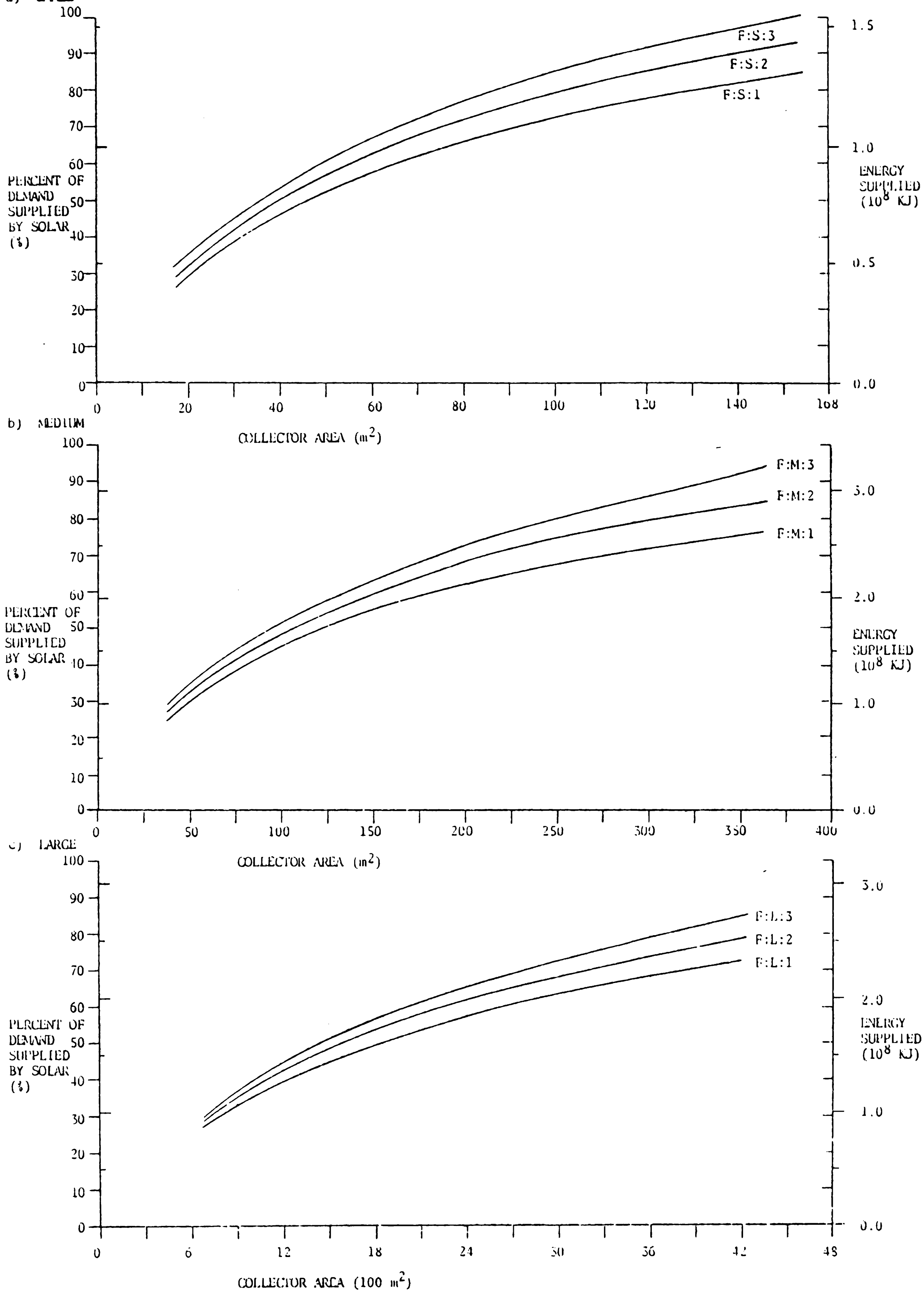

Figure 6.4a,b,c Meat Plant Solar Water Heater Performance Curves.

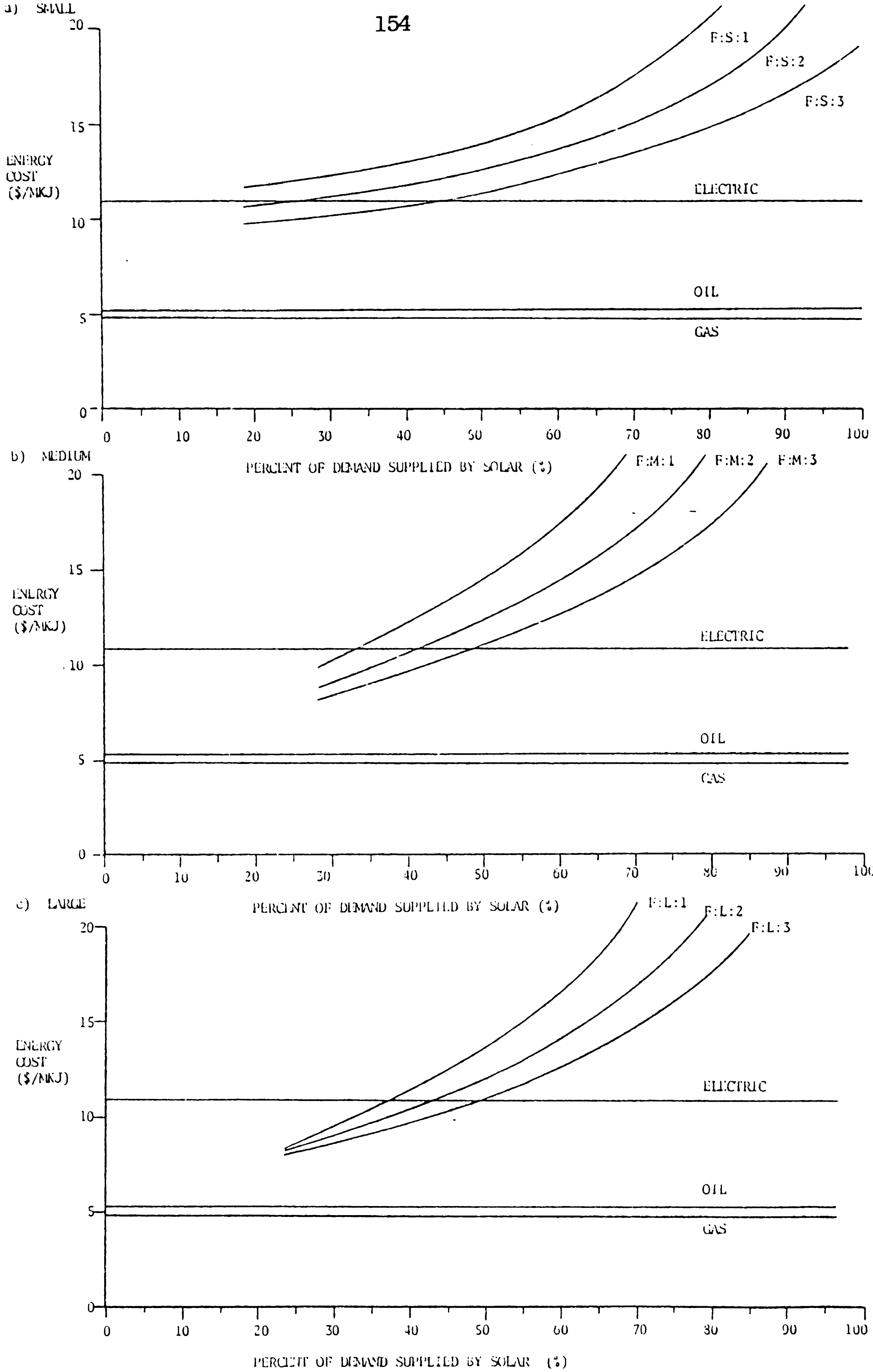

Figure 6.5a,b,c Meat Plant Solar Water Heater Energy Cost Comparison.

A look at the demand schedules for the meat processing plants, Figure 3.6, illustrates that the small and medium plants have a time varying schedule, while the large plant schedule is constant during the total 6-day period. Since the medium and large plants show an energy cost curve similarity, the effect of demand schedule appears insignificant. The medium and large plants, however, both require the same warm water temperature, as shown in Table 3.3. Thus, effect of increasing temperature above that of the small plant is responsible for the increase in performance and lower energy costs of the medium and large plants below the 50 percent supply level. Above this level, the rate of increase in energy cost for the two larger plants is greater than for the small plant. This illustrates the limiting effect of the higher collector operating temperature as the system supplies more of the energy demand load.

The capital investment analysis results for the meat plants are given in Figure 6.6. All three plants show a cost advantage over electricity below the 70 percent supply level. The small plant shows a justified percent supply level greater than the medium and large plants of 20 to 30 percent. This illustrates the effect of the lower warm water supply temperature delivered by the solar water heater for the small plant relative to the medium and large plants. Near the 30 percent supply level all three plants approach the break even point for oil.

The benefits of solar water heating for the meat processing industry appear to be real and independent of plant size. The effect of warm water temperatures appears to be minor with respect to the overall performance. The feasibility of using solar energy shows real promise for replacing

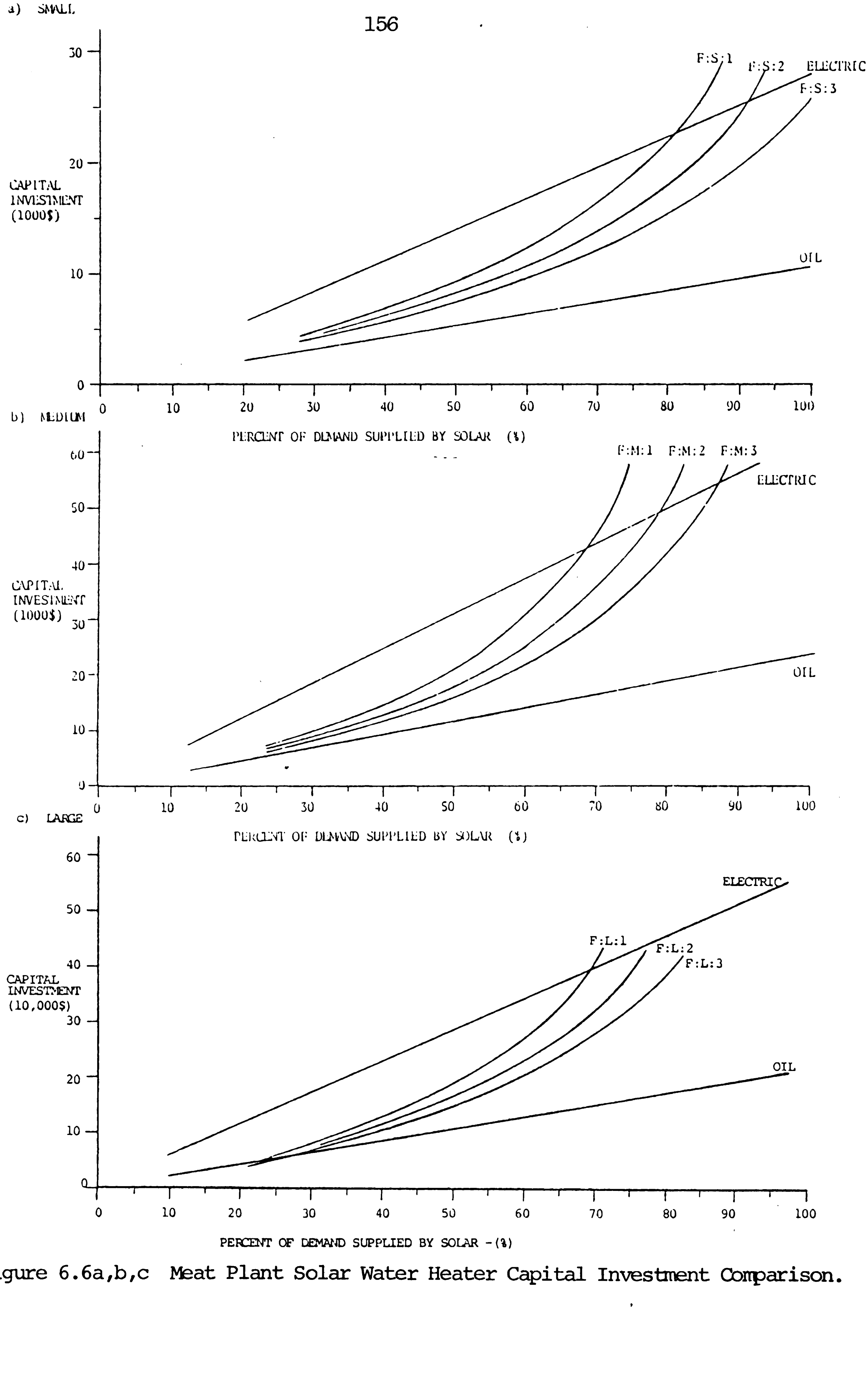

Figure 6.6a,b,c Meat Plant Solar Water Heater Capital Investment Comparison.

electricity. The replacement of petroleum fuel is real for only small demand percentage applications, while a future potential exists for a significant contribution with an increase in oil and gas prices.

6.3 Fruit and Vegetable Plant Feasibility

Performance curves for the fruit and vegetable plants are presented in Figure 6.7a,b,c. These curves follow similar trends established by the dairy and meat plants even though the fruit and vegetable plants are generally seasonal in their operation. The medium plant has an annual demand schedule according to Table 3.4 compared to the seasonal demand schedules of the small and large plants. This factor does not noticably affect the performance curves. For the East Lansing test location the curves are extended beyond the Indianapolis and Columbia curves. This is a result of the extra simulation performed at East Lansing.

Energy cost comparisons for the fruit and vegetable plants are shown in Figure 6.8. The small and large plants show a greater solar energy cost compared to the medium plant. This is primarily a result of the seasonal usage patterns characteristic of many canning plants. The large plant has a greater solar energy cost than the small plant because of the extremely short processing period, as shown in Table 3.4. The small plant indicates a favorable cost comparison with electricity near the less than 10 percent supply level. The effect of daily demand schedules cannot be observed because of the extreme variations due to the seasonal use patterns. The medium plant exhibits an energy cost comparable to electricity near the 40 percent supply level and approaches a break even point with oil in the less than 10 percent range.

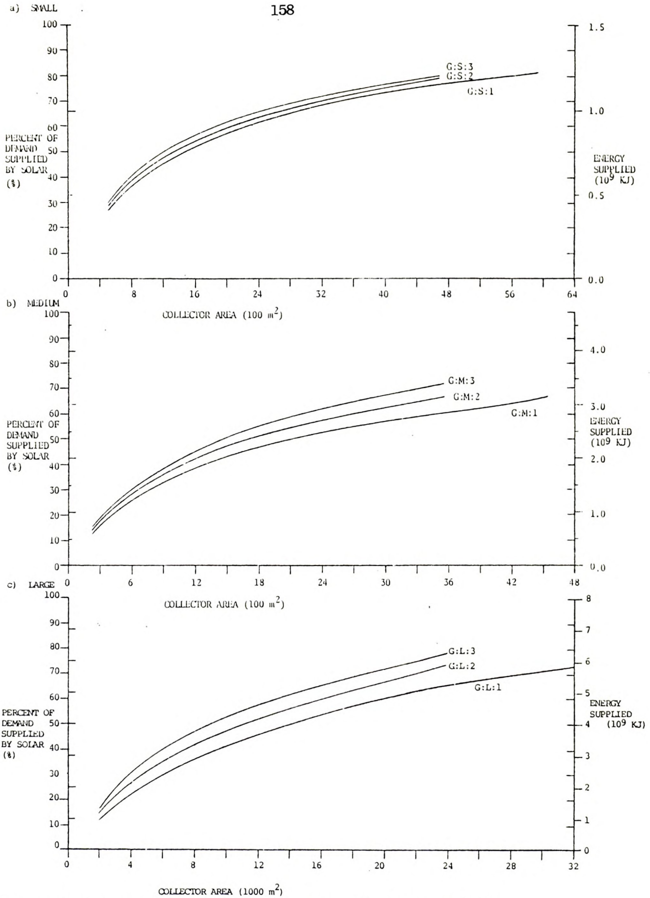

Figure 6.7a,b,c Fruit and Vegetable Plant Solar Water Heater Performance Curves.

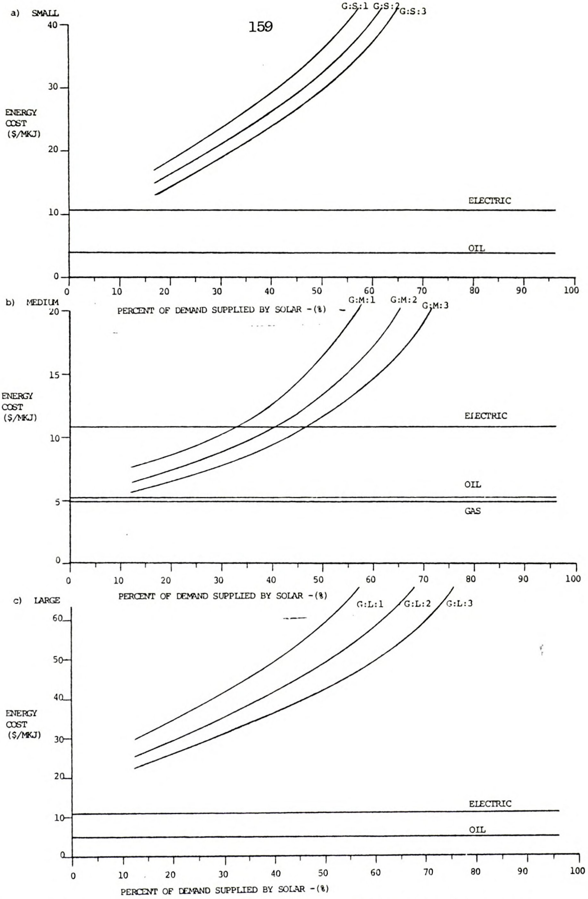

Figure 6.8a,b,c Fruit and Vegetable Plant Solar Water Heater Energy Cost Comparison.

Since the medium plant has year around operation, the comparison of present day costs appears quite favorable to a solar energy application. The other plants do not show this result. If a different energy demand can be justified for these plants in order to increase their use factor, the cost comparison is likely to be favorable.

The long range results for the fruit and vegetable plants are shown in Figure 6.9. It is notable that even with the very high costs of solar water heating systems in these plants, the capital investment approaches a break even point with electricity near the 30 percent level for the small plant and 10 percent for the large plant. This indicates that a potential does exist for these plants also because an off season energy demand could significantly improve the solar energy feasibility.

The medium plant shows favorable results (see Figure 6.9) for long-term replacement of petroleum fuel at the 30 percent supply level. The feasibility associated with this plant appears very favorable, since the energy demand remains constant during the winter months and increases during the summer period when the availability of solar energy also increases.

The results of this analysis indicate a definite benefit for solar energy applications for those fruit and vegetable processing plants (in this case a freezing plant) which exhibit a uniform annual demand schedule. A possible application exists for the seasonal canning plants if an appropriate use of the water heating capactiy can be found to increase the overall use factor.

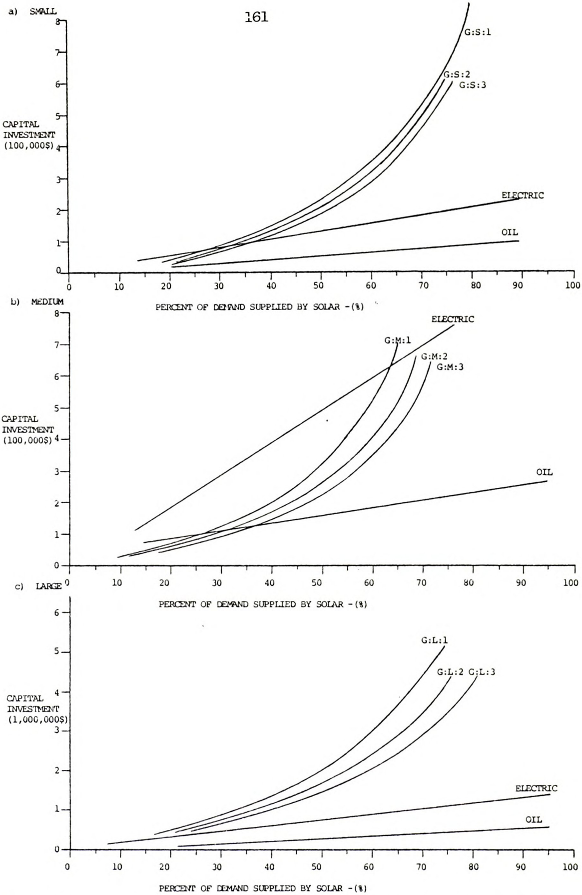

Figure 6.9a,b,c Fruit and Vegetable Plant Solar Water Heater Capital Investment Comparison.

7. SUMMARY

Five insolation models were tested for their accuracy in predicting hourly insolation data for simulating solar water heaters. The ASHRAE weekly model shown in Appendix A, which uses weekly averages of daily total measured insolation (Appendix F) and average air temperature (Appendix E) data to calculate hourly data, was chosen for simulating input insolation data for the "average" year. This model was shown to give annual simulation results within 0.2 percent of a control model which used actual measured hourly values of insolation and air temperatures for the same period. The ASHRAE daily and the Whillier models also gave results within 10 percent of the control model. Tests using 1, 3, and 6-hour average insolation data showed an unacceptable decrease in performance, when using averages greater than one hour.

Parametric tests were performed to determine the best storage tank volume and collector fluid flow rate for a solar water heater of 100 m^2 and a small dairy demand load. Results from these tests produced ratios, of storage volume and collector fluid flow rate to collector surface area, which were used to simulate the food processing plants. Values of the storage tank volume ratio of 0.03875 m^3/m^2 of collector and the collector fluid flow rate ratio of 34.11 $kg/hr/m^2$ of collector were obtained.

A solar water heating model developed with TRNSYS, was used to simulate a solar water heater using water usage surveys for three sizes of dairy, meat, and fruit and vegetable processing plants chosen as representative of the Midwest region. Each plant was simulated for a period of two weeks in September using data for two years at two locations: 1965 and 1974 at East Lansing, Michigan, and 1949 and 1952 at Columbia, Missouri. The medium dairy plant with a collector area of 140 m^2 was simulated for three actual years: 1974 at East Lansing, Michigan and 1949 and 1952 at Columbia, Missouri, and for the average year using the ASHRAE weekly insolation model for all three test locations: East Lansing, Michigan, Indianapolis, Indiana, and Columbia, Missouri. Projected results of these simulations are presented in Tables 5.3, 5.16, and 5.22, and Figures 6.1, 6.4, 6.7. The long-term annual percentage of solar energy which can be delivered to the load as a function of collector area, for each plant and geographic location is given.

From the resulting annual performance projections, an economic comparison of present day energy costs and long-term capital investments was made between solar energy, electricity, fuel oil, and natural gas. A summary of these results is given in Table 7.1. The present day cost of solar energy for most plants compares favorably with electricity when replacing 20 to 45 percent of the demand. The small dairy and the small and large fruit and vegetable plants indicated an overall higher cost of solar energy compared to electricity, oil, and gas. Only the large dairy, medium and large meat plants and the medium fruit and vegetable plant indicated a favorable cost comparison with oil and gas at a supply level below 10 percent.

The long-term capital investment analysis showed a favorable comparison of solar energy with electricity for all plants, ranging from 100

Table 7.1 - Summary of Economic Results of Solar Water Heating and Conventional Energy Sources (Location of the break even point of percentage of demand supplied by solar).

Plant	Solar Energy Unit Cost Comparison Electric %	Oil %	Gas %	Capital Investment Electric %	Oil %
Small Dairy	high	high	high	below 50-70	near 0
Medium Dairy	below 20	high	high	below 65-80	near 0-5
Large Dairy	30-40	0-10	0-10	below 60-75	below 20
Small Meat	0-40	high	high	below 80-100	near 20
Medium Meat	below 35-45	0-10	0-10	below 70-85	near 20
Large Meat	below 35-50	0-5	0-5	below 65-80	near 25
Small F & V	near 0	high	high	below 30-35	near 20
Medium F & V	below 30-45	0-10	0-10	below 60-70	below 25-35
Large F & V	high	high	high	near 20	high

percent supply for the small meat plant to 20 percent supply for the large fruit and vegetable plant. The long-term results of solar energy and oil showed an advantage of solar energy, below 35 percent for all plants. The small dairy and the large fruit and vegetable plants indicated an overall higher cost of solar energy compared to oil.

Generally the application of solar water heating to food processing plants is economically feasible for supplying a major percentage of the energy demand when replacing electricity and a significant percentage when replacing fuel oil and natural gas over the long run. The differences between the type and size of processing plant generally reflected the plant solar water heater use factor. A constant annual demand schedule and a lower warm water supply temperature were shown to improve the overall use factor and feasibility.

These economic results showed the future contribution solar energy can make in supplying energy for food processing plants. Future changes in energy prices and economic trends will realize a greater potential for solar water heating applications.

8. CONCLUSIONS

The following conclusions of this study are:

1. The simulation of hourly insolation and temperature data using the ASHRAE weekly model is acceptable for simulating a solar energy system for long-term periods and for locations where hourly insolation data is unavailable.
2. An engineering feasibility exists for solar water heating for food processing plants for supplying up to 90 to 100 percent of the annual energy demand. Over 100 percent of the demand may be supplied during the summer periods. Auxiliary energy is still necessary for winter time operation and periods of low insolation.
3. Geographic location has a definite effect upon solar water heating feasibility for food processing plants. The Columbia test location showed a significant advantage over East Lansing for solar water heating.
4. The current economic feasibility of solar water heating for food processing plants in the midwestern United States is limited to saving 20 to 50 percent of the conventional energy sources. The realization of this savings is dependent upon the type of plant, use factor, annual demand schedule, warm water supply temperature, type of conventional energy currently employed in the plant, the cost of this energy, and the required

payback period of the capital investment. Larger savings may be realized by the replacement of electricity than of fuel oil or natural gas.

5. All processing plants studied (dairy, meat, and fruit and vegetable) show some degree of energy savings potential. Fruit and vegetable processing plants show a lower use potential because of their seasonal demands. In order to realize the fossil fuel savings, a capital investment is required with a payback period of up to 20 years.

9. SUGGESTIONS FOR FUTURE RESEARCH

The economic analysis performed on solar water heaters for food processing plants generally illustrates the current overall feasibility. Further simulation work should be conducted. In particular:

1. Test other solar water heating models using TRNSYS, to determine the potential of using heat pumps, and of other types of collectors.
2. Study the effects of daily processing plant demand schedules and water temperatures on solar water heater performance.
3. Test the validity of the ASHRAE weekly data simulation model for other geographic locations.

REFERENCES

10. REFERENCES

ASHRAE Applications Handbook, 1974. American Society of Heating, Refrigeration and Air Conditioning Engineers, New York, NY.

Baker, D. G. and D. A. Haines, 1969. Solar Radiation and Sunshine Duration Relationships, North Central Regional Research Publication 195, University of Minnesota, Agricultural Experiment Station Technical Bulletin 262, 372p.

Baker, D. G. and J. C. Klink, 1975. Solar Radiation Reception, Probabilities, and Areal Distribution in the North Central Region, North Central Regional Research Publication 225, University of Minnesota Agricultural Experiment Station Technical Bulletin 300, 54p.

Daniels, F. and J. A. Duffie, ed., 1955. Solar Energy Research, The University of Wisconsin Press, Madison, WI, 290p.

Dansbury, K. P., 1977. A study of the warm water usage in food processing plants. Department of Food Science and Human Nutrition, Michigan State University, East Lansing, MI, Personal communication.

Duffie, J. A. and W. A. Beckman, 1974. Solar Energy Thermal Processes. John Wiley and Sons, New York, NY, 386p.

Edenburn, M. W., 1973. Systems Analysis Computer Program for Solar Community Total Energy Concept. NTIS, SLA-73-0950, October, 1973.

Edenburn, M. W., 1975. Sandia Laboratories Energy System Simulation Computer Program. Solar Systems Division, Sandia Laboratories, Albuquerque, NM, NTIS-75-0712.

Edenburn, M. W. and Grandjean, N. R., 1975. Energy System Simulation Computer Program: SOLSYS. Sandia Laboratories, Albuquerque, NM, 22p.

Fritz, S., 1957. "Solar Energy on Clear and Cloudy Days", The Scientific Monthly, 84:55-65.

Fryling, G. R. ed., 1966. Combustion Engineering, Combustion Engineering Co., New York, NY.

Furnival, G., Wyler, E., Reifsnyder, W., and Siccama, T. G., 1969. SOLAR, a Fortran computer program. Yale School of Forestry, New Haven, CT.

Graven, Robert M., 1974. A Comparison of Computer Programs Used for Modeling Solar Heating and Air Conditioning Systems for Buildings. Lawrence Berkley Laboratory, University of California, Berkley, CA, LBL-3066.

Gutierrez, G., F. Hincapie, J. A. Duffie, and W. A. Beckman, 1974. "Simulation of Forced Circulation Water Heaters; Effects of Auxiliary Energy Supply, Load Type, and Storage Capacity", Solar Energy, 15:(4):287-298.

Holman, J. P., 1972. Heat Transfer, McGraw Hill, Inc., New York, NY, 462p.

Kays, W. M., and A. L. London, 1958. Compact Heat Exchangers, McGraw Hill, Inc., New York, NY.

Klein, S. A., 1974. "Calculation of flat-plate collector loss coefficients", Solar Energy, vol. 17:(11):79-80.

Klein, S. A., P. I. Cooper, W. A. Beckman, and J. A. Duffie, 1974. TRNSYS - A Transient Simulation Program, Madison, University of Wisconsin Engineering Experiment Station Report #38, Madison, WI.

Klein, S. A., P. I. Cooper, T. L. Freeman, D. M. Beekman, W. A. Beckman, and J. A. Duffie, 1975. "A Method of Simulation of Solar Processes and its Application", Solar Energy, vol. 17:(1):29-37.

Kreider, Jan F., and Frank Kreith, 1975. Solar Heating and Cooling: Engineering, Practical Design, and Economics. McGraw Hill, Inc., New York, NY, 341p.

Kreith, Frank, 1973. Principles of Heat Transfer, Intext Educational Publishers, New York, NY, 656p.

Linvill, Dale, 1977. Professor, Department of Agricultural Engineering, Michigan State University, East Lansing, MI, Personal communication.

Local Climatological Data, National Oceanic and Atmospheric Administration, March 1974 to February 1975 at Capitol City Airport, Lansing, MI, Washington, DC.

Löf, G. O. G., 1977. Director, Solar Energy Applications Laboratory, Colorado State University, Ft. Collins, CO. Presentation at the Management Briefing Seminar: Solar Energy-Opportunities and Applications, Dearborn, MI, May 24, 1977.

Liu, Benjamin Y. H., and Richard C. Jordan, 1960. "The Interrelationship and Characteristic Distribution of Direct, Diffuse and Total Solar Radiation", Solar Energy, 4(3):1-19.

Michigan Department of Agriculture, 1974. Climate of Michigan, Michigan Weather Service/NOAA/US Department of Commerce, Washington, DC.

Moon, P., 1940. "Proposed Standard Solar Radiation Curves for Engineering Use", Journal of Franklin Institute, 230:583.

Oonk, R. L., W. A. Beckman, and J. A. Duffie, 1975. "Modeling of the CSU Heating/Cooling System", Solar Energy, 17:(1)21-28.

Owens-Illinois, 1977. The Owens-Illinois SUNPAK Solar Collector.

Solar Research, 1977. The Flat Plate Solar Collector, Solar Research, Division of Refrigeration Research, Inc., Brighton, MI.

Ramsey, J. W., 1975. Development of Flat-Plate Solar Collectors for Heating and Cooling of Buildings, NASA-CR-134804, 209p.

Reding, J. T., and B. P. Shepard, 1975. Energy Consumption: Paper, Stone/Clay/Glass/Concrete/and Food Industries. Report No. EPA-650/2-75-032-C.

Reynolds, William C., and Henry C. Perkins, 1970. Engineering Thermodynamics, McGraw Hill, Inc., New York, NY, 585p.

Sadler, G. W., 1975. "Direct and Diffuse Insolation Using Approximation Methods Applied to Horizontal Surface Insolation", Solar Energy, 17:39-46.

Siegel, Robert, and John R. Howell, 1972. Thermal Radiation Heat Transfer, McGraw Hill, Inc., New York, NY, 814p.

Solar Radiation Considerations in Building Planning and Design, 1976. Proceedings of a Working Conference, National Academy of Sciences, Washington, DC.

Thomas, S. M., 1977. Michigan Solar Insolation and Its Weather Dependence. Unpublished Technical Problem Report, Department of Agricultural Engineering, Michigan State University, East Lansing, MI.

Threlkeld, J. L., and R. C. Jordan, 1957. "Direct Solar Radiation Available on Clear Days". Heating, Piping, and Air Conditioning, 29:(12):135-145.

Whillier, A., 1956. "The Determination of Hourly Values of Total Solar Radiation from Daily Summations", Arch, Met. Geoph, Biolk, B. Bd. 7. H.2:-97-244.

Whillier, A., 1967. "Design Factors Influencing Solar Collector Performance". Low Temperature Engineering Applications of Solar Energy, ASHRAE, New York, NY, pp 27-39.

Williams, W. A., R. S. Loomis, and M. B. Carter, 1974. "Computing Hourly Values of Diffuse and Direct Sunlight", Crop Science, 14:492-493.

U. S. Department of Commerce, 1964. Climatic Summary of the United States - Supplement for 1951-1960, Indiana. Climatography of the United States No. 86-10, Decennial census of U. S. Climate, Washington, DC.

U. S. Department of Commerce, 1968. Climates of the Untied States-Missouri, Washington, DC.

APPENDICES

APPENDIX A

Table A. ASHRAE Insolation Model Ratios (Hourly horizontal insolation per daily total horizontal insolation)[4].

	Solar Time[1]							
Periods[2]	11:30/ 12:30	10:30/ 11:30	9:30/ 10:30	8:30/ 9:30	7:30/ 8:30	6:30/ 7:30	5:30/ 6:30	4:30/ 5:30
3/1-3/14[3]	.146	.139	.123	.093	.057	.016		
3/15-3/28	.139	.133	.118	.093	.062	.025		
3/29-4/11	.132	.127	.114	.080	.050	.016		
4/12-5/2	.126	.122	.110	.067	.038	.009		
5/3-5/16	.122	.118	.108	.078	.053	.018	.090	
5/17-5/30	.118	.115	.105	.089	.069	.045	.019	
5/31-6/13[3]	.116	.114	.104	.089	.069	.046	.021	
6/14-6/27	.115	.112	.103	.088	.069	.047	.023	.002
6/28-7/11	.113	.113	.104	.088	.069	.046	.021	
7/12-8/1	.118	.114	.105	.089	.069	.045	.020	
8/2-8/15	.122	.118	.108	.090	.069	.042	.015	
8/16-8/29	.126	.122	.110	.091	.067	.039	.009	
8/30-9/12[3]	.132	.128	.114	.092	.063	.042	.005	
9/13-10/3	.139	.134	.118	.093	.061	.039		
10/4-10/17	.146	.141	.122	.093	.056	.031		
10/18-10/31	.145	.148	.126	.094	.050	.024		
11/1-11/14	.164	.155	.130	.090	.040	.014		
11/15-11/28	.173	.162	.134	.087	.030	.005		
11/29-12/12[3]	.178	.167	.136	.085	.024	.003		
13/13-12/26	.183	.171	.137	.083	.018			
12/27-1/16	.178	.166	.136	.086	.024			
1/17-1/30	.173	.162	.134	.088	.030			
1/31-2/13	.163	.154	.130	.090	.041	.0036		
2/14-2/28	.153	.146	.126	.093	.052	.007		

[1]Ratios are the same for morning and afternoon

[2]Based on climatological weekly periods beginning March 1

[3]Ratios used for the insolation model tests

[4]From ASHRAE 1974

APPENDIX B

Table B. Daylength Table for East Lansing (Calculated using program SOLAR).

DATE	JAN	FEB	MAR	APR	MAY	JUNE	JULY	AUG	SEPT	OCT	NOV	DEC
1	9.06	9.58	11.13	12.43	14.05	15.07	15.17	14.30	13.11	11.45	10.19	9.17
2	9.07	10.00	11.16	12.46	14.08	15.08	15.16	14.28	13.08	11.42	10.17	9.15
3	9.08	10.03	11.19	12.49	14.10	15.09	15.15	14.25	13.05	11.39	10.14	9.14
4	9.09	10.05	11.22	12.52	14.13	15.10	15.14	14.23	13.02	11.37	10.12	9.13
5	9.10	10.08	11.25	12.55	14.15	15.11	15.13	14.21	13.00	11.34	10.09	9.12
6	9.11	10.10	11.27	12.58	14.18	15.12	15.13	14.18	12.57	11.31	10.07	9.10
7	9.12	10.13	11.30	13.00	14.20	15.13	15.12	14.16	12.54	11.28	10.04	9.09
8	9.13	10.15	11.33	13.03	14.22	15.14	15.10	14.14	12.51	11.25	10.02	9.08
9	9.14	10.18	11.36	13.06	14.25	15.15	15.09	14.11	12.48	11.22	9.59	9.07
10	9.16	10.21	11.39	13.09	14.27	15.16	15.08	14.09	12.45	11.19	9.57	9.07
11	9.17	10.23	11.42	13.12	14.29	15.17	15.07	14.06	12.43	11.17	9.55	9.06
12	9.18	10.26	11.45	13.15	14.31	15.17	15.06	14.04	12.40	11.14	9.52	9.05
13	9.20	10.28	11.48	13.17	14.34	15.18	15.04	14.01	12.37	11.11	9.50	9.04
14	9.22	10.31	11.51	13.20	14.36	15.18	15.03	13.59	12.34	11.08	9.48	9.04
15	9.23	10.34	11.54	13.23	14.38	15.19	15.01	13.56	12.31	11.05	9.46	9.03
16	9.25	10.37	11.57	13.26	14.40	15.19	15.00	13.54	12.28	11.02	9.44	9.03
17	9.27	10.39	11.60	13.28	14.42	15.19	14.58	13.51	12.25	11.00	9.41	9.02
18	9.28	10.42	12.02	13.31	14.44	15.20	14.57	13.49	12.23	10.57	9.39	9.02
19	9.30	10.45	12.05	13.34	14.46	15.20	14.55	13.46	12.20	10.54	9.37	9.02
20	9.32	10.48	12.08	13.37	14.48	15.20	14.53	13.43	12.17	10.51	9.35	9.02
21	9.34	10.50	12.11	13.39	14.50	15.20	14.52	13.41	12.14	10.49	9.33	9.02
22	9.36	10.53	12.14	13.42	14.51	15.20	14.50	13.38	12.11	10.46	9.32	9.02
23	9.38	10.56	12.17	13.45	14.53	15.20	14.48	13.35	12.08	10.43	9.30	9.02
24	9.40	10.59	12.20	13.47	14.55	15.20	14.46	13.33	12.05	10.40	9.28	9.02
25	9.42	11.02	12.23	13.50	14.56	15.19	14.44	13.30	12.02	10.38	9.26	9.02
26	9.44	11.04	12.26	13.53	14.58	15.19	14.42	13.27	11.60	10.35	9.24	9.02
27	9.47	11.07	12.29	13.55	15.00	15.19	14.40	13.25	11.57	10.32	9.23	9.03
28	9.49	11.10	12.32	13.58	15.01	15.18	14.38	13.22	11.54	10.30	9.21	9.03
29	9.51	0.00	12.35	14.00	15.03	15.18	14.36	13.19	11.51	10.27	9.20	9.04
30	9.53	0.00	12.37	14.03	15.04	15.17	14.34	13.16	11.48	10.24	9.18	9.04
31	9.56	0.00	12.40	0.00	15.05	0.00	14.32	13.14	0.00	10.22	0.00	9.05

APPENDIX C

Table C. Whillier Insolation Model Ratios (Ratio of hourly total horizontal insolation to daily total horizontal insolation)[1].

Day length (hrs)	1/2	1 1/2	2 1/2	3 1/2	4 1/2	5 1/2	6 1/2
9.00	.180	.155	.108	.052	0		
9.25	.176	.153	.108	.056	.005		
9.50	.172	.150	.110	.059	.011		
9.75	.168	.147	.110	.063	.016		
10.00	.165	.145	.110	.065	.020	0	
10.25	.162	.143	.110	.067	.023	.002	
10.50	.158	.140	.109	.069	.027	.003	
10.75	.155	.138	.108	.071	.028	.004	
11.00	.152	.136	.108	.072	.032	.005	
11.25	.149	.134	.107	.073	.034	.007	
11.50	.147	.132	.106	.074	.037	.008	
11.75	.145	.130	.105	.075	.038	.010	
12.00	.142	.128	.105	.076	.041	.011	
12.25	.140	.126	.104	.077	.043	.013	0
12.50	.138	.124	.104	.077	.045	.015	.002
12.75	.135	.123	.103	.078	.047	.018	.002
13.00	.132	.121	.102	.078	.048	.018	.003
13.25	.131	.119	.101	.078	.049	.021	.004
13.50	.128	.118	.101	.078	.059	.023	.005

Table C. (COntinued).

13.75	.127	.116	.100	.078	.052	.025	.007
14.00	.124	.114	.099	.079	.053	.027	.008
14.25	.122	.113	.098	.079	.053	.028	.009
14.50	.120	.111	.098	.079	.054	.030	.010
14.75	.118	.110	.097	.078	.055	.031	.012
15.00	.117	.108	.096	.078	.056	.033	.013
15.25	.115	.107	.095	.078	.057	.034	.015
15.50	.113	.106	.095	.078	.058	.035	.016

[1]From Whillier 1956

APPENDIX D

Table D. Atmospheric Transmissivity Insolation Model Ratios (Average weekly ratio of hourly total horizontal insolation to extraterrestrial hourly horizontal radiation)[1].

Period	Atmospheric Transmissivity
3/1-3/7	.370
3/8-3/14	.421
6/1-6/7	.494
6/8-6/14	.446
9/1-9/7	.470
9/8-9/14	.417
11/30-12/6	.395
12/7-12/13	.292

[1]From Thomas 1977

APPENDIX E

Table E. Average Ambient Air Temperature Used In Average Year ASHRAE Weekly Insolation Model.

1974 Month	East Lansing[1] (MI)	Indianapolis[2] (IN)	Columbia[3] (MO)
January	22.2	30.3	29.1
February	22.2	33.8	31.1
March	32.3	41.9	38.9
April	44.8	54.6	50.8
May	56.5	64.4	61.4
June	66.2	74.0	71.1
July	70.7	78.7	75.2
August	68.9	77.2	73.7
September	61.9	69.3	66.5
October	50.8	58.7	55.4
November	38.0	43.3	40.9
December	26.6	33.8	31.1

[1] Michigan Department of Agriculture 1974
[2] U. S. Department of Commerce 1964
[3] U. S. Department of Commerce 1968

APPENDIX F

Table F. Weekly Averages Of Daily Insolation For All Test Locations.

Climatological Week Beginning March 1	East Lansing (MI) (ly/day)	Indianapolis (IN) (ly/day)	Columbia (MO) (ly/day)
1	256.9	273.7	312
2	292.4	288.3	310.4
3	326.0	332.8	327
4	338.2	336.2	387.6
5	353.2	363.6	364.4
6	378.6	397.2	430.9
7	395.1	414.3	430.8
8	380.9	439.9	451.7
9	423.6	462.5	476.3
10	487.1	515.2	502.3
11	465.1	445.6	503.7
12	501.0	519.4	531.6
13	538.7	524.8	534.7
14	543.6	540.4	529.3
15	529.1	523.0	569.9
16	555.1	571.8	556.2
17	551.9	573.9	583.1
18	539.8	573.7	595.1
19	546.6	560.8	561.4
20	522.8	531.2	589.1

Table F. (Continued).

Climatological Week Beginning March 1	East Lansing (MI) (ly/day)	Indianapolis (IN) (ly/day)	Columbia (MO) (ly/day)
21	546.7	527.5	569.2
22	513.8	545.0	572.4
23	485.8	507.5	553.4
24	475.4	500.9	507.5
25	462.9	490.6	513.3
26	429.3	492.9	502.8
27	411.6	448.6	466.7
28	403.6	443.5	460.4
29	367.6	396.6	426.8
30	310.9	379.6	389.4
31	332.0	361.3	384.1
32	288.4	338.3	345.1
33	255.9	303.5	333.9
34	223.6	280.4	311.1
35	196.7	238.3	260.1
36	160.8	205.1	219.0
37	145.9	193.4	223.3
38	117.3	167.0	185.8
39	123.0	145.3	188.9
40	119.1	149.3	174.0

Table F. (Continued).

41	105.0	124.1	157.9
42	111.9	140.3	169.5
43	104.9	123.7	155.9
44	115.4	135.8	150.2
45	115.5	153.9	178.5
46	137.3	164.8	169.4
47	147.4	161.1	180.6
48	163.0	181.4	199.1
49	190.1	190.0	221.8
50	201.7	213.3	240.9
51	240.8	255.7	276.5
52	251.8	277.4	270.8

Source Baker and Klink 1975

APPENDIX G

Table G. Program SOLAR (Furnival, *et al.*, 1969).

```
      PROGRAM SOLAR ( INPUT=65, OUTPUT, TAPE5=INPUT, TAPE6=OUTPUT )
C MODIFIED TO PRINT RADIATION VALUES IN EASTERN STANDARD TIME
C  BY C THOMAS DEPT OF AE 2/25/77.
C                        PROGRAM SOLAR  -  FIMCIF 103
C
C    WRITTEN BY G. FURNIVAL, E. WYLIE, N. REIFSNYDER AND T. G. SICCAMA
C                  YALE SCHOOL OF FORESTRY,  DECEMBER 1969
C
C THIS PROGRAM CALCULATES SOLAR CLIMATE DATA AND PRINTS OUT TABLES OF HO
C DAILY VALUES OF SOLAR ENERGY OUTSIDE THE EARTHS ATMOSPHERE,DAY LENGTH
C OF SUNRISE,TIME OF SUNSET,AND TIME OF SOLAR NOON. IT IS WRITTEN IN FOR
C VERSION 13. IT IS BASED ON THE PROGRAM/ASTRONOMICOLOGICAL ESTIMATOR
C ROBERTSON AND D.A.RUSSELO,PUBLISHED BY THE AGROMETEOROLOGY SECTION,PLA
C RESEARCH INSTITUTE,CANADA DEPARTMENT OF AGRICULTURE,OTTAWA,ONTARIO,AS
C MET. TECH. BULLETIN 14.JANUARY 1965. THE PROGRAM ASSUMES THE SOLAR CONS
C TO BE 1.95 LANGLEYS PER MINUTE. IT IS IDENTIFIED AS SCON IN A DATA ST
C PROGRAM IS SUITABLE FOR YEARS 1930 - 2000. SOLAR ELEVATION IS ASSUMED
C  - 50 MIN.
C
C ONE CONTROL CARD IS REQUIRED FOR EACH LOCATION ON EARTH FOR WHICH CALC
C ARE DESIRED. THEY ARE PLACED AS DATA CARDS AT THE END OF THE PROGRAM D
C
C                  COLUMN 1-4      YEAR
C                  COLUMN 15-30    STATION IDENTIFICATION (16 ALPHAMERIC SYMBOLS
C                  COLUMN 31       SIGN OF LATITUDE  (N=+,S=-)
C                  COLUMN 32-33    LATITUDE, DEGREES
C                  COLUMN 35-36    LATITUDE,MINUTES
C                  COLUMN 38       SIGN OF LONGITUDE (W=+,E=-)
C                  COLUMN 39-41    LONGITUDE, DEGREES
C                  COLUMN 43-44    LONGITUDE, MINUTES
C                  COLUMN 52-55    MERIDIAN OF STANDARD TIME ZONE (W=+, E=-)
C
      INTEGER STALA2,STLON2,DECL2,DCLO2
      REAL MNLONG,MNSUN,LNOON
      DIMENSION NAME(4),MONDOY(12),MONTH(12),TITLE(9,9),SS(31,12,4),X(4)
      DIMENSION THIRG(13),ENERGA(12)
      DATA                 TITLE  /4H    ,4H     ,4HDAY ,4HLENG,4HTH I
     1,4HN HO,4HURS ,4*4H    ,4H   A,4HND M,4HINUT,4HES  ,3*4H    ,4H  T
     2I,4HME O,4HF SU,4HNRIS,4HE, L,4HOCAL,4H STD,4H TIM,4HE   ,4H    ,
     3 4H  IN,4H HOU,4HRS A,4HND M,4HINUT,4HES  ,2*4H    ,4H  TI,4HME O,
     44HF SU,4HNSET,4H, LO,4HCAL ,4HSTD ,4HTIME,2*4H    ,4H  IN,4H HOU,
     54HRS A,4HND M,4HINUT,4HES  ,2*4H    ,4HTIME,4H OF ,4HSOLA,4HR NO,
     54HON, ,4HLOCA,4HL ST,4HD TI,4HME  ,44   ,4H  IN,4H HOU,4HRS A,
     64HND M,4HINUT,4HES  ,2*4H    /
      DATA    MONTH         /4H JAN,4H FEB,4H MAR,4H APR,4H MAY,4HJUNE,
     14HJULY,4H AUG,4HSEPT,4H OCT,4H NOV,4H DEC/
      DATA   MONDOY          /31,00,31,30,31,30,31,31,30,31,30,31/
      DATA  ,SCON,PI,PPI,RAD,RAH,FIRST,THIRD,POW,A1,A2,A3,SLONG,SANOM,
     1  DLONG,DANOM,OSUN,SINOB,COTOB,SINE /
     2  0.0167247,1.95,3.1415927,6.2831854,0.0174533,0.2617994,
     3  1.5707963,4.712389,0.9997203,3.3344567E-01,0.3495545-03,
     4  0.3061E5-05,4.3950836,6.2413117,0.17202079-01,0.1720196E-01,
     5 -0.23942E-04,0.3978478,2.30b65F3,-0.0145399/
C
C                                   EXPLANATION OF CONSTANTS
C
C  PPI=2.0*PI  RAD=180.0/PI  RAH=12.0/PI  FIRST=PI/2.0  THIRD=3.0*PI/2.0
C  POW=1.0-.05    A1=1.915294*RAD  A2=0.020028*RAD  A3=0.00020*RAD
C  SLONG=(279.95555-20.503500.0)*RAD  SANOM=357.5020*RAD
C  DLONG=0.98564735*RAD  DANOM=0.9856002*RAD  OSUN=SLONG-279.95223*RAD
C  SINOB=SIN(23.44371*RAD)  COTOB=COTAN(23.44371*RAD)
C  SINE=-SIN(50.0/60.0*RAD)
C                                   READ CONTROL CARD
 1000 READ(5,2) NYR,NAME,STALA2,DECL2,STLON2,DCLO2,ZONAS
    2 FORMAT(I4,10X,4A2,2I3,I5,I3,7X,F4.0)
      IF ( NYR.EQ.0 ) CALL EXIT
      STALA = STALA2
      STLON= STLON2
      DCLON = DCLO2
      DECLA = DECL2
      IF(STALA.LT.0.0) DECLA=-DECLA
      IF(STLON.LT.0.0) DCLON=-DCLON
      STALA=STALA+DECLA/60.0
      STLON=STLON+DCLON/60.0
      COSL=COS(STALA/RAD)
      SINL=SIN(STALA/RAD)
      LNOON=12.0+(STLON-ZONAS)/15.0

      DO 40 I=1,4
      DO 40 J=1,12
      DO 40 K=29,31
      SS(K,J,I) = 0.0
   40 CONTINUE
C                                   INITIALIZE EPHEMERIS
      IF(NYR.LE.1956) DAZ=(NYR-1956)/.+365*(NYR-1956)
      IF(NYR.GT.1956) DAZ=(NYR-1957)/4+365*(NYR-1956)
      DAZ=DAZ+STLON/360.0-0.25
      MNLONG=AMOD(SLONG+DLONG*DAZ,PPI)
      ANOM=AMOD(SANOM+DANOM*DAZ,PPI)
      IF(MNLONG.LT.0.0) MNLONG=MNLONG+PPI
      MONDOY(2)=28
      IF((NYR/4)*4.EQ.NYR) MONDOY(2)=29
      IDAY = 0
```

Table G. (Continued).

```
C                                              BEGIN DAY LOOP
      WRITE(6,701)
  701 FORMAT(1X,*DAY      1      2      3      4      5      6      7      8      9      10
     Z  11     12     13     14     15     16     17     18     19     20     21     22     23
     Z 24   TOTAL*)
      DO 110 I=1,12
      J = MONDAY(I)
      DO 109 K=1,J
      IDAY= IDAY + 1
C                                              COMPUTE EPHEMERIS
      MNLONG=MNLONG+DLONG
      ANOM=ANOM+DANOM
      CTERM=A1*SIN(ANOM)+A2*SIN(2.0*ANOM)+A3*SIN(3.0*ANOM)
      TLONG=MNLONG+CTERM
      RHO=ECH/(1.0+E*COS(ANOM+CTERM))
      SIND=SIN(TLONG)*SINOB
      COSD=SQRT(1.0-SIND*SIND)
      APSUN=A SIN(SIND/COSD*COTOB)
      IF(TLONG.GT.PPI)TLONG=TLONG-PPI
      IF(TLONG.GT.FIRST.AND.TLONG.LE.THIRD) APSUN=PI-APSUN
      IF(TLONG.GT.THIRD) APSUN=APSUN+PPI
      TIME=(MNLONG-DSUN-APSUN)/RAH
      IF(TIME.LT.-12.0) TIME=TIME+24.0
      IF(TIME.GT.12.0) TIME=TIME-24.0
C                                              DAYLENGTH,SUNRISE,SUNSET,LOCAL NOON
      DIGA=SINL*SIND
      BIGB=COSL*COSD
      COSS=(SINE-DIGA)/BIGB
      IF(COSS.LT.-1.0) COSS=-1.0
      IF(COSS.GT.1.0) COSS=1.0
      HOURS=A COS(COSS)/RAH
      IF(STALA.GT.60.0) GO TO 111
      X(4)=LNOON-TIME
      X(1)=2.0*HOURS
      X(2)=X(4)-HOURS
      X(3)=X(4)+HOURS
  111 DO 41 KL = 1,4
      IX=X(KL)+0.0067
      H = IX
      SS(K,I,KL) = H + (X(KL)-H)*0.60
   41 CONTINUE
C                                              CALCULATE HOURLY ENERGIES
      COSS=-DIGA/BIGB
      IF(COSS.LT.-1.0) COSS=-1.0
      IF(COSS.GT.1.0) COSS=1.0
      HOURS=A COS(COSS)/RAH
      ITEST=HOURS+1.0
      ANN =(DIGA*60.0*SCON)/(RHO*RHO)
      B = (BIGB*60.0*SCON)/(RHO*RHO*RAH)
      BFN=(SS(K,I,4)-12.00)/60. *100.
      ZINO=0.0
      ZINL=ANN*BFN+B*SIN(RAH*BFN)
      ENERG(1)=ZINL-ZINO
      ZINO=ZINL
      DO 500 NUM=2,13
      ENERG(NUM)=0.0     $     ANUM=NUM-1.
      AJAX=ANUM+BFN
      IF(AJAX.LT.ITEST) GO TO 500
      IF(AJAX.GT.HOURS) AJAX=HOURS
      ZINL=ANN*AJAX+B*SIN(RAH*AJAX)
      ENERG(NUM)=ZINL-ZINO
      ZINO=ZINL
  500 CONTINUE
      AJEN=ZINL      $     ZINO=0.0
      AFN=(12.00-SS(K,I,4))/60.*100.
      ZINL=ANN*AFN+B*SIN(RAH*AFN)
      ENERGA(1)=ZINL
      ZINO=ZINL
      DO 600 IK=2,12
      ENERGA(IK)=0.0              $   ANUM=IK-1
      AJAX=ANUM+AFN
      IF(AJAX.GT.ITEST)GO TO 600
      IF(AJAX.GT.HOURS)AJAX=HOURS
      ZINL=ANN*AJAX+B*SIN(RAH*AJAX)
      ENERGA(IK)=ZINL-ZINO
      ZINO=ZINL
  600 CONTINUE
      AJAXX= ENERGA(1)    $    ENERGA(1)=AJAXX+ENERG(1)
      AJ1=ENERG(2) $ AJ2=ENERG(3) $ AJ3=ENERG(4)   $   AJ4=ENERG(5)
      AJ5=ENERG(6) $ AJ6=ENERG(7) $ AJ7=ENERG(8) $ AJ8=ENERG(9)
      AJ9=ENERG(10)  $  AJ10=ENERG(11) $ AJ11=ENERG(12) $ AJ12=ENERG(13)
      TOTAL=ZINL+AJEN
      WRITE (6,702)K,IDAY,AJ12,AJ11,AJ10,AJ9,AJ8,AJ7,AJ6,AJ5,AJ4,AJ3,
     7AJ2,AJ1,ENERGA,TOTAL
  702 FORMAT(1X,I2,I3,24F5.1,F6.1)
  109 CONTINUE
  110 CONTINUE
C                                              PRINT DAYLENGTH TABLES
      DO 112 I=1,4
      M=2*(I-1)+1
      WRITE(6,708) NAME, NYR
  708 FORMAT(1H1//// 57X,8A2,1X,I4)
      WRITE(6,709) (TITLE(J,M),J=1,9), (TITLE(J,M+1),J=1,9)
  709 FORMAT(1H0,44X,9A4/49X,9A4)
      WRITE(6,710) MONTH
  710 FORMAT(///31X,*DATE*,12(2X,A4)//)
      DO 130 II = 1,31
      WRITE(6,711) II, (SS(II,J,I),J=1,12)
  711 FORMAT(25X,I4,3X,12F6.2)
      IF((II/5)*5.EQ.II) WRITE(6,709)
  130 CONTINUE
  112 CONTINUE
      IF(STALA.GT.60.0) GO TO 1000
      END
```

APPENDIX H

Table H.1 TRNSYS Control Card Deck.

```
              TRNSYS - A TRANSIENT SIMULATION PROGRAM
      FROM THE SOLAR ENERGY LAB AT THE UNIVERSITY OF WISCONSIN
                      VERSION 7.3  2/9/76

SIMULATION        0.            7.360E+02    2.000E-01

TOLERANCES        1.000E-01     1.000E-01

LIMITS    30    30

WIDTH    132

UNIT   9      TYPE   9      CARD READER
    PARAMETERS  11
    1.000E+01   1.000E+00    7.000E+00    5.556E-01    -1.778E+01    9.000E+00    1.150E+03    0.          1.600E+01
    4.187E+01   0.

UNIT  16      TYPE  16      RADIATION PROCESSOR
    PARAMETERS   7
    1.000E+00   2.440E+02    4.270E+01    3.900E+01     0.           4.875E+03    0.
    INPUTS   1
     9,10
    0.

UNIT   1      TYPE   1      SOLAR COLLECTOR
    PARAMETERS   7
    1.000E+00   2.500E+01    9.500E-01    2.386E+00     9.000E-01    2.000E+01    8.333E-01
    INPUTS   4
     3, 1        3, 2         9, 7         16, 1
    1.000E+01   0.           9.000E+00    0.

UNIT   2      TYPE   2      SOLAR CONTROLLER
    PARAMETERS   3
    1.000E+01   3.000E+00    5.000E-01
    INPUTS   3
     1, 1       13, 1         2, 1
    2.000E+01   2.000E+01    0.

UNIT   3      TYPE   3      COLLECTOR PUMP
    PARAMETERS   1
    8.580E+02
    INPUTS   3
     5, 1        5, 2         2, 1
    1.000E+01   0.           0.

UNIT   5      TYPE   5      HEAT EXCHANGER
    PARAMETERS   4
    2.000E+00   4.750E+03    2.386E+00    4.196E+00
    INPUTS   4
     1, 1        1, 2        13, 1        13, 2
    2.000E+01   0.           2.000E+01    0.

UNIT  13      TYPE   3      HEAT EXCHANGER PUMP
    PARAMETERS   1
    1.135E+03
    INPUTS   3
     4, 1        4, 2         2, 1
    2.000E+01   0.           0.
```

Table H.1 (Continued).

```
UNIT  4        TYPE   4      STORAGE TANK
     PARAMETERS  5
     9.462E-01     2.000E+00     4.196E+00     1.000E+03     5.960E+00
     INPUTS   5
      5, 3           5, 4          5, 1          14, 1          0, 1
     2.000E+01      0.                         1.273E+01     0.            1.600E+01
     DERIVATIVES   1
     2.000E+01

UNIT  6        TYPE   6      AUXILIARY HEATER
     PARAMETERS  4
     1.700E+05     6.553E+01     2.000E+00     4.196E+00
     INPUTS   2
      4, 3           4, 4
     6.553E+01      0.

UNIT 14        TYPE 14      FORCING FUNCTION CYCLE 48 HOURS
*SMALL DAIRY DEMAND DATA
     PARAMETERS 40
     0.            0.            1.200E+01     0.            1.200E+01     1.390E+02     1.600E+01     1.390E+02     1.600E+01
     6.920E+02     1.310E+01     6.920E+02     1.800E+01     0.            6.920E+01     0.            6.900E+01     1.390E+02
     6.400E+01     1.390E+02     6.400E+01     6.920E+02     6.600E+01     6.920E+02     6.600E+01     0.            1.390E+02
     0.            1.390E+02     1.390E+02     1.120E+02     1.390E+02     1.120E+02     6.920E+02     1.140E+02     6.920E+02
     1.140E+02     0.            1.630E+02     0.
UNIT 25        TYPE 25      SECOND PRINTER
     PARAMETERS  4
     6.000E+00     0.            2.160E+03     6.000E+00
     INPUTS 10
      1, 1           4, 1          24, 1          24, 2          24, 5          24, 6          24, 4          24, 3          24, 7
     24, 7
     TCOL          TTANK         RADT          QCOL           QTANK          QAUX           QENVT          QHX            FLOW
     XXX

UNIT 24        TYPE 24      INTEGRATOR
     INPUTS   8
     16, 1           1, 3          5, 5          4, 5           4, 6           6, 3           1, 2          14, 1
     0.             0.            0.            0.             0.             0.             0.            0.

UNIT 26        TYPE 26      PLOTTER
     PARAMETERS  4
     6.000E+00     0.            2.280E+03     1.000E+01
     INPUTS  4
      1, 1           4, 1          6, 1           0, 7
     TCOL          TTANK         TAUX           TAMB
END
```

Table H.1 (Continued).

```
  TRNSYS COMPONENT OUTPUT MAP

UNIT   9 TYPE   9    UNIT/TYPE/INPUT
      OUTPUT   3        1   1   3
                       26  26   4
      OUTPUT  13       16  16   1

UNIT  16 TYPE  16    UNIT/TYPE/INPUT
      OUTPUT   1        1   1   4
                       24  24   1

UNIT   1 TYPE   1    UNIT/TYPE/INPUT
      OUTPUT   1        2   2   1
                        5   5   1
                       35  25   1
                       26  26   1
      OUTPUT   2        5   5   2
                       24  24   3
      OUTPUT   3       24  24   2

UNIT   2 TYPE   2    UNIT/TYPE/INPUT
      OUTPUT   1        2   2   3
                        3   3   3
                       13   3   3

UNIT   3 TYPE   3    UNIT/TYPE/INPUT
      OUTPUT   1        1   1   1
      OUTPUT   2        1   1   2

UNIT   5 TYPE   5    UNIT/TYPE/INPUT
      OUTPUT   1        3   3   1
      OUTPUT   2        3   3   2
      OUTPUT   3        4   4   1
      OUTPUT   4        4   4   2
      OUTPUT   5       24  24   3

UNIT  13 TYPE   3    UNIT/TYPE/INPUT
      OUTPUT   1        2   2   2
                        5   5   3
      OUTPUT   2        5   5   4

UNIT   4 TYPE   4    UNIT/TYPE/INPUT
      OUTPUT   1       13   3   1
                       35  25   2
                       26  26   2
      OUTPUT   2       13   3   2
      OUTPUT   3        6   6   1
      OUTPUT   4        6   6   2
      OUTPUT   5       24  24   4
      OUTPUT   6       24  24   5

UNIT   6 TYPE   6    UNIT/TYPE/INPUT
      OUTPUT   1       35  25   3
      OUTPUT   3       24  24   6

UNIT  14 TYPE  14    UNIT/TYPE/INPUT
      OUTPUT   1        4   4   4
                       24  24   9

UNIT  35 TYPE  25    UNIT/TYPE/INPUT

UNIT  24 TYPE  24    UNIT/TYPE/INPUT
      OUTPUT   1       35  25   3
      OUTPUT   2       35  25   4
      OUTPUT   3       35  25   9
      OUTPUT   4       35  25   7
      OUTPUT   5       35  25   5
      OUTPUT   6       35  25   6
      OUTPUT   7       35  25  10
      OUTPUT   8       35  25   9

UNIT  26 TYPE  26    UNIT/TYPE/INPUT
```

Table H.2 Sample Simulation Results.

```
TRANSIENT SIMULATION              STARTING AT TIME = 0.
                                  STOPPING AT TIME = 3.360E+02
                                          TIMESTEP = 2.000E-01
         DIFFERENTIAL EQUATION ERROR TOLERANCE = 1.000E-01
                   ALGEBRAIC CONVERGENCE TOLERANCE = 1.000E-01
```

0.0000	8.839E+00	2.000E+01	0.	0.	0.	0.	0.	0.	0.	0.
6.0000	1.382E+01	1.976E+01	6.737E+10	0.	0.	0.	9.434E+02	0.	0.	0.
12.0000	5.321E+01	4.791E+01	1.257E+14	1.647E+05	0.	0.	4.644E+03	1.414E+05	0.	5.933E+03
18.0000	1.722E+01	1.946E+01	1.774E+14	1.979E+05	1.497E+05	2.643E+05	1.016E+04	1.736E+05	1.971E+03	8.318E+03
24.0000	1.333E+01	1.351E+01	1.774E+14	1.979E+05	1.558E+05	2.773E+05	1.079E+04	1.756E+05	1.940E+03	8.318E+03
30.0000	1.990E+01	1.835E+01	1.774E+14	1.939E+05	1.558E+05	2.773E+05	1.137E+04	1.756E+05	1.940E+03	8.018E+03
36.0000	1.022E+01	1.842E+01	1.875E+14	1.941E+05	1.559E+05	2.774E+05	1.194E+04	1.767E+05	1.940E+03	8.359E+03
42.0000	4.733E+00	1.328E+01	1.978E+14	1.941E+05	1.559E+05	2.779E+05	1.251E+04	1.767E+05	1.940E+03	8.359E+03
48.0000	7.225E+00	1.414E+01	1.979E+14	1.941E+05	1.559E+05	2.779E+05	1.305E+04	1.767E+05	1.940E+03	8.359E+03
54.0000	7.335E+01	1.892E+01	1.979E+14	1.941E+05	1.559E+05	2.779E+05	1.355E+04	1.767E+05	1.940E+03	8.359E+03
60.0000	6.549E+01	4.937E+01	3.368E+14	3.712E+05	1.559E+05	2.779E+05	1.711E+04	3.291E+05	1.940E+03	1.322E+04
66.0000	1.444E+01	2.135E+01	4.097E+14	4.426E+05	3.269E+05	5.150E+05	2.353E+04	4.077E+05	3.911E+03	1.621E+04
72.0000	5.910E+00	1.966E+01	4.097E+14	4.426E+05	3.291E+05	5.281E+05	2.445E+04	4.077E+05	3.990E+03	1.621E+04
78.0000	7.707E+00	1.940E+01	4.098E+14	4.426E+05	3.291E+05	5.281E+05	2.531E+04	4.007E+05	3.990E+03	1.621E+04
84.0000	6.339E+01	4.709E+01	5.343E+14	6.045E+05	3.291E+05	5.281E+05	2.992E+04	5.400E+05	3.930E+03	2.107E+04
90.0000	1.556E+01	5.825E+01	6.335E+14	6.793E+05	3.291E+05	5.281E+05	3.885E+04	6.053E+05	3.930E+03	2.405E+04
96.0000	3.899E+00	5.554E+01	6.335E+14	6.793E+05	3.291E+05	5.281E+05	4.972E+04	6.053E+05	3.930E+03	2.405E+04
102.0000	9.135E+00	5.319E+01	6.335E+14	6.793E+05	3.291E+05	5.281E+05	5.904E+04	6.053E+05	3.930E+03	2.405E+04
108.0000	7.237E+01	5.726E+01	7.519E+14	7.761E+05	3.291E+05	5.281E+05	6.839E+04	6.849E+05	3.990E+03	2.823E+04
114.0000	1.333E+01	2.230E+01	8.237E+14	8.024E+05	5.572E+05	7.177E+05	7.699E+04	7.272E+05	5.731E+03	3.156E+04
120.0000	6.111E+00	2.139E+01	8.237E+14	8.024E+05	5.559E+05	7.303E+05	7.834E+04	7.272E+05	5.920E+03	3.156E+04
126.0000	7.017E+00	2.106E+01	9.237E+14	8.024E+05	5.559E+05	7.303E+05	7.961E+04	7.272E+05	5.820E+03	3.156E+04
132.0000	6.130E+01	4.776E+01	9.450E+14	9.570E+05	5.559E+05	7.303E+05	8.352E+04	8.602E+05	5.920E+03	3.642E+04
138.0000	1.722E+01	5.643E+01	1.027E+15	1.023E+06	5.559E+05	7.303E+05	9.313E+04	9.179E+05	5.820E+03	3.958E+04
144.0000	6.667E+00	5.440E+01	1.027E+15	1.023E+06	5.559E+05	7.303E+05	1.028E+05	9.178E+05	5.820E+03	3.958E+04
150.0000	6.434E+00	5.212E+01	1.027E+15	1.023E+06	5.559E+05	7.303E+05	1.118E+05	9.178E+05	5.820E+03	3.958E+04
156.0000	7.643E+01	6.376E+01	1.133E+15	1.100E+06	5.559E+05	7.303E+05	1.216E+05	9.850E+05	5.820E+03	4.376E+04
162.0000	1.773E+01	6.659E+01	1.199E+15	1.132E+06	5.559E+05	7.303E+05	1.341E+05	1.013E+06	5.920E+03	4.599E+04
168.0000	1.222E+01	6.351E+01	1.199E+15	1.132E+06	5.559E+05	7.303E+05	1.468E+05	1.013E+06	5.920E+03	4.599E+04
174.0000	1.616E+01	6.275E+01	1.199E+15	1.132E+06	5.559E+05	7.303E+05	1.572E+05	1.013E+06	5.820E+03	4.569E+04
180.0000	8.841E+01	7.493E+01	1.322E+15	1.225E+06	5.559E+05	7.303E+05	1.692E+05	1.095E+06	5.920E+03	4.990E+04
186.0000	2.279E+01	2.357E+01	1.455E+15	1.272E+06	8.152E+05	8.925E+05	1.794E+05	1.150E+06	7.691E+03	5.272E+04
192.0000	1.722E+01	2.249E+01	1.455E+15	1.272E+06	8.183E+05	9.044E+05	1.810E+05	1.150E+06	7.760E+03	5.272E+04
198.0000	1.650E+01	2.211E+01	1.495E+15	1.272E+06	8.193E+05	9.048E+05	1.825E+05	1.150E+06	7.760E+03	5.272E+04
204.0000	6.759E+01	5.356E+01	1.530E+15	1.440E+06	8.193E+05	9.049E+05	1.970E+05	1.294E+06	7.760E+03	5.775E+04
210.0000	2.333E+01	5.771E+01	1.596E+15	1.493E+06	8.193E+05	9.043E+05	1.971E+05	1.341E+06	7.760E+03	6.039E+04
216.0000	1.933E+01	5.522E+01	1.596E+15	1.493E+06	8.193E+05	9.049E+05	2.060E+05	1.341E+06	7.760E+03	6.039E+04
222.0000	2.250E+01	5.249E+01	1.596E+05	1.493E+06	8.193E+05	9.049E+05	2.161E+05	1.341E+06	7.759E+03	6.039E+04
228.0000	6.923E+01	5.717E+01	1.661E+15	1.527E+06	8.193E+05	9.048E+05	2.252E+05	1.371E+06	7.760E+03	6.399E+04
234.0000	2.500E+01	2.021E+01	1.709E+15	1.553E+06	9.969E+05	1.141E+06	2.324E+05	1.423E+06	9.631E+03	6.636E+04
240.0000	2.111E+01	1.952E+01	1.709E+15	1.553E+06	9.990E+05	1.153E+06	2.329E+05	1.423E+06	9.710E+03	6.636E+04
246.0000	2.111E+01	1.933E+01	1.709E+15	1.553E+06	9.990E+05	1.153E+06	2.338E+05	1.413E+06	9.710E+03	6.636E+04
252.0000	6.691E+01	4.631E+01	1.814E+15	1.710E+06	9.990E+05	1.153E+06	2.367E+05	1.537E+06	9.710E+03	7.140E+04
258.0000	2.556E+01	5.637E+01	1.894E+15	1.749E+06	9.990E+05	1.153E+06	2.453E+05	1.598E+06	9.700E+03	7.387E+04
264.0000	2.110E+01	5.396E+01	1.894E+15	1.749E+06	9.990E+05	1.153E+06	2.558E+05	1.598E+06	9.710E+03	7.387E+04
270.0000	2.163E+01	5.170E+01	1.894E+15	1.789E+06	9.990E+05	1.153E+06	2.648E+05	1.598E+06	9.700E+03	7.357E+04
276.0000	5.959E+01	5.693E+01	1.948E+15	1.921E+06	9.990E+05	1.153E+06	2.736E+05	1.674E+06	9.700E+03	7.634E+04
282.0000	2.393E+01	2.075E+01	2.005E+15	1.962E+06	1.188E+06	1.377E+06	2.895E+05	1.690E+06	1.157E+04	7.916E+04
288.0000	2.000E+01	1.994E+01	2.035E+15	1.962E+06	1.193E+06	1.390E+06	2.916E+05	1.690E+06	1.164E+04	7.916E+04
294.0000	1.914E+01	1.971E+01	2.035E+15	1.962E+06	1.193E+06	1.390E+06	2.827E+05	1.690E+06	1.164E+04	7.916E+04
300.0000	4.416E+01	3.545E+01	2.075E+15	1.954E+06	1.193E+06	1.390E+06	2.951E+05	1.759E+06	1.164E+04	8.402E+04
306.0000	1.444E+01	3.953E+01	2.116E+15	1.979E+06	1.193E+06	1.390E+06	2.985E+05	1.791E+06	1.164E+04	8.761E+04
312.0000	7.222E+00	3.710E+01	2.116E+15	1.978E+06	1.193E+06	1.390E+06	2.959E+05	1.781E+06	1.164E+04	8.741E+04
318.0000	1.070E+01	3.593E+01	2.116E+15	1.978E+06	1.193E+06	1.390E+06	3.068E+05	1.781E+06	1.164E+04	8.741E+04
324.0000	5.913E+01	4.546E+01	2.193E+15	2.039E+06	1.193E+06	1.390E+06	3.064E+05	1.833E+06	1.164E+04	9.153E+04
330.0000	1.719E+01	5.413E+01	2.274E+15	2.039E+06	1.193E+06	1.390E+06	3.153E+05	1.886E+06	1.164E+04	9.469E+04
336.0000	1.111E+01	5.196E+01	2.274E+15	2.099E+06	1.193E+06	1.390E+06	3.247E+05	1.886E+06	1.164E+04	9.468E+04

Table H.3 Sample Output Plot.

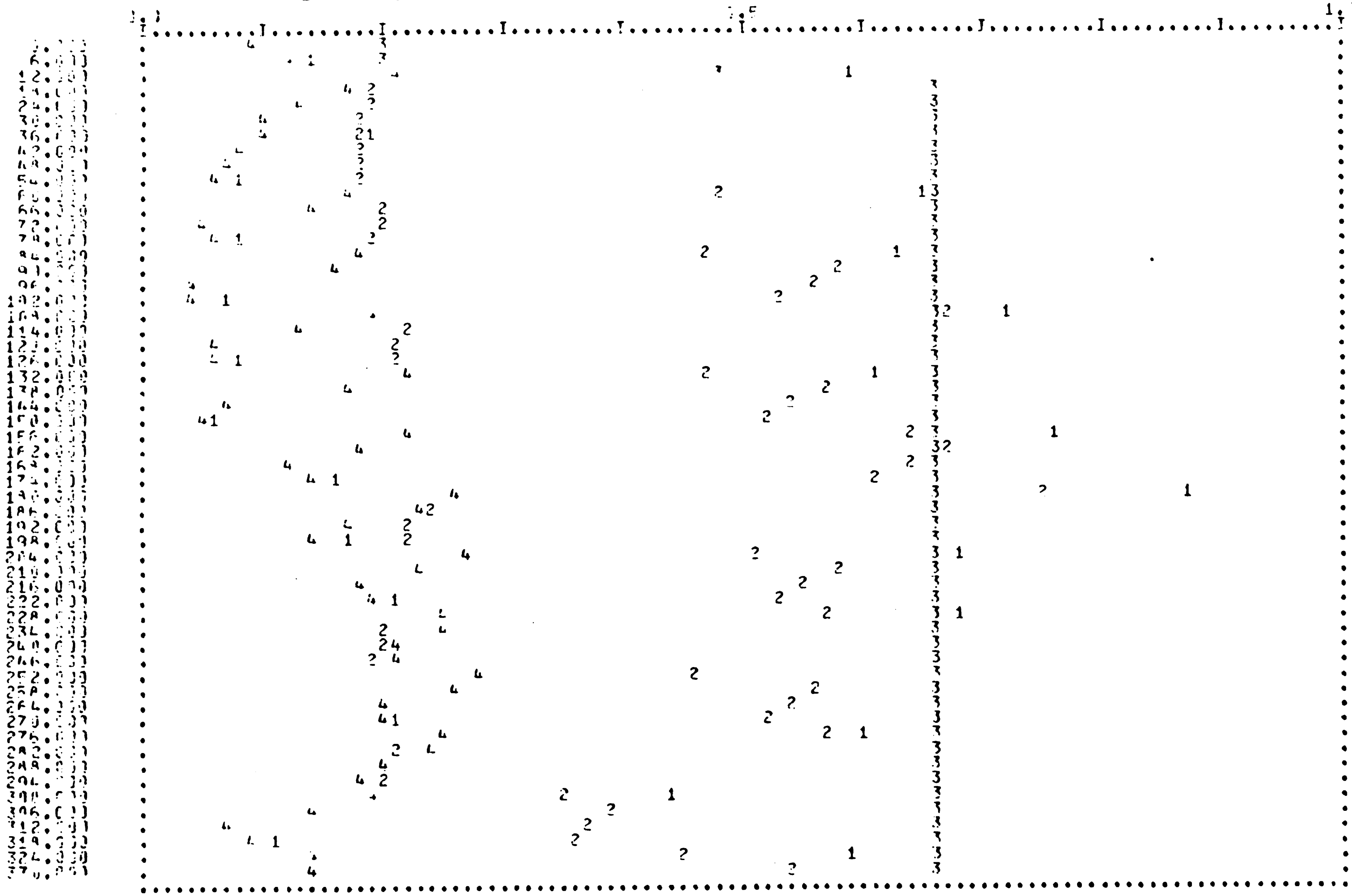

SYMBOL	IDENTIFIER	SCALE FACTOR	ZERO POINT
1	TCOL	1.000E+02	0.
2	TTANK	1.000E+02	0.
3	TAUX	1.000E+02	0.
4	TAMB	1.000E+02	0.

APPENDIX I

Table I.1 Small Dairy Plant Simulation Results For September 1965 - East Lansing.

Run: E:S:1:65:FA:K:336:a,b,c,d

Scale:	a	b	c	d
Collector area (m^2)	25	40	65	100
RADTOTAL (10^6KJ)	5.753	9.200	14.96	23.01
QCOL (10^6KJ)	2.091	3.007	4.257	5.714
QTANK (10^6KJ)	1.199	1.551	1.921	2.225
QAUX (10^6KJ)	1.382	1.044	0.717	0.477
QTOTAL (10^6KJ)	2.581	2.595	2.638	2.702
QENV (10^6KJ)	0.326	0.517	0.842	1.283
QHX (10^6KJ)	1.892	2.689	3.769	5.044
MCOL (10^5Kg)	1.029	1.547	2.346	3.356
COLEF (%)	36.3	32.7	28.5	24.8
SOLAR (%)	46.7	60.4	74.7	86.6
SOLAR - total (%)	46.5	59.8	72.8	82.3
SYSOP (hrs/dav)	8.6	8.1	7.6	7.0
TANK LOSS (%)	15.6	17.2	19.8	22.5
Avg. Temp. (^oC)	37.4	44.6	52.2	58.4

Table I.2 Small Dairy Plant Simulation Results
For September 1974 - East Lansing.

Run: E:S:1:74:FA:K:336:a,b,c,d

Scale:	a	b	c	d
Collector area (m^2)	25	40	65	100
RADTOTAL (10^6KJ)	5.685	9.096	14.78	22.74
QCOL (10^6KJ)	2.099	3.036	4.310	5.802
QTANK (10^6KJ)	1.190	1.567	1.966	2.297
QAUX (10^6KJ)	1.390	1.025	0.654	0.385
QTOTAL (10^6KJ)	2.580	2.592	2.620	2.682
QENV (10^6KJ)	0.324	0.521	0.860	1.321
QHX (10^6KJ)	1.886	2.697	3.805	5.094
MCOL (10^5Kg)	0.947	1.419	2.124	3.084
COLEF (%)	36.9	33.4	29.2	25.5
SOLAR (%)	46.3	61.0	76.5	89.4
SOLAR - total (%)	46.1	60.5	75.0	85.6
SYSOP (hrs/day)	7.9	7.4	6.8	6.5
TANK LOSS (%)	15.5	17.2	19.9	22.8
Avg. Temp. (^oC)	37.2	44.9	53.1	59.9

Table I.3 Small Dairy Plant Simulation Results For September 1949 - Columbia.

Run: E:S:3:49:FA:K:336:a,b,c,d

Scale:	a	b	c	d
Collector area (m^2)	25	40	65	100
RADTOTAL (10^6KJ)	6.865	10.98	17.85	27.46
QCOL (10^6KJ)	2.772	3.946	5.666	7.746
QTANK (10^6KJ)	1.723	2.249	2.758	3.177
QAUX (10^6KJ)	0.892	0.449	0.150	0.035
QTOTAL (10^6KJ)	2.615	2.698	2.808	3.212
QENV (10^6KJ)	0.426	0.700	1.158	1.784
QHX (10^6KJ)	2.560	3.619	5.108	6.903
MCOL (10^5Kg)	0.884	1.290	1.920	2.783
COLEF (%)	40.4	35.9	31.7	28.2
SOLAR (%)	67.0	87.5	107.3	124.0
SOLAR - total (%)	65.9	83.4	98.2	98.9
SYSOP (hrs/day)	7.4	6.8	6.2	5.8
TANK LOSS (%)	15.4	17.7	20.4	23.0
Avg. Temp. (^oC)	48.2	58.9	69.4	78.0

Table I.4 Small Dairy Plant Simulation Results For September 1952 - Columbia.

Run: E:S:3:52:FA:K:336:a,b,c,d

Scale	a	b	c	d
Collector area (m^2)	25	40	65	100
RADTOTAL (10^6KJ)	8.795	14.07	22.90	35.18
QCOL (10^6KJ)	3.312	4.768	6.831	9.223
QTANK (10^6KJ)	1.988	2.518	3.024	3.474
QAUX (10^6KJ)	0.743	0.364	0.117	0.042
QTOTAL (10^6KJ)	2.731	2.882	3.141	3.516
QENV (10^6KJ)	0.558	0.869	1.381	2.086
QHX (10^6KJ)	3.071	4.316	6.091	8.163
MCOL (10^5Kg)	1.027	1.536	2.315	3.309
COLEF (%)	37.7	33.9	29.9	26.2
SOLAR (%)	77.4	98.0	117.7	135.2
SOLAR - total (%)	72.8	87.4	96.3	98.8
SYSOP (hrs/day)	8.6	8.0	7.5	6.9
TANK LOSS (%)	16.9	18.2	20.2	22.6
Avg. Temp. (^oC)	53.6	64.5	74.8	84.1

Table I.5 Medium Dairy Plant Simulation Results For September 1965 - East Lansing .

Run: E:M:1:65:FA:K:336:a,b,c,d

Scale:	a	b	c	d
Collector area (m^2)	80	140	200	330
RADTOTAL (10^7KJ)	1.841	3.221	4.602	7.593
QCOL (10^7KJ)	0.774	1.208	1.559	2.174
QTANK (10^7KJ)	0.482	0.695	0.846	1.0627
QAUX (10^7KJ)	0.959	0.747	0.596	0.388
QTOTAL (10^7KJ)	1.441	1.441	1.442	1.450
QENV (10^6KJ)	0.509	0.961	1.458	2.573
QHX (10^7KJ)	6.813	1.057	1.362	1.899
MCOL (10^6Kg)	0.358	0.566	0.771	1.164
COLEF (%)	42.0	37.5	33.9	28.6
SOLAR (%)	33.5	48.2	58.8	73.8
SOLAR - total (%)	33.5	48.2	58.7	73.2
SYSOP (hrs/day)	9.4	8.5	8.1	7.4
TANK LOSS (%)	6.6	8.0	9.4	11.8
Avg. Temp. (^oC)	30.6	38.5	44.1	52.1

Table I.6 Medium Dairy Plant Simulation Results
For September 1974 - East Lansing.

Run: E:M:1:74:FA:K:336:a,b,c,d

Scale:	a	b	c	d
Collector area (m^2)	80	140	200	330
RADTOTAL (10^7KJ)	1.819	3.184	4.548	7.500
QCOL (10^7KJ)	0.761	1.195	1.553	2.176
QTANK (10^7KJ)	0.466	0.691	0.852	1.087
QAUX (10^7KJ)	0.978	0.758	0.600	0.383
QTOTAL (10^7KJ)	1.445	1.448	1.453	1.470
QENV (10^6KJ)	0.513	0.970	1.471	2.611
QHX (10^7KJ)	0.668	1.043	1.353	1.899
MCOL (10^6Kg)	0.335	0.538	0.731	1.099
COLEF (%)	41.8	37.5	34.1	29.0
SOLAR (%)	32.4	48.0	59.2	75.5
SOLAR - total (%)	32.3	47.7	58.7	73.9
SYSOP (hrs/day)	8.8	8.0	7.7	7.0
TANK LOSS (%)	6.7	8.1	9.5	12.0
Avg. Temp. (^oC)	29.9	38.3	44.3	53.0

Table I.7 Medium Dairy Plant Simulation Results For September 1949 - Columbia.

Run: E:M:3:49:FA:K:336:a,b,c,d

Scale:	a	b	c	d
Collector area (m^2)	80	140	200	330
RADTOTAL (10^7KJ)	2.197	3.844	5.492	9.062
QCOL (10^7KJ)	1.012	1.585	2.060	2.932
QTANK (10^7KJ)	0.673	0.971	1.188	1.506
QAUX (10^7KJ)	0.770	0.492	0.310	0.099
QTOTAL (10^7KJ)	1.442	1.463	1.498	1.605
QENV (10^6KJ)	0.544	1.099	1.738	3.231
QHX (10^7KJ)	0.907	1.403	1.814	2.567
MCOL (10^6Kg)	0.346	0.505	0.671	0.986
COLEF (%)	46.1	41.2	37.5	32.4
SOLAR (%)	46.7	67.4	82.5	104.6
SOLAR - total (%)	46.6	66.4	79.3	93.8
SYSOP (hrs/day)	9.0	7.6	7.0	6.3
TANK LOSS (%)	5.4	6.9	8.4	11.0
Avg. Temp. (^oC)	37.7	48.7	56.7	68.5

Table I.8 Medium Dairy Plant Simulation Results For September 1952 - Columbia.

Run: E:M:3:52:FA:K:336:a,b,c,d

Scale:	a	b	c	d
Collector area (m^2)	80	140	200	330
RADTOTAL (10^7KJ)	2.814	4.930	7.040	11.61
QCOL (10^7KJ)	1.207	1.891	2.459	3.470
QTANK (10^7KJ)	0.748	1.066	1.297	1.629
QAUX (10^7KJ)	0.709	0.431	0.260	0.102
QTOTAL (10^7KJ)	1.457	1.496	1.557	1.731
QENV (10^6KJ)	0.866	1.598	2.389	4.161
QHX (10^7KJ)	1.074	1.659	2.151	3.026
MCOL (10^6Kg)	0.354	0.560	0.756	1.144
COLEF (%)	42.9	38.4	34.9	29.9
SOLAR (%)	51.9	47.0	90.1	113.1
SOLAR - total (%)	51.3	71.3	83.3	94.1
SYSOP (hrs/day)	9.3	8.4	7.9	7.3
TANK LOSS (%)	7.2	8.5	9.7	12.0
Avg. Temp. (^oC)	40.4	52.2	60.8	73.1

Table I.9 Large Dairy Plant Simulation Results
For September 1965 - East Lansing

Run: E:L:1:65:FA:K:336:a,b,c,d

Scale:	a	b	c	d
Collector area (m^2)	400	700	1000	1600
RADTOTAL (10^8KJ)	0.920	1.611	2.301	3.682
QCOL (10^7KJ)	3.942	5.797	7.290	9.716
QTANK (10^7KJ)	2.832	3.844	4.524	5.432
QAUX (10^7KJ)	5.531	4.519	3.839	2.931
QTOTAL (10^7KJ)	8.363	8.363	8.363	8.363
QENV (10^6KJ)	1.468	3.052	4.648	7.846
QHX (10^7KJ)	3.574	5.210	6.504	8.635
MCOL (10^6Kg)	1.864	2.918	3.820	5.567
COLEF (%)	42.8	36.0	31.7	26.4
SOLAR (%)	33.9	46.0	54.1	65.0
SOLAR - total (%)	33.9	46.0	54.1	65.0
SYSOP (hrs/dav)	9.8	8.7	8.0	7.3
TANK LOSS (%)	3.7	5.3	6.4	8.1
Avg. Temp. (^oC)	35.4	43.4	48.8	56.1

Table I.10 Large Dairy Plant Simulation Results For September 1974 - East Lansing.

Run: E:L:1:74:FA:K:336:a,b,c,d

Scale:	a	b	c	d
Collector area (m^2)	400	700	1000	1600
RADTOTAL (10^8KJ)	0.910	1.592	2.274	3.638
QCOL (10^7KJ)	3.944	5.886	7.436	9.925
QTANK (10^7KJ)	2.774	3.845	4.588	5.582
QAUX (10^7KJ)	5.589	4.519	3.776	2.784
QTOTAL (10^7KJ)	8.363	8.364	8.364	8.366
QENV (10^6KJ)	1.502	3.121	4.778	8.108
QHX (10^7KJ)	3.551	5.258	6.594	8.756
MCOL (10^6Kg)	1.670	2.670	3.561	5.152
COLEF (%)	43.4	37.0	32.7	27.3
SOLAR (%)	33.2	46.0	54.9	66.8
SYSOP (hrs/day)	3.7	8.0	7.5	6.7
TANK LOSS (%)	3.8	5.3	6.4	8.2
Avg. Temp. (^oC)	34.9	43.4	49.4	57.3

Table I.11 Large Dairy Plant Simulation Results For September 1949 - Columbia.

Run: E:L:3:49:FA:K:336:a,b,c,d

Scale:	a	b	c	d
Collector area (m^2)	400	700	1000	1600
RADTOTAL (10^8KJ)	1.098	1.922	2.746	4.394
QCOL (10^7KJ)	5.018	7.584	9.702	13.29
QTANK (10^7KJ)	3.466	4.881	5.894	7.292
QAUX (10^7KJ)	4.897	3.483	2.506	1.315
QTOTAL (10^7KJ)	8.363	8.364	8.400	8.607
QENV (10^6KJ)	1.786	3.845	6.005	1.047
QHX (10^7KJ)	4.531	6.784	8.644	11.76
MCOL (10^6Kg)	1.591	2.460	3.152	4.628
COLEF (%)	45.7	39.5	35.3	30.2
SOLAR (%)	41.5	58.4	70.5	87.2
SOLAR - total (%)	41.4	58.4	70.2	84.7
SYSOP (hrs/day)	8.3	7.4	6.6	6.1
TANK LOSS (%)	3.6	5.1	6.2	7.9
Avg. Temp. (^oC)	40.4	51.7	59.8	70.9

Table I.12 Large Dairy Plant Simulation Results For September 1952 - Columbia.

Run: E:L:3:52:FA:K:336:a,b,c,d

Scale:	a	b	c	d
Collector area (m^2)	400	700	1000	1600
RADTOTAL (10^8KJ)	1.407	2.463	3.518	5.629
QCOL (10^7KJ)	6.232	9.284	11.75	15.78
QTANK (10^7KJ)	4.319	5.908	6.990	8.420
QAUX (10^7KJ)	4.046	2.479	1.588	0.849
QTOTAL (10^7KJ)	8.365	8.387	8.578	9.269
QENV (10^6KJ)	2.511	5.094	7.685	12.83
QHX (10^7KJ)	5.632	8.315	10.45	13.96
MCOL (10^6Kg)	1.768	2.784	3.691	5.491
COLEF (%)	44.3	37.7	33.4	28.0
SOLAR (%)	51.7	70.7	83.6	100.7
SOLAR - total (%)	51.6	70.4	81.4	90.8
SYSOP (hrs/day)	9.3	8.3	7.7	7.2
TANK LOSS (%)	4.0	5.5	6.5	8.1
Avg. Temp. (^oC)	47.2	59.9	68.5	79.9

Table I.13 Medium Dairy Plant Simulation Results for East Lansing 1974-75.

Run - E:M:1:74:SP, SU, FA, WI:K:2184, 2184, 2160, 2184:b

Season:	SP	SU	FA	WI
Collector area (m^2)	140	140	140	140
RADTOTAL (10^8KJ)	1.837	2.481	1.793	1.498
QCOL (10^7KJ)	5.833	8.930	6.138	4.245
QTANK (10^7KJ)	3.606	5.578	3.813	2.617
QAUX (10^7KJ)	5.781	3.912	5.577	6.751
QTOTAL (10^7KJ)	9.387	9.490	9.390	9.368
QENV (10^6KJ)	5.390	8.341	5.770	3.874
QHX (10^7KJ)	5.108	7.830	5.393	3.743
MCOL (10^6Kg)	2.955	3.802	2.731	2.212
COLEF (%)	31.8	36.0	34.2	28.3
SOLAR (%)	38.5	59.5	40.7	27.9
SOLAR--Total (%)	38.4	58.8	40.6	27.9
SYSOP (hrs/day)	6.8	8.7	6.3	5.1
TANK LOSS (%)	9.2	9.3	9.4	9.1
Average Temperature (°C)	33.3	44.5	34.5	27.7

Table I.14 Medium Dairy Plant Simulation Results for Columbia 1949.

Run - E:M:3:49:SP, SU, FA, WI:K:2184, 2184, 1320, 2160:b

Season:	SP	SU	FA	WI
Collector area (m^2)	140	140	140	140
RADTOTAL (10^8KJ)	2.460	2.923	1.688	1.607
QCOL (10^7KJ)	8.148	10.90	6.102	5.039
QTANK (10^7KJ)	5.045	7.010	4.015	3.061
QAUX (10^7KJ)	4.466	2.813	2.022	6.396
QTOTAL (10^7KJ)	9.511	9.823	6.037	9.457
QENV (10^6KJ)	7.417	10.12	5.420	4.835
QHX (10^7KJ)	7.124	9.641	5.391	4.413
MCOL (10^6Kg)	3.118	3.907	2.154	2.005
COLEF (%)	33.1	37.3	37.2	31.4
SOLAR (%)	53.9	74.8	69.7	32.7
SOLAR--Total (%)	53.0	71.4	66.5	32.4
SYSOP (hrs/day)	7.2	9.0	8.2	4.7
TANK LOSS (%)	9.1	9.3	8.9	9.6
Average Temperature (°C)	41.5	52.7	49.9	30.2

Table I.15 Medium Dairy Plant Simulation Results for Columbia 1952.

Run - E:M:3:52:SP, SU, FA, WI:K:2184, 2184, 2184, 2160:b

Season:	SP	SU	FA	WI
Collector area (M^2)	140	140	140	140
RADTOTAL (10^8KJ)	2.554	3.037	3.200	2.279
QCOL (10^7KJ)	8.646	11.27	11.37	7.289
QTANK (10^7KJ)	5.337	7.065	7.229	4.478
QAUX (10^7KJ)	4.200	2.784	2.618	5.052
QTOTAL (10^7KJ)	9.537	9.849	9.847	9.530
QENV (10^7KJ)	0.771	1.053	1.020	0.680
QHX (10^7KJ)	7.556	9.891	9.985	6.413
MCOL (10^6Kg)	3.071	3.910	3.442	2.481
COLEF (%)	33.9	37.1	37.1	32.8
SOLAR (%)	57.0	75.4	77.2	47.8
SOLAR--Total (%)	56.0	71.7	73.4	47.0
SYSOP (hrs/day)	7.1	9.0	7.9	5.8
TANK LOSS (%)	8.9	9.3	8.9	9.3
Average Temperature (°C)	43.2	53.0	53.9	38.3

Table I.16 ASHRAE Average Simulation Results for Medium Dairy Plant--East Lansing.

Run - H:M:1:A:SP, SU, FA, WI:N:2160:b

Season:	SP	SU	FA	WI
Collector area (m^2)	140	140	140	140
RADTOTAL (10^8KJ)	2.076	2.692	2.100	1.775
QCOL (10^7KJ)	6.193	9.244	6.949	4.736
QTANK (10^7KJ)	3.889	5.799	4.342	3.064
QAUX (10^7KJ)	5.479	3.676	5.059	6.304
QTOTAL (10^7KJ)	9.368	9.475	9.401	9.368
QENV (10^6KJ)	5.434	8.641	6.446	4.208
QHX (10^7KJ)	5.421	8.091	6.094	4.215
MCOL (10^6Kg)	3.384	3.932	3.171	2.614
COLEF (%)	29.8	34.3	33.1	26.7
SOLAR (%)	41.5	61.9	46.4	32.7
SOLAR--Total (%)	41.5	61.2	46.2	32.7
SYSOP (hrs/day)	7.9	9.1	7.4	6.1
TANK LOSS (%)	8.8	9.3	9.3	8.9
Average Temperature (°C)	34.9	45.8	37.5	30.2

Table I.17 ASHRAE Average Simulation Results for Medium Dairy Plant--Indianapolis.

Run - H:M:2:A:SP, SU, FA, WI:N:2160:b

Season:	SP	SU	FA	WI
Collector area (m^2)	140	140	140	140
RADTOTAL (10^8KJ)	2.202	2.720	2.412	1.886
QCOL (10^7KJ)	6.838	9.627	8.223	5.364
QTANK (10^7KJ)	4.297	6.037	5.139	3.447
QAUX (10^7KJ)	5.081	3.464	4.306	5.925
QTOTAL (10^7KJ)	9.378	9.501	9.445	9.367
QENV (10^6KJ)	6.106	9.010	7.776	4.849
QHX (10^7KJ)	5.989	8.433	7.215	4.759
MCOL (10^6Kg)	3.543	3.972	3.221	2.741
COLEF (%)	31.1	35.4	34.1	28.4
SOLAR (%)	45.9	64.4	54.9	36.7
SOLAR--Total (%)	45.8	63.5	54.4	36.7
SYSOP (hrs/day)	8.2	9.2	7.5	6.4
TANK LOSS (%)	8.9	9.4	9.5	7.6
Average Temperature (°C)	37.2	47.2	42.0	32.4

Table I.18 ASHRAE Average Simulation Results for Medium Dairy Plant--Columbia .

Run - H:M:3:A:SP, SU, FA, WI N:2160:b

Season:	SP	SU	FA	WI
Collector area (m^2)	140	140	140	140
RADTOTAL (10^8KJ)	2.335	2.814	2.533	2.086
QCOL (10^7KJ)	7.446	10.12	8.780	6.133
QTANK (10^7KJ)	4.676	6.342	5.474	3.941
QAUX (10^7KJ)	4.719	3.208	4.001	5.418
QTOTAL (10^7KJ)	9.395	9.550	9.475	9.369
QENV (10^6KJ)	6.727	9.509	8.312	5.704
QHX (10^7KJ)	6.524	8.864	7.701	5.464
MCOL (10^6Kg)	3.587	4.021	3.265	2.782
COLEF (%)	31.9	36.0	34.7	29.4
SOLAR (%)	49.9	67.7	57.8	42.2
SOLAR--Total (%)	49.8	66.4	57.8	42.2
SYSOP (hrs/day)	8.4	9.4	7.6	6.5
TANK LOSS (%)	9.0	9.4	9.5	9.3
Average Temperature (°C)	39.4	48.9	43.9	35.3

APPENDIX J

Table J.1 Small Meat Plant Simulation Results For September 1965 - East Lansing.

Run: F:S:1:65:FA:K:336:a.b.c.d

Scale:	a	b	c	d
Collector area (m^2)	35	65	100	150
RADTOTAL (10^6KJ)	8.054	14.96	23.01	34.52
QCOL (10^6KJ)	3.430	5.429	7.313	9.522
QTANK (10^6KJ)	2.670	3.748	4.535	5.258
QAUX (10^6KJ)	3.311	2.233	1.458	0.98
QTOTAL (10^6KJ)	5.981	5.981	5.993	6.156
QENV (10^6KJ)	0.307	0.617	0.991	1.521
QHX (10^6KJ)	3.301	5.121	6.805	8.817
MCOL (10^5Kg)	1.607	2.669	3.820	4.865
COLEF (%)	42.6	36.3	31.8	27.6
SOLAR (%)	44.6	62.7	75.8	87.9
SOLAR - total (%)	44.6	62.7	75.7	85.4
SYSOP (hrs/day)	9.6	8.6	8.0	7.4
TANK LOSS (%)	8.9	11.4	13.6	16.0
Avg. Temp. (^oC)	33.9	43.4	48.6	54.3

Table J.2 Small Meat Plant Simulation Results For September 1974 - East Lansing.

Run: F:S:1:74:FA:K:336:a,b,c,d

Scale:	a	b	c	d
Collector area (m^2)	35	65	100	150
RADTOTAL (10^6KJ)	7.959	14.78	22.74	34.11
QCOL (10^6KJ)	3.401	5.458	7.397	9.674
QTANK (10^6KJ)	2.679	3.784	4.613	5.403
QAUX (10^6KJ)	3.319	2.258	1.513	0.913
QTOTAL (10^6KJ)	5.998	6.042	6.126	6.316
QENV (10^6KJ)	0.294	0.592	0.963	1.500
QHX (10^6KJ)	3.280	5.118	6.815	8.864
MCOL (10^5Kg)	1.555	2.567	3.629	4.612
COLEF (%)	42.7	36.9	32.5	28.4
SOLAR (%)	44.8	63.3	77.1	90.4
SOLAR - total (%)	44.7	62.6	75.3	85.5
SYSOP (hrs/day)	9.3	8.3	7.6	7.0
TANK LOSS (%)	8.6	8.3	7.6	7.0
Avg. Temp. (^oC)	33.9	42.7	49.2	55.4

Table J.3 Small Meat Plant Simulation Results For September 1949 - Columbia.

Run: F:S:3:49:FA:K:336:a,b,c,d

Scale:	a	b	c	d
Collector area (m^2)	35	65	100	150
RADTOTAL (10^6KJ)	9.611	17.85	27.46	41.19
QCOL (10^6KJ)	4.458	7.094	9.637	12.72
QTANK (10^6KJ)	3.528	5.109	6.274	7.367
QAUX (10^6KJ)	2.453	0.932	0.376	0.130
QTOTAL (10^6KJ)	5.981	6.041	6.650	7.497
QENV (10^6KJ)	0.383	0.804	1.312	2.056
QHX (10^6KJ)	4.336	6,800	9.107	11.92
MCOL (10^5Kg)	1.364	2.297	3.179	4.003
COLEF (%)	46.4	39.7	35.1	30.9
SOLAR (%)	59.0	85.4	105.0	123.2
SOLAR - total (%)	59.0	84.6	94.3	98.3
SYSOP (hrs/day)	8.2	7.4	6.7	6.1
TANK LOSS (%)	8.6	11.3	13.6	16.2
Avg. Temp. (^oC)	40.6	53.1	62.3	70.9

Table J.4 Small Meat Plant Simulation Results
For September 1952 - Columbia

Run: F:S:3:52:FA:K:336:a,b,c,d

Scale:	a	b	c	d
Collector area (m^2)	35	65	100	160
RADTOTAL (10^6KJ)	21.31	22.87	35.18	52.77
QCOL (10^6KJ)	5.389	8.529	11.55	15.17
QTANK (10^6KJ)	4.088	5.726	6.932	8.057
QAUX (10^6KJ)	1.994	0.671	0.390	0.244
QTOTAL (10^6KJ)	6.082	6.397	7.322	8.303
QENV (10^6KJ)	0.552	1.073	1.675	2.521
QHX (10^6KJ)	5.199	8.093	10.79	14.05
MCOL (10^5Kg)	1.562	2.660	3.752	4.790
COLEF (%)	43.8	37.3	32.8	28.7
SOLAR (%)	69.4	95.8	115.9	134.7
SOLAR - total (%)	67.2	89.5	94.7	97.0
SYSOP (hrs/day)	9.3	8.6	7.9	7.3
TANK LOSS (%)	10.3	12.6	14.5	16.6
Avg. Temp. (^oC)	45.1	58.0	67.5	76.4

Table J.5 Medium Meat Plant Simulation Results for September 1965--East Lansing.

Run - F:M:1:65:FA:K:336:a, b, c, d

Scale:	a	b	c	d
Collector area (m^2)	80	140	200	320
RADTOTAL (10^7KJ)	1.841	3.220	4.602	7.363
QCOL (10^7KJ)	0.733	1.093	1.388	1.889
QTANK (10^7KJ)	0.558	0.740	0.858	1.006
QAUX (10^7KJ)	0.763	0.581	0.463	0.315
QTOTAL (10^7KJ)	1.321	1.321	1.321	1.321
QENV (10^6KJ)	0.594	1.127	1.676	2.769
QHX (10^7KJ)	0.700	1.027	1.289	1.730
MCOL (10^5Kg)	3.456	5.549	7.436	10.81
COLEF (%)	39.8	33.9	30.2	25.7
SOLAR (%)	42.2	56.0	65.0	76.2
SOLAR--Total (%)	42.2	56.0	65.0	76.2
SYSOP (hrs/day)	9.0	8.3	7.8	7.1
TANK LOSS (%)	8.1	10.3	12.1	14.7
Average Temperature (°C)	37.4	45.5	50.7	57.2

Table J.6 Medium Meat Plant Simulation Results for September 1974--East Lansing.

Run - F:M:1:74:FA:K:336:a, b, c, d

Scale:	a	b	c	d
Collector area (m^2)	80	140	200	320
RADTOTAL (10^7KJ)	1.819	3.184	4.548	7.277
QCOL (10^7KJ)	0.731	1.101	1.406	1.919
QTANK (10^7KJ)	0.560	0.748	0.874	1.039
QAUX (10^7KJ)	0.762	0.577	0.456	0.306
QTOTAL (10^7KJ)	1.322	1.324	1.329	1.344
QENV (10^6KJ)	0.564	1.084	1.631	2.747
QHX (10^7KJ)	0.695	1.024	1.293	1.737
MCOL (10^5Kg)	3.358	5.329	7.040	10.24
COLEF (%)	40.2	34.6	30.9	26.4
SOLAR (%)	42.4	56.6	66.1	78.7
SOLAR--Total (%)	42.4	56.5	65.7	77.3
SYSOP (hrs/day)	8.8	8.0	7.4	6.7
TANK LOSS (%)	7.7	9.8	11.6	14.3
Average Temperature (°C)	37.5	45.8	51.4	58.6

Table J.7 Medium Meat Plant Simulation Results for September 1949--Columbia.

Run - F:M:3:49:FA:K:336:a, b, c, d

Scale:	a	b	c	d
Collector area (m^2)	80	140	200	320
RADTOTAL (10^7KJ)	2.197	3.844	5.492	8.787
QCOL (10^7KJ)	0.955	1.430	1.835	2.542
QTANK (10^7KJ)	0.749	1.019	1.195	1.421
QAUX (10^7KJ)	0.572	0.302	0.155	0.055
QTOTAL (10^7KJ)	1.321	1.321	1.350	1.476
QENV (10^6KJ)	0.756	1.482	2.237	3.787
QHX (10^7KJ)	0.925	1.364	1.726	2.351
MCOL (10^5Kg)	2.987	4.699	6.126	8.950
COLEF (%)	43.5	37.2	33.4	28.9
SOLAR (%)	56.7	77.1	90.5	107.6
SOLAR--Total (%)	56.7	77.1	88.5	96.3
SYSOP (hrs/day)	7.8	7.0	6.4	5.9
TANK LOSS (%)	7.8	10.4	12.2	14.9
Average Temperature (°C)	45.9	57.8	65.5	75.5

Table J.8 Medium Meat Plant Simulation Results for September 1952--Columbia.

Run - F:M:3:52:FA:K:336:a, b, c, d

Scale:	a	b	c	d
Collector area (m^2)	80	140	200	320
RADTOTAL (10^7KJ)	2.814	4.925	7.036	11.26
QCOL (10^7KJ)	1.149	1.717	2.195	3.015
QTANK (10^7KJ)	0.849	1.133	1.314	1.545
QAUX (10^7KJ)	0.478	0.213	0.134	0.088
QTOTAL (10^7KJ)	1.327	1.346	1.448	1.633
QENV (10^6KJ)	1.055	1.931	2.811	4.557
QHX (10^7KJ)	1.104	1.620	2.040	2.760
MCOL (10^5Kg)	3.473	5.482	7.286	10.78
COLEF (%)	40.8	34.9	31.2	26.8
SOLAR (%)	64.3	75.3	99.5	117.0
SOLAR--Total (%)	64.0	84.2	90.7	94.6
SYSOP (hrs/day)	9.1	8.2	7.6	7.1
TANK LOSS (%)	9.2	11.2	12.8	15.1
Average Temperature (°C)	50.3	62.8	70.8	81.0

Table J.9 Large Meat Plant Simulation Results for September 1965--East Lansing .

Run - F:L:1:65:FA:K:336:a, b, c, d

Scale:	a	b	c	d
Collector area (m^2)	600	1050	1600	2400
RADTOTAL (10^8KJ)	1.381	2.416	3.682	5.522
QCOL (10^8KJ)	0.605	0.897	1.178	1.512
QTANK (10^8KJ)	0.439	0.606	0.742	0.875
QAUX (10^8KJ	0.792	0.625	0.489	0.357
QTOTAL (10^8KJ)	1.231	1.231	1.231	1.232
QENV (10^7KJ)	0.192	0.394	0.648	1.017
QHX (10^8KJ)	0.549	0.808	1.054	1.345
MCOL (10^6Kg)	2.800	4.425	6.091	8.432
COLEF (%)	43.8	37.1	32.0	27.4
SOLAR (%)	35.6	49.2	60.3	71.0
SOLAR--Total (%)	35.6	49.2	60.3	71.0
SYSOP (hrs/day)	9.8	8.8	8.0	7.4
TANK LOSS (%)	3.2	4.4	5.5	6.7
Average Temperature (°C)	33.6	41.5	47.9	54.3

Table J.10 Large Meat Plant Simulation Results for September 1974--East Lansing.

Run - F:L:1:74:FA:K:336:a, b, c, d

Scale:	a	b	c	d
Collector area (m^2)	600	1050	1600	2400
RADTOTAL (10^8KJ)	1.364	2.388	3.638	5.458
QCOL (10^8KJ)	0.604	0.906	1.197	1.539
QTANK (10^8KJ)	0.431	0.608	0.755	0.900
QAUX (10^8KJ)	0.800	0.623	0.477	0.338
QTOTAL (10^8KJ)	1.231	1.231	1.232	1.238
QENV (10^7KJ)	0.196	0.402	0.664	1.047
QHX (10^8KJ)	5.455	8.124	1.067	1.362
MCOL (10^6Kg)	2.513	4.053	5.687	7.826
COLEF (%)	44.2	37.9	32.9	28.2
SOLAR (%)	35.0	49.4	61.3	73.1
SOLAR--Total (%)	35.0	49.4	61.3	72.7
SYSOP (hrs/day)	8.8	8.1	7.4	6.8
TANK LOSS (%)	3.2	4.4	5.5	6.8
Average Temperature (°C)	33.2	41.6	48.6	55.4

Table J.11 Large Meat Plant Simulation Results for September 1949--Columbia.

Run - F:L:3:49:FA:K:336:a, b, c, d

Scale:	a	b	c	d
Collector area (m^2)	600	1050	1600	2400
RADTOTAL (10^8KJ)	1.648	2.883	4.394	6.590
QCOL (10^8KJ)	0.770	1.173	1.575	2.065
QTANK (10^8KJ)	0.531	0.764	0.964	1.169
QAUX (10^8KJ)	0.699	0.471	0.292	0.144
QTOTAL (10^8KJ)	1.231	1.235	1.256	1.313
QENV (10^7KJ)	0.232	0.490	0.827	1.337
QHX (10^8KJ)	0.692	1.049	1.397	1.823
MCOL (10^6Kg)	2.435	3.745	5.076	6.991
COLEF (%)	46.7	40.7	35.8	31.3
SOLAR (%)	43.1	62.1	78.3	94.9
SOLAR--Total (%)	43.2	61.9	76.8	89.0
SYSOP (hrs/day)	8.5	7.5	6.6	6.1
TANK LOSS (%)	3.0	4.2	5.3	6.5
Average Temperature (°C)	37.9	49.0	58.5	68.2

Table J.12 Large Meat Plant Simulation Results for September 1952--Columbia.

Run - F:L:3:52:FA:K:336:a, b, c, d

Scale:	a	b	c	d
Collector area (m^2)	600	1050	1600	2400
RADTOTAL (10^8KJ)	2.111	3.694	5.630	8.443
QCOL (10^8KJ)	0.953	1.432	1.898	2.451
QTANK (10^8KJ)	0.662	0.923	1.138	1.349
QAUX (10^8KJ)	0.570	0.330	0.183	0.103
QTOTAL (10^8KJ)	1.232	1.253	1.320	1.452
QENV (10^7KJ)	0.329	0.658	1.068	1.660
QHX (10^8KJ)	0.859	1.280	1.687	2.171
MCOL (10^6Kg)	2.673	4.196	5.971	8.317
COLEF (%)	45.2	38.8	33.7	29.0
SOLAR (%)	53.8	75.0	92.4	109.6
SOLAR--Total (%)	53.7	73.7	86.2	92.9
SYSOP (hrs/day)	9.3	8.4	7.8	7.3
TANK LOSS (%)	3.5	4.6	5.6	6.8
Average Temperature (°C)	44.2	56.5	66.7	76.7

APPENDIX K

Table K.1 Small Fruit and Vegetable Plant Simulation Results For September 1965 - East Lansing.

Run: G:S:1:65:FA:K:336:a,b,c,d,e

Scale:	a	b	c	d	e
Collector area (m^2)	670	1340	2340	3340	5365
RADTOTAL (10^8KJ)	1.542	3.083	5.384	7.685	12.34
QCOL (10^8KJ)	0.729	1.308	1.753	2.197	2.964
QTANK (10^8KJ)	0.591	0.893	1.170	1.356	1.591
QAUX (10^8KJ)	1.964	1.661	1.385	1.198	0.964
QTOTAL (10^8KJ)	2.555	2.555	2.555	2.555	2.555
QENV (10^6KJ)	1.706	4.735	10.02	15.76	28.09
QHX (10^8KJ)	0.688	1.122	1.605	2.002	2.672
MCOL (10^6Kg)	3.258	5.833	8.908	11.94	17.17
COLEF (%)	47.3	39.2	32.6	28.6	24.0
SOLAR (%)	23.1	35.0	45.8	53.1	62.3
SYSOP (hrs/day)	10.2	9.1	8.0	7.5	6.7
TANK LOSS (%)	2.3	3.9	5.7	7.2	9.5
Avg. Temp. (^oC)	29.4	38.0	45.8	51.0	57.6

Table K.2 Small Fruit and Vegetable Plant Simulation Results For September 1974 - East Lansing.

Run: G:S:1:74:FA:K:336:a,b,c,d,e[1]

Scale:	a	b	c	d	e
Collector area (m^2)	670	1340	2340	3340	5365
RADTOTAL (10^8KJ)	1.417	2.835	4.950	7.070	11.35
QCOL (10^8KJ)	0.691	1.160	1.694	2.129	2.867
QTANK (10^8KJ)	0.581	0.897	1.201	1.404	1.667
QAUX (10^8KJ)	1.969	1.652	1.349	1.145	0.882
QTOTAL (10^8KJ)	2.550	2.550	.2550	2.550	2.550
QENV (10^6KJ)	1.454	4.178	9.091	14.47	26.18
QHX (10^8KJ)	0.650	1.073	1.546	1.926	2.574
MCOL (10^6Kg)	2.815	4.992	7.790	10.32	15.15
COLEF (%)	48.7	40.2	34.2	30.1	25.3
SOLAR (%)	22.8	35.2	47.1	55.1	65.4
SYSOP (hrs/day)	9.5	8.4	7.6	7.0	6.4
TANK LOSS (%)	2.1	3.6	5.4	6.8	9.1
Avg. Temp (^oC)	29.2	38.1	46.7	52.4	60.2

[1]The total design energy load is 2.549×10^8 KJ and total mass flow is 8.455×10^5Kg. This simulation was truncated at 306 hours.

Table K.3 Small Fruit and Vegetable Plant Simulation Results For September 1949 - Columbia.

Run: G:S:3:49:FA:K:336:a,b,c,d

Scale:	a	b	c	d
Collector area (m^2)	670	1340	2340	3340
RADTOTAL (10^8KJ)	1.840	3.680	6.426	9.172
QCOL (10^8KJ)	0.926	1.597	2.377	3.029
QTANK (10^8KJ)	0.709	1.130	1.548	1.831
QAUX (10^8KJ)	1.846	1.425	1.007	7.259
QTOTAL (10^8KJ)	2.555	2.555	2.555	2.557
QENV (10^6KJ)	2.119	5.906	12.83	20.55
QHX (10^8KJ	0.86	1.461	2.151	2.722
MCOL (10^6Kg)	2.843	4.955	7.679	10.03
COLEF (%)	50.4	43.4	37.0	33.0
SOLAR (%)	27.7	44.2	60.6	71.6
SYSOP (hrs/day)	8.9	7.7	6.9	6.3
TANK LOSS (%)	2.3	3.7	5.4	6.6
Avg. Temp. (^oC)	32.8	44.6	56.4	64.4

Table K.4 Small Fruit and Vegetable Plant Simulation Results For September 1952 - Columbia.

Run: G:S:3:52:FA:K:336:a,b,c,d

Scale:	a	b	c	d
Collector area (m^2)	670	1340	2340	3340
RADTOTAL (10^8KJ)	2.357	4.714	8.232	11.75
QCOL (10^8KJ)	1.141	1.923	2.822	3.559
QTANK (10^8KJ)	0.877	1.345	1.788	2.079
QAUX (10^8KJ)	1.678	1.212	0.779	0.529
QTOTAL (10^8KJ)	2.555	2.557	2.567	2.608
QENV (10^6KJ)	3.101	8.039	16.60	25.76
QHX (10^8KJ)	1.065	1.766	2.566	3.212
MCOL (10^6Kg)	3.172	5.659	8.860	11.76
COLEF (%)	48.4	40.8	33.0	30.3
SOLAR (%)	34.3	52.6	70.0	81.4
SOLAR - total (%)	34.3	52.6	69.7	79.7
SYSOP (hrs./day)	9.9	8.8	7.9	7.4
TANK LOSS (%)	2.7	4.2	5.8	7.2
Avg. Temp. (^oC)	37.5	50.7	63.2	71.4

Table K.5 Medium Fruit and Vegetable Plant Simulation Results For September 1965 - East Lansing.

Run: G:M:1:65:FA:K:336:a,b,c,d,e

Scale:	a	b	c	d	e
Collector area (m^2)	525	1050	1850	2650	4200
RADTOTAL (10^8KJ)	1.208	2.416	4.257	6.098	9.664
QCOL (10^8KJ)	0.566	0.928	1.342	1.679	2.238
QTANK (10^8KJ)	0.449	0.672	0.871	1.002	1.158
QAUX (10^8KJ)	1.300	1.078	0.878	0.748	0.592
QTOTAL (10^8KJ)	1.750	1.750	1.749	1.750	1.750
QENV (10^6KJ)	1.461	4.045	8.527	13.37	23.23
QHX (10^8KJ)	0.528	0.853	1.218	1.514	2.001
MCOL (10^6Kg)	2.560	4.561	7.042	9.438	13.58
COLEF (%)	46.8	38.4	31.5	27.5	23.2
SOLAR (%)	25.7	38.4	49.8	57.3	66.2
SYSOP (hrs/day)	10.2	9.1	8.0	7.5	6.8
TANK LOSS (%)	2.6	4.4	6.4	8.0	10.4
Avg. Temp. (^oC)	31.2	40.3	48.4	53.8	60.2

Table K.6 Medium Fruit and Vegetable Plant Simulation Results For September 1974 - East Lansing.

Run: G:M:1:74:FA:K:336:a,b,c,d,e[1]

Scale:	a	b	c	d	e
Collector area (m^2)	525	1050	1850	2650	4200
RADTOTAL (10^8KJ)	1.111	2.222	3.915	5.607	8.887
QCOL (10^8KJ)	0.530	0.882	1.286	1.614	2.149
QTANK (10^8KJ)	0.436	0.665	0.882	1.022	1.193
QAUX (10^8KJ)	1.290	1.060	0.844	0.704	0.532
QTOTAL (10^8KJ)	1.726	1.725	1.725	1.726	1.725
QENV (10^6KJ)	1.321	3.729	8.014	12.63	22.11
QHX (10^8KJ)	0.494	0.809	1.165	1.451	1.922
MCOL (10^6Kg)	2.166	3.809	6.045	7.901	11.61
COLEF (%)	47.7	39.7	32.9	28.8	24.2
SOLAR (%)	25.3	38.6	51.1	59.2	69.2
SYSOP (hrs/day)	9.3	8.2	7.4	6.7	6.2
TANK LOSS (%)	2.5	4.2	6.2	7.8	10.3
Avg. Temp. (^oC)	30.9	40.4	49.4	55.2	62.3

[1]The total design energy load is 1.725×10^8KJ and the total mass flow is 5.755×10^5Kg. This simulation was truncated at 306 hours.

Table K.7 Medium Fruit and Vegetable Plant Simulation Results For September 1949 - Columbia.

Run: G:M:3:49:FA:K:336:a,b,c,d

Scale:	a	b	c	d
Collector area (m^2)	525	1050	1850	2650
RADTOTAL (10^8KJ)	1.442	2.88	5.080	7.277
QCOL (10^8KJ)	0.709	1.209	1.801	2.299
QTANK (10^8KJ)	0.530	0.832	1.128	1.329
QAUX (10^8KJ)	1.219	0.918	0.621	0.431
QTOTAL (10^8KJ)	1.749	1.749	1.749	1.760
QENV (10^6KJ)	1.856	5.164	11.16	17.83
QHX (10^8KJ)	0.654	1.099	1.618	2.055
MCOL (10^6Kg)	2.234	3.816	5.856	7.756
COLEF (%)	49.2	41.9	35.5	31.6
SOLAR (%)	30.3	47.5	64.5	76.0
SOLAR - total (%)	30.3	47.5	64.5	75.5
SYSOP (hrs/day)	8.9	7.6	6.6	6.1
TANK LOSS (%)	2.6	4.3	6.2	7.8
Avg. Temp. (^oC)	34.5	46.8	59.0	67.2

Table K.7 Medium Fruit and Vegetable Plant Simulation Results For September 1949 - Columbia.

Run: G:M:3:49:FA:K:336:a,b,c,d

Scale:	a	b	c	d
Collector area (m^2)	525	1050	1850	2650
RADTOTAL (10^8KJ)	1.442	2.88	5.080	7.277
QCOL (10^8KJ)	0.709	1.209	1.801	2.299
QTANK (10^8KJ)	0.530	0.832	1.128	1.329
QAUX (10^8KJ)	1.219	0.918	0.621	0.431
QTOTAL (10^8KJ)	1.749	1.749	1.749	1.760
QENV (10^6KJ)	1.856	5.164	11.16	17.83
QHX (10^8KJ)	0.654	1.099	1.618	2.055
MCOL (10^6Kg)	2.234	3.816	5.856	7.756
COLEF (%)	49.2	41.9	35.5	31.6
SOLAR (%)	30.3	47.5	64.5	76.0
SOLAR - total (%)	30.3	47.5	64.5	75.5
SYSOP (hrs/day)	8.9	7.6	6.6	6.1
TANK LOSS (%)	2.6	4.3	6.2	7.8
Avg. Temp. (^oC)	34.5	46.8	59.0	67.2

Table K.8 Medium Fruit and Vegetable Plant Simulation Results For September 1952 - Columbia.

Run: G:M:3:52:FA:K:336:a,b,c,d

Scale:	a	b	c	d
Collector area (m^2)	525	1050	1850	2650
RADTOTAL (10^8KJ)	1.847	3.694	6.508	9.323
QCOL (10^8KJ)	0.888	1.481	2.170	2.731
QTANK (10^8KJ)	0.672	1.017	1.336	1.541
QAUX (10^8KJ)	1.077	0.733	0.424	0.275
QTOTAL (10^8KJ)	1.749	1.750	1.760	1.816
QENV (10^6KJ)	2.611	6.840	14.14	21.92
QHX (10^8KJ)	0.822	1.351	1.954	2.445
MCOL (10^6Kg)	2.452	4.317	6.891	9.275
COLEF (%)	48.1	40.1	33.3	29.3
SOLAR (%)	38.4	58.1	76.4	88.1
SOLAR - total (%)	38.4	58.1	84.9	75.9
SYSOP (hrs/day)	9.8	8.6	7.8	7.3
TANK LOSS (%)	2.9	4.6	6.5	8.0
Avg. Temp. (^oC)	40.3	54.4	67.5	75.9

Table K.9 Large Fruit and Vegetable Plant Simulation Results For September 1965 - East Lansing.

Run: G:L:1:65:FA:K:336:a,b,c,d,e

Scale:	a	b	c	d	e
Collector area (m^2)	4015	8030	14050	20070	32100
RADTOTAL (10^9KJ)	0.924	1.848	3.233	4.618	8.290
QCOL (10^9KJ)	0.462	0.777	1.130	1.418	1.894
QTANK (10^9KJ)	0.387	0.598	0.801	0.934	1.111
QAUX (10^9KJ)	1.268	1.057	0.854	0.721	0.543
QTOTAL (10^9KJ)	1.655	1.655	1.660	1.654	1.654
QENV (10^7KJ)	0.574	1.829	4.26	7.074	13.28
QHX (10^9KJ)	0.436	0.720	1.036	1.288	1.707
MCOL (10^7Kg)	2.102	3.699	5.767	7.549	10.93
COLEF (%)	50.0	42.0	35.0	30.7	22.8
SOLAR (%)	23.4	36.1	48.4	56.4	67.1
SYSOP (hrs/day)	11.0	9.6	8.6	7.9	7.1
TANK LOSS (%)	1.2	2.4	3.8	5.0	7.0
Avg. Temp. (^oC)	28.0	36.3	44.2	49.5	56.4

Table K.10 Large Fruit and Vegetable Plant Simulation Results For September 1974 - East Lansing.

Run: G:L:1:74:FA:K:336:a,b,c,d,e[1]

Scale:	a	b	c	d	e
Collector area (m^2)	4015	8030	14050	20070	32100
RADTOTAL (10^9KJ)	0.850	1.699	2.973	4.247	6.792
QCOL (10^9KJ)	0.431	0.734	1.081	1.360	1.819
QTANK (10^9KJ)	0.371	0.587	0.801	0.948	1.141
QAUX (10^9KJ)	1.264	1.048	0.834	0.686	0.495
QTOTAL (10^9KJ)	1.635	1.635	1.635	1.635	1.636
QENV (10^7KJ)	0.509	1.669	3.957	6.651	12.59
QHX (10^9KJ)	0.406	0.679	0.987	1.233	1.636
MCOL (10^7Kg)	1.718	3.058	4.847	6.439	9.264
COLEF (%)	50.7	43.2	36.4	32.0	26.8
SOLAR (%)	22.7	35.9	49.0	58.0	69.8
SYSOP (hrs/day)	9.6	8.6	7.8	7.2	6.5
TANK LOSS (%)	1.2	2.3	3.7	4.9	6.9
Avg. Temp. (^oC)	27.5	36.1	44.6	50.5	58.1

[1]The total design energy load is 1.635×10^9 and the total water demand is 6.008×10^6kg. This simulation was truncated at 306 hours.

Table K.11 Large Fruit and Vegetable Plant Simulation Results For September 1949 - Columbia.

Run: G:L:3:49:FA:K:336:a,b,c,d

Scale:	a	b	c	d
Collector area (m^2)	4015	8030	14050	20070
RADTOTAL (10^9KJ)	1.103	2.205	3.858	5.511
QCOL (10^9KJ)	0.573	0.995	1.495	1.911
QTANK (10^9KJ)	0.449	0.724	1.013	1.216
QAUX (10^9KJ)	1.206	0.931	0.642	0.451
QTOTAL (10^9KJ)	1.655	1.655	1.655	1.667
QENV (10^8KJ)	0.074	0.233	0.551	0.931
QHX (10^9KJ)	0.533	0.911	1.354	1.717
MCOL (10^7Kg)	1.888	3.102	4.838	6.275
COLEF (%)	51.9	45.1	38.7	34.7
SOLAR (%)	27.1	43.7	61.2	73.5
SOLAR - total (%)	27.1	43.7	61.2	72.9
SYSOP (hrs/day)	9.8	8.1	7.2	6.5
TANK LOSS (%)	1.3	2.3	3.7	4.9
Avg. Temp. (^oC)	30.4	41.2	52.6	60.6

Table K.12 Large Fruit and Vegetable Plant Simulation Results For September 1952 - Columbia.

Run: G:L:3:52:FA:K:336:a,b,c,d

Scale:				
Collector area (m^2)	4015	8030	14058	20070
RADTOTAL (10^9KJ)	1.412	2.825	4.943	7.061
QCOL (10^9KJ)	0.721	1.230	1.816	2.293
QTANK (10^9KJ)	0.574	0.901	1.220	1.434
QAUX (10^9KJ)	1.080	0.755	0.445	0.283
QTOTAL (10^9KJ)	1.654	1.656	1.665	1.717
QENV (10^8KJ)	0.106	0.317	0.714	1.172
QHX (10^9KJ)	0.673	1.129	1.648	2.066
MCOL (10^7Kg)	1.959	3.535	5.508	7.343
COLEF (%)	51.0	46.7	36.7	32.5
SOLAR (%)	34.7	54.5	73.7	86.6
SOLAR-total (%)	34.7	54.4	73.3	83.5
SYSOP (hrs/day)	10.2	9.2	8.2	7.7
TANK LOSS (%)	1.5	2.6	3.9	5.1
Avg. Temp. (^oC)	35.3	48.2	60.7	69.1

Table K.13 Small Fruit and Vegetable Plant Simulation Results for Period A

Runs - G:S:1:74:SP:K:864:b

G:S:3:52:SP:K:864:b

Location:	1 (East Lansing, 74)	3 (Columbia, 52)
Collector area (m^2)	1340	1340
RADTOTAL (10^9KJ)	0.767	1.146
QCOL (10^8KJ)	1.940	2.902
QTANK (10^8KJ)	1.379	2.073
QAUX (10^8KJ)	1.008	0.374
QTOTAL (10^8KJ)	2.487	2.447
QENV (10^7KJ)	1.990	3.166
QHX (10^8KJ)	1.818	2.738
MCOL (10^7Kg)	1.087	1.188
COLEF (%)	25.3	25.3
SOLAR (%)	57.8	86.8
SOLAR--Total (%)	55.4	84.7
SYSOP (hrs/day	6.6	7.2
TANK LOSS (%)	10.3	10.9
Average Temperature (°C)	54.4	75.3

Table K.14 Small Fruit and Vegetable Plant Simulation Results for Period B.

Runs - G:S:1:74:SU:K:360:b

G:S:3:52:SU:K:360:b

Location:	1 (East Lansing, 74)	3 (Columbia, 52)
Collector area (m^2)	1340	1340
RADTOTAL (10^8KJ)	2.892	4.823
QCOL (10^7KJ)	6.221	9.699
QTANK (10^7KJ)	2.283	3.570
QAUX (10^7KJ)	0.735	0.129
QTOTAL (10^7KJ)	3.020	3.699
QENV (10^7KJ)	1.169	1.758
QHX (10^7KJ)	5.499	8.640
MCOL (10^6Kg)	3.602	4.566
COLEF (%)	21.5	20.1
SOLAR (%)	75.9	118.8
SOLAR--Total (%)	75.6	96.5
SYSOP (hrs/day)	5.2	6.7
TANK LOSS (%)	18.8	18.1
Average Temperature (°C)	67.5	98.3

Table K.15 Small Fruit and Vegetable Plant Simulation Results for Period C.

Runs - G:S:1:74:SU:K:432:b
G:S:3:52:SU:K:432:b

Location:	1 (East Lansing, 74)	3 (Columbia, 52)
Collector area (m^2)	1340	1340
RADTOTAL (10^8KJ)	3.274	5.171
QCOL (10^8KJ)	1.531	2.261
QTANK (10^8KJ)	1.119	1.766
QAUX (10^8KJ)	2.363	1.716
QTOTAL (10^8KJ)	3.482	3.482
QENV (10^6KJ)	5.839	8.728
QHX (10^8KJ)	1.388	2.096
MCOL (10^6Kg)	6.166	7.775
COLEF (%)	46.8	43.7
SOLAR (%)	32.1	50.7
SOLAR--Total (%)	32.1	50.7
SYSOP (hrs/day)	7.5	9.5
TANK LOSS (%)	3.8	3.9
Average Temperature (°C)	35.9	49.3

Table K.16 Small Fruit and Vegetable Plant Simulation Results for Period D.

Runs - G:S:1:74:FA:K:1440:b

G:S:3:52:FA:K:1440:b

Location:	1 (East Lansing, 74)	3 (Columbia, 52)
Collector area (m^2)	1340	1340
RADTOTAL (10^9KJ)	1.451	1.931
QCOL (10^8KJ)	3.110	4.362
QTANK (10^8KJ)	1.613	2.213
QAUX (10^8KJ)	0.021	0.023
QTOTAL (10^8KJ)	1.634	2.236
QENV (10^7KJ)	7.784	10.79
QHX (10^8KJ)	2.937	4.123
MCOL (10^6Kg)	8.612	8.694
COLEF (%)	21.4	22.6
SOLAR (%)	134.2	184.1
SOLAR--Total (%)	98.7	99.0
SYSOP (hrs/day)	3.1	3.2
TANK LOSS (%)	25.0	24.7
Average Temperature (°C)	109.4	145.3

Table K.17 Medium Fruit and Vegetable Plant Simulation Results for Period B.

Runs - G:M:1:74:SU:K:432:b
G:M:3:52:SU:K:432:b

Location:	1 (East Lansing, 74)	3 (Columbia, 52)
Collector area (m^2)	1340	1340
RADTOTAL (10^8KJ)	2.565	4.052
QCOL (10^8KJ)	1.234	1.836
QTANK (10^8KJ)	0.905	1.432
QAUX (10^8KJ)	2.012	1.485
QTOTAL (10^8KJ)	2.917	2.917
QENV (10^6KJ)	4.470	6.658
QHX (10^8KJ)	1.118	1.698
MCOL (10^6Kg)	4.944	6.233
COLEF (%)	48.1	45.3
SOLAR (%)	31.0	49.1
SOLAR--Total (%)	31.0	49.1
SYSOP (hrs/day)	7.7	9.7
TANK LOSS (%)	3.6	3.6
Average Temperature (°C)	35.0	47.9

Table K.18 Large Fruit and Vegetable Plant Simulation Results for Summer Period.

Runs - G:L:1:74:SU:K:432:b

G:L:3:52:SU:K:432:b

Location:	1 (East Lansing, 74)	3 (Columbia, 52)
Collector area (m^2)	8030	8030
RADTOTAL (10^9KJ)	1.962	3.099
QCOL (10^9KJ)	0.959	1.433
QTANK (10^9KJ)	0.721	1.146
QAUX (10^9KJ)	1.485	1.060
QTOTAL (10^9KJ)	2.206	2.206
QENV (10^7KJ)	2.341	3.463
QHX (10^8KJ)	8.717	1.330
MCOL (10^7Kg)	3.806	4.847
COLEF (%)	48.9	46.2
SOLAR (%)	32.7	51.9
SOLAR--Total (%)	32.7	51.9
SYSOP (hrs/day)	7.7	9.8
TANK LOSS (%)	2.4	2.4
Average Temperature (°C)	34.0	46.5